



Universidade do Porto

FEUP Faculdade de
Engenharia

Drug-induced bone regeneration in a diabetic model

José Carlos Osório Rodrigues da Silva

Orientador

Professor Doutor Pedro Sousa Gomes

Co-orientadora

Professora Doutora Maria Helena Raposo Fernandes

Porto

Fevereiro de 2017

Dissertação submetida à Faculdade de Engenharia, U. do Porto para
obtenção do grau de Doutor em Engenharia Biomédica

This thesis was supervised by:

Prof. Doutor Pedro Sousa Gomes

Faculdade de Medicina Dentária, U. Porto

Prof. Doutora Maria Helena Raposo Fernandes

Faculdade de Medicina Dentária, U. Porto

Advisor:

Prof. Doutor Bruno Jorge Antunes Colaço

Universidade de Trás-os-Montes e Alto Douro

The host institutions in which the experimental work was conducted were:

Laboratório de Metabolismo e Regeneração Óssea

Faculdade de Medicina Dentária, U. Porto

- Cell cultures establishment and characterization

Serviço de Biotério

Universidade de Trás-os-Montes e Alto Douro

- Animal housing and experimental surgeries

The research was supported by:

Laboratório de Metabolismo e Regeneração Óssea, FMDUP

“Nothing in life is to be feared, it is only to be understood.

Now is the time to understand more, so that we may

fear less.”

Marie Curie

...to Leonardo

...to my brother

...to my parents

Table of Contents

Acknowledgements	vii
Abstract	xi
Resumo	xiii
Abbreviations	xv
List of figures	xix
List of Tables	xxv
Chapter 1 – Aim and Structure of the Thesis	1
1.1 – Aim and structure	3
Chapter 2 - Background and Literature overview	9
2.1 - Bone Tissue.....	11
2.1.1 - Macrostructure.....	12
2.1.2 - Microstructure	17
2.1.3 - Bone minerals	22
2.1.4 - Bone cells	23
2.1.5 - Bone remodelling	31
2.1.6 - Bone healing	36
2.2 - Diabetes mellitus.....	38

2.2.1 - Diabetes classification	40
2.2.2 - Diabetes diagnosis	48
2.2.3 - Diabetes and Bone.....	50
2.2.4 - Diabetes and Biomaterials Implantation	57
2.3 - Tetracyclines.....	60
2.3.1 - Chemistry and anti-microbial properties	63
2.3.2 - Non-antibiotic properties	66
2.3.3 – Doxycycline	68
2.3.4 - Minocycline.....	71
Chapter 3 – The Osteogenic priming of mesenchymal stem cells is impaired in experimental diabetes	73
3.1 – Introduction.....	75
3.2 – Research hypothesis and objectives	77
3.3 – Materials and methods	78
3.3.1 – Animals.....	78
3.3.2 – Diabetic bone alterations.....	79
3.3.3 – Establishment of bone-marrow cell cultures	79
3.3.4 – Optical microscopy	80
3.3.5 – Cell proliferation and metabolic activity	81
3.3.6 – Cell morphology.....	81
3.3.7 – Alkaline phosphatase activity and total Protein content	82

3.3.8 – Programmed cell death	84
3.3.9 – Collagen synthesis.....	84
3.3.10 – Gene expression	85
3.3.11 – Osteogenic induction and culture characterization	86
3.3.12 – Activation of specific signaling pathways in STZ-derived cultures ..	87
3.3.13 – Statistical analysis	88
3.4 – Results.....	89
3.4.1 – Diabetic experimental model	89
3.4.2 – Diabetic bone alterations.....	89
3.4.3 – Cell proliferation and metabolic activity	90
3.4.4 – Cell morphology	93
3.4.5 – Alkaline phosphatase activity	94
3.4.6 – Programmed cell death	95
3.4.7 – Collagen synthesis.....	96
3.4.8 – Gene expression in standard conditions and in osteogenic-inducing conditions.....	99
3.4.9 – Mineralization assessment in osteogenic- and STZ-induced conditions	101
3.4.10 – Evaluation of specific signaling pathways.....	102
3.5 – Discussion	104
3.6 – Conclusion	111

Chapter 4 – Doxycycline enhances the osteogenic functionality of diabetic-derived mesenchymal stem cells	113
4.1 – Introduction	115
4.2 – Research hypothesis and objectives	118
4.3 – Materials and Methods	119
4.3.1 – Animals.....	119
4.3.2 – Characterization of the experimental groups.....	120
4.3.3 – Cell cultures	120
4.3.4 – Cell proliferation and metabolic activity	121
4.3.5 – Cell morphology	121
4.3.6 – Alkaline phosphatase activity	122
4.3.7 – Apoptotic behaviour	122
4.3.8 – Collagen synthesis.....	122
4.3.9 – Gene expression	123
4.3.10 – Neonatal calvaria defect ex vivo model.....	124
4.3.11 – Statistical analysis	126
4.4 Results	127
4.4.1 – Establishment of a diabetes experimental model	127
4.4.2 – Evaluation of diabetes effects on bone	127
4.4.3 – Characterization of MSCs cultures grown in the presence of doxycycline	129

4.4.4 – Calvarial bone defect regeneration – Ex vivo model	139
4.5 – Discussion	146
4.6 Conclusion	151
Chapter 5 – Minocycline-loaded PMMA bone Cement as a delivery system to enhance bone healing – Biocompatibility evaluation in a diabetic model	153
5.1 – Introduction	155
5.2 – Research hypothesis and Objectives	158
5.3 – Materials and Methods	159
5.3.1 – PMMA and minocycline-loaded Pmma samples preparation	159
5.3.2 – PMMA and minocycline-loaded Pmma samples Characterization .	159
5.3.3 – Animals.....	162
5.3.4 – Subcutaneous implantation of minocycline-loaded PMMA.....	163
5.3.5 – Sample gathering and fixation	165
5.3.6 – Histological analysis of inflammatory response	165
5.4 – Results.....	166
5.4.1 – FTIR evaluation of PMMA and minocycline-loaded Pmma samples	166
5.4.2 – Surface analysis of PMMA and minocycline-loaded Pmma samples	166
5.4.3 – Minocycline release evaluation	168
5.4.4 – Diabetic experimental model	169

5.4.5 – Inflammatory response to PMMA and minocycline-impregnated PMMA.....	169
5.5 – Discussion	179
5.6 – Conclusions.....	189
Chapter 6 – Conclusions and future perspectives	191
6.1 – General conclusions.....	193
6.2 – Future perspectives	195
References	197

ACKNOWLEDGEMENTS

The development of a work driven to obtain a Doctor degree is a hard and complex path and it can also be a very lonely walk. During this process many changes emerge, which can be either personal or professional and may happen to be major causes of difficulties and discouragement.

However, my walk was neither lonely, nor demotivating. On the other hand, I can state that this was one of the most precious journeys I have experienced and also the most enriching. All the goals and results were achieved with plenty of work, dedication, and the support of teams that helped me during these four years in the Doctoral Program of Biomedical Engineering. Thus, I wish to share this moment of great importance with those who have been crucial during this stage and in my personal development as well.

Therefore, I would like to express my gratitude to those without whom this victory would not have been possible:

To Professor Maria Helena Raposo Fernandes for all of the transmitted knowledge, constant encouragement and support. For all of the opportunities given to me, from the possibility of integrating her research team at the Laboratory for Bone Metabolism and Regeneration, to the possibility of participating in several works and for all the results of this collaboration. I am sincerely grateful for the friendship and for all the advices that helped me through the last years and that will still help me to grow both as a person and as a professional.

To Professor Pedro de Sousa Gomes, for all of the knowledge I acquired during these six years we worked together. For the exemplar orientation and professional accuracy that allowed me to grow scientifically. For all of the support, encouragement and persistence. For all of the opportunities offered to me to acquire knowledge in many different areas from my initial training, namely Tissue Regeneration and Science in Laboratory Animals which became my main preference areas and greater scientific interest. I would also like to thank for his friendship and counseling during the most difficult times. For all the constant calmness and tolerance during my experience at the Laboratory for Bone Metabolism and Regeneration, as well as the availability he has shown to me under any circumstance. I also want to thank him for having accepted to supervise my work, since he represents an example for me to follow.

To Professor Bruno Jorge Antunes Colaço, I thank for all of the availability and cooperation during this work development. I am also grateful for the academic basis and encouragement he transmitted to me in what concerns the work with laboratory animals.

To my colleagues of the Laboratory for Bone Metabolism and Regeneration of the Faculty of Dental Medicine: Elisabete Gonçalves, Fábio Costa, Gabriel Fidelis, Liliana Grenho and Mónica Garcia for all of the excellent team work and cooperation, friendship and aid in the final phase of my PhD.

To my friends, Joana Venâncio, Jorge Cerdeira and Rita Carmona who supported me through this journey sharing with me moments of happiness and who always transmitted me the most positive strength and encouragement.

To Hélder Martinho and Nuno Magalhães, my deepest and heartfelt gratitude for having been present in all of the occasions. As earning a PhD involves hard work and may have consequences in one's personal life and relationships, I appreciate the understanding and care given to me during this more difficult period. I thank you for all of those days when I could not be with you because I had work to do and yet you came to meet me to support me and give strength. Above all, I appreciate the unwavering friendship.

To my grandparents, I thank the values they instilled in me and for having been present in every stages of my life until today and I wish that they always keep the same faith in me. For the strength that they always gave me and for teaching me that "willpower can move mountains". I would also still like to thank for all of their trust in me and for the unconditional support throughout all these years always with all of the availability, affection and love.

To my parents, my deepest gratitude for the trust, for the transmitted values and education and for the support in my whole academic and personal life. For the unlimited love and for being role-models of humility, strength and perseverance for me. Also, for being the most solid pillars of my training and in both of my personal and professional development and finally for being by my side in all of the moments. Last but not the least, thank you for having taught me everyday, that together we are able of overcome any difficulty and to take down any obstacle.

To my brother, Pedro Gustavo, I acknowledge so much more than I can here describe. I am thankful for the friendship, the unconditional support in my personal and professional life, whatever the circumstances are. For all of the tight hugs during good and bad moments. For being an integral part of my life and for having been and still being my biggest inspiration and

example of loyalty and positivism under any circumstance.

To Leonardo, I thank how he converted all of the complications in a smile or a laugh. All the moments we spent together, for the unrestricted support during the development of this work. I appreciate the tolerance and understanding during the weakest moments throughout this path, either at a personal or professional level. For all the happy moments, for all of the positivity and energy. I also thank the affection, intimacy and love that have been the biggest sources of motivation to continue until here and hereafter.

Diabetes mellitus (DM) is one of the most established systemic conditions, with increasing epidemiological importance. It is known to cause numerous complications and severe damage among a variety of tissues and organs, including bone. Accordingly, type 1 diabetes mellitus (T1D) has been associated decreased skeletal mass, higher risk of fractures and delayed healing. Despite the numerous studies on diabetes and its influence on bone, the molecular events affecting both osteoblasts and progenitor cells, within the diabetic milieu, are still not fully understood.

In this context, a detailed study was carried out in order to assess the functionality of diabetic-derived bone marrow-derived mesenchymal stem cells – i.e., osteoblastic precursor cells – regarding proliferation, functional activity, osteogenic priming, and relevant signalling pathways modulating these processes. Data showed that the diabetic environment affected both mesenchymal stem cells signalling and functionality, in a long-lasting way, contributing to a decreased osteogenic priming and increased adipogenic activation, which may converges to the verified bone alterations and weakening.

Given the verified hindrances in diabetes, a novel therapeutic strategy for the enhancement of osteogenic activation was developed, based on the delivery of minocycline and doxycycline, two semi-synthetic derivatives of tetracycline, known to enhance cell proliferation and the functional activity of osteoblasts. Initially, the osteogenic enhancement of bone marrow-derived mesenchymal stem cells and osteoblasts, developed under diabetic-induced conditions, was validated *in vitro*, in

established cell culture models, and *ex vivo*, in a model of calvarial bone regeneration. Assayed regimens of low dosage tetracyclines, were able to normalize the impaired osteogenic commitment of osteoblastic precursor populations, enhancing the metabolic equilibrium, as assessed within the *in vitro* system. Furthermore, tetracycline administration were found to increase tissue healing and tissue mineralization in simulated diabetic conditions, as assayed *ex vivo*.

Subsequently, and envisaging the development of a translational therapeutic application with reliable effectiveness within the clinical scenario, a PMMA cement-based minocycline delivery system was developed and assayed for biocompatibility. Developed system was subcutaneously implanted in experimental animals, either in control or diabetic conditions. The controlled release of minocycline was able to enhance several inflammation-related factors, suggesting an enhanced tissue healing and biomaterial integration which may further be applied as a local therapy for bone regeneration.

Overall, a novel therapeutic approach – the application of a low dosage regimen of tetracyclines – for the management of the verified hindrances in the osteogenic activation within the diabetic milieu was assayed and validated within *in vitro*, *ex vivo* and *in vivo* models, exhibiting an improved biological outcome and a prospective clinical application.

A diabetes mellitus é uma patologia sistêmica, com elevada incidência, e cuja relevância epidemiológica tem vindo a aumentar. A longo prazo, a diabetes está associada a inúmeras complicações e lesões graves nos tecidos e órgãos, incluindo o osso. Em particular, a diabetes tipo 1 está associada à perda de conteúdo mineral ósseo, aumento do risco de fraturas e atraso nos processos de regeneração. Apesar de terem sido realizados diversos estudos para compreender os efeitos da diabetes no osso, não estão claros quais os mecanismos moleculares envolvidos na afetação, tanto dos osteoblastos como das suas células progenitoras.

Neste sentido, foi realizado um estudo pormenorizado, focado na avaliação da funcionalidade das células estaminais mesenquimais provenientes da medula óssea – células precursoras dos osteoblastos – na condição diabética. Foram avaliados parâmetros como a proliferação, atividade funcional, expressão osteogénica e vias de sinalização relevantes, que modulam estes processos. Os resultados mostraram que a condição diabética afeta tanto vias de sinalização como a funcionalidade das células mesenquimais de forma duradoura, contribuindo para uma diminuída expressão osteogénica e aumento da expressão adipogénica, convergindo desta forma para alterações na estrutura óssea, e seu consequente enfraquecimento.

Tendo por base a identificação das alterações vigentes na condição diabética, foi desenvolvida uma nova abordagem terapêutica para melhorar a ativação osteogénica, baseada na libertação de minociclina e doxiciclina, dois derivados semissintéticos da tetraciclina, que demonstraram um efeito indutor na proliferação celular e na atividade

funcional de osteoblastos. Inicialmente, foi realizada uma validação *in vitro* dos efeitos promotores da expressão osteogénica de células estaminais mesenquimais da medula óssea, bem como os efeitos da doxiciclina num modelo *ex vivo* da regeneração da óssea da calote. As baixas doses de tetraciclinas que foram estudadas permitiram a normalização do comprometimento com a linhagem osteogénica, melhorando assim o equilíbrio metabólico no osso diabético.

Com o intuito de desenvolver uma aplicação terapêutica com uma efetividade clínica, foi desenvolvido um sistema de libertação controlada de minociclina, a partir de um cimento de polimetil metacrilato (PMMA). O sistema desenvolvido foi implantado subcutaneamente em animais controlo e animais diabéticos, para avaliação da sua biocompatibilidade. A libertação controlada de minociclina permitiu melhorar determinados fatores relacionados com a resposta inflamatória, sugerindo uma melhoria tanto nos processos de regeneração dos tecidos envolventes como na integração do biomaterial que, por sua vez, poderá ser posteriormente aplicado em terapias locais de regeneração óssea.

No geral, foi estudada uma nova abordagem terapêutica, baseada na aplicação de baixas doses de tetraciclinas, tendo em vista a indução osteogénica, que se encontra alterada na condição diabética. Esta abordagem foi validada com estudos *in vitro*, *in vivo* e *ex vivo*, e revelou resultados biológicos favoráveis para futuras aplicações clínicas.

ABBREVIATIONS

α MEM	Alpha-modification minimum essential medium
ALP	Alkaline phosphatase
AP2	Adipocyte protein 2
BMD	Bone mineral density
BSP-1	Bone sialoprotein 1, osteopontin
BSP-2	Bone sialoprotein 2
CAP	Fibrotic capsule
CLSM	Confocal laser scanning microscopy
DGAV	<i>Direção Geral de Alimentação e Veterinária</i>
DM	Diabetes mellitus
DO	Diabetic osteopenia
ECM	Extracellular matrix
EDS	Energy-dispersive x-ray spectroscopy
EDTA	Ethylenediaminetetraacetic acid
FB	Fibroblasts
FBS	Foetal bovine serum
FTIR	Fourier Transform Infrared (spectroscopy)
GAPDH	Glyceraldehyde 3-phosphate dehydrogenase

GC	Giant cells
GDM	Gestational diabetes mellitus
GH	Growth hormone
IGF-1	Insulin-like growth factor-1
IP	Intraperitoneal (injection)
IR	Inflammatory reaction
IRS1	Insulin receptor substrate 1
IRS2	Insulin receptor substrate 2
LYM	Lymphocytes
MAC	Macrophages
MAP	Mycobacterium avium subspecies paratuberculosis
μCT	Microcomputed tomography
M-CSF	Macrophage colony-stimulating factor
MMP	Matrix metalloproteinase
MMP-9	Matrix metalloproteinase 9
mPMMA	Minocycline-loaded poly(methyl methacrylate)
ND	Neonatal diabetes
NEO	Neovascularization
NO	Nitric oxide
OC	Osteocalcin

OPG	Osteoprotegerin
OPN	Osteopontin
ON	Osteonectin
PBS	Phosphate buffered saline
PMMA	Poly(methyl methacrylate)
PMNs	Polymorphonuclear neutrophils
PPAR γ	Peroxisome proliferator-activated receptor gamma
PTH	Parathyroid hormone
RANKL	Receptor activator of nuclear factor kappa- β ligand
RUNX2	Runt-related transcription factor 2
SC	Subcutaneous (injection)
SDD	Subantibacterial dose doxycycline
STZ	Streptozotocin
T1D	Type 1 diabetes mellitus
T2D	Type 2 diabetes mellitus
TC	Tetracycline
TGF- β	Transforming growth factor β

Chapter 2

Figure 2.1	Different types of bone morphology	13
Figure 2.2	Microstructural organization of mature lamellar bone comprising areas of compact and cancellous bone	18
Figure 2.3	Scanning electron microscopy image of collagen fibers of human cancellous bone	20
Figure 2.4	Rat multinucleated osteoclast; Histological analysis of human bone	24
Figure 2.5	Histological analysis of rat bone section stained with toluidine blue	27
Figure 2.6	Bone lining cells	30
Figure 2.7	Schematic representation of the four stages of bone remodelling cycle	34
Figure 2.8	Schematic representation of the four stages of bone fracture repair	37
Figure 2.9	Chemical structure of naphthacene ring system, first-generation antibiotics, and second-generation antibiotics	62
Figure 2.10	Chemical structure of tetracycline	63

Chapter 3

Figure 3.1	Representative 2D microtomographic images of the proximal tibia methaphysis, in control and STZ animals	90
Figure 3.2	Cell proliferation (DNA assay) of STZ-derived bone marrow mesenchymal stem cell cultures	91
Figure 3.3	Cell viability/metabolic activity (MTT assay) of STZ-derived bone marrow mesenchymal stem cell cultures	92
Figure 3.4	Confocal laser scanning microscopy imaging of rat bone marrow-derived mesenchymal stem cell cultures	94
Figure 3.5	Alkaline phosphatase activity (ALP per total protein content) of STZ-derived bone marrow mesenchymal stem cell cultures	95
Figure 3.6	Apoptotic analysis (caspase-3 activity assay) of STZ-derived bone marrow mesenchymal cell cultures	96
Figure 3.7	Total collagen staining of STZ-derived bone marrow mesenchymal stem cell cultures	97
Figure 3.8	Colorimetric determination of the total collagen stained product within the established STZ-derived bone marrow mesenchymal stem cell cultures	98
Figure 3.9	qPCR gene expression analysis of ALP, RUNX2, Col1 α 1, osteopontin, osteocalcin, and osteoprotegerin in MSCs cultures	99
Figure 3.10	qPCR gene expression assessment of adipogenic genes PPAR γ , IRS1, IRS2, and AP2, in undifferentiated STZ-derived MSCs cultures	100

Figure 3.11	Colorimetric determination of the mineralization nodules within the established control- and STZ-derived bone marrow mesenchymal stem cell cultures	101
Figure 3.12	Metabolic activity and gene expression analysis (of ALP, RUNX2, and PPAR γ) of MSCs cultures	102

Chapter 4

Figure 4.1	Representative 2D microtomographic images of the proximal tibia metaphysis, in control and STZ animals	128
Figure 4.2	Cell viability/metabolic activity (MTT assay) of rat bone marrow-derived cells cultured in presence and absence of doxycycline	130
Figure 4.3	Confocal laser scanning microscopy imaging of rat bone marrow-derived cell cultures, from control and STZ-induced diabetic animals in presence and absence of doxycycline	132
Figure 4.4	Alkaline phosphatase activity (ALP per total protein content) of rat bone marrow-derived cells cultured in presence and absence of doxycycline from both control and STZ-induced animals	133
Figure 4.5	Alkaline phosphatase staining of rat bone marrow-derived cell cultures	134
Figure 4.6	Apoptotic analysis (caspase-3 activity assay) of rat bone marrow-derived cells cultured in presence and in absence of doxycycline from both control and STZ-induced animals	135

Figure 4.7	Total type 1 collagen staining of rat bone marrow-derived cell cultures, from control and STZ-induced diabetic animals in presence and in absence of doxycycline	136
Figure 4.8	Colorimetric determination of the total collagen stained product within the established MSCs cultures from both control and STZ-induced diabetic animals in presence and absence of doxycycline	137
Figure 4.9	qPCR gene expression analysis of ALP, BMP-2, Col 1, OPN, LRP5, OC, and OPG in MSCs cultures, established for days 5 and 8, from control and STZ-induced diabetic animals	139
Figure 4.10	Phase contrast optical microscopy images obtained at days 0, 10 and 20 for the established experimental conditions of new-born rat calvarial organ culture	141
Figure 4.11	SEM images of new-born rat parietal bone at days 8 and 15	143
Figure 4.12	SEM images of mineralization deposits after 15 days of culture of newborn rat parietal bones	144
Figure 4.13	Percentage of regenerated area along the 15 days of new-born rat parietal bones' culture, in both control and diabetic conditions, in presence and absence of doxycycline	145

Chapter 5

Figure 5.1	Subcutaneous mPMMA implantation	164
-------------------	---------------------------------------	-----

Figure 5.2	FTIR spectra of PMMA, minocycline-loaded PMMA and free minocycline	167
Figure 5.3	SEM micrographs of the control BC matrix (PMMA), and BC loaded with minocycline	167
Figure 5.4	<i>In vitro</i> release profiles of minocycline, in both LOW and HIGH concentrations	168
Figure 5.5	Histological analysis of the tissues surrounding PMMA constructs implantation in control and diabetic animals	171
Figure 5.6	Histological analysis of PMMA and mPMMA surrounding tissue, in control animals	173
Figure 5.7	Histological analysis of PMMA and mPMMA surrounding tissue, in diabetic animals	174

Chapter 2

Table 2.1	Differences between human cortical and cancellous bone	14
Table 2.2	Etiologic types and stages of glycemc disorders	41
Table 2.3	Criteria for the diagnosis of diabetes mellitus	49

Chapter 3

Table 3.1	Forward and reverse sequences of the primers used for the qPCR analysis	86
------------------	---	----

Chapter 4

Table 4.1	Forward and reverse sequences of the primers used for the qPCR analysis	124
------------------	---	-----

Chapter 5

Table 5.1	Semi-qualitative analysis of overall inflammatory reaction and inflammatory response parameters around PMMA and mPMMA samples, in both control and diabetic conditions	177
------------------	--	-----

CHAPTER 1 – AIM AND STRUCTURE OF THE THESIS

1.1 – AIM AND STRUCTURE

Of worldwide importance, diabetes mellitus represents one of most established systemic conditions with increasing epidemiological importance. It encompasses a group of metabolic disorders which are ultimately characterized by a hyperglycaemic state and consequent requirement for continuous medical care with multifactorial risk-reduction strategies (1). Diabetic hyperglycaemia is strongly associated with long-term tissue and organs failure due to severe damaged and unbalanced carbohydrate metabolism. The most well-known complications related with diabetes comprise neuropathy, nephropathy, retinopathy and osteopenia, among others (2).

In which concerns the bone tissue, uncontrolled hyperglycaemia was broadly described to affect the normal bone metabolism interfering with the natural bone renewal, as well as, increasing the risk of fractures due abnormal cellular function to produce new bone, impaired mineralization and consequent altered bone mineral density (3, 4). Despite the contradictory reports, regarding bone tissue affection in the different types of diabetic condition (5), it is established that type 1 diabetes, in particular, exerts severe effects in bone through a variety of mechanisms including impairment of osteoblastic recruitment, maturation and function to produce new bone; promoting a disorganized and defective deposition of collagen matrix; inhibiting the expression of growth factors, essential for bone mineralization to occur; among other which culminate in a weakened structure (6).

Recently, several studies reported that, tetracycline's semi-synthetic derivatives, i.e., minocycline and doxycycline, were able to modulate osteoblastic cells and

improving the bone regeneration process in a mechanism independent of the antibacterial activity (7, 8). Furthermore, these non-antibacterial properties of minocycline and doxycycline were demonstrated to exert a significant beneficial effects in pathological conditions involving abnormal immune and inflammatory response and unbalanced apoptotic behaviour (such as rheumatoid arthritis, periodontitis, rosacea, among others) (9, 10). Accordingly, these semisynthetic tetracyclines may represent promising candidates to support bone healing therapies in both cases of fractures in physiological or pathological conditions.

The increased risk of fracture among diabetic patients, lead to an increased requirement for orthopaedic implants. However, diabetes systemic abnormalities include defective host response and impaired wound healing which greatly increases the risk of infection among the patients with the disease (11).

In this context, this work aims to achieve a deeper insight on the effects of minocycline and doxycycline as osteogenic agents, promoters of bone regeneration and tissue healing, in the tissues and cells of a well-established animal model of diabetes – the streptozotocin-induced diabetic rat.

The thesis is organized into six chapters:

Chapter 1

General considerations about the aim and structural organization of the present PhD thesis.

Chapter 2

The second chapter is divided in three parts. The first part consists of an overview of bone tissue including composition, structure and metabolic activity; bone remodelling and bone healing processes. Following, in the second part, a review of diabetes mellitus is made focusing the systemic unbalances, classifications and diagnosis; with especial relevance, the effects of diabetes in bone tissue; and biomaterial implants to support bone healing in diabetic-mediated pathological conditions. In the third part, a revision of tetracycline derivatives, minocycline and doxycycline, is carried out. In addition to their role as antibiotics, their properties as modulatory agents of bone metabolism and regeneration in physiological and pathological conditions are reviewed.

Chapter 3

The third chapter describes a detailed characterization of bone marrow-derived mesenchymal stem cells, harvested from both healthy and streptozotocin-induced diabetic Wistar rats, and cultured in control and osteogenic-induced conditions. In this module, *in vitro* assays leading to the characterizations of cell proliferation, metabolic

activity, as well as the assessment of gene expression and significant signalling pathways activated within the osteogenic priming and functionality, were critically detailed.

Chapter 4

In chapter 4, the effect of doxycycline is assessed on both *in vitro* and *ex vivo* models of control and diabetic conditions. In the first part, the effect of a low dosage regimen of doxycycline was assayed in the previously described cell culture model of bone marrow-derived mesenchymal stem cells, harvested from control and diabetic-induced Wistar rats. Culture functionality was critically detailed, regarding cell proliferation, metabolic activity, osteogenic priming and activation. In a second part, an *ex vivo* experiment was conducted with new-born rats' calvaria to assess the effect of the low dosage regimen of doxycycline in the bone regeneration process, in both control and diabetic simulated conditions.

Chapter 5

In the chapter 5, a novel PMMA cement-based system for the controlled release of minocycline, aiming the development of a clinical relevant formulation for drug delivery in diabetic conditions, was characterized for solid state parameters and biocompatibility. The tissue response to the implanted minocycline-loaded constructs was detailed, in both control and diabetic animal models, by histological and histomorphometric analysis, at several time points following subcutaneous implantation.

Chapter 6

In the last chapter, a general conclusion is presented, based on the data gathered from the experimental studies presented on chapter 3, 4 and 5.

Prospective studies and future perspectives are further discussed.

CHAPTER 2 - BACKGROUND AND LITERATURE

OVERVIEW

2.1 - BONE TISSUE

The bone is a highly complex and hard form of connective tissue which may be both coped as a tissue or as organ system, making up most of the skeleton. It combines the endurance and toughness of a mineralized matrix composed essentially by proteins and hydroxyapatite crystals with a dynamic organic/inorganic matrix. As a component of the skeleton, bone tissue plays crucial functions in the human organism including protection, support, motion of the entire organism and metabolic homeostasis. Bone unique and individual properties such as a high flexibility and elasticity promote the protection of vital organs. Yet its stiffness also underwrites to the conservation of the structural support and mechanical action allowing for the precise and controlled muscular movement. The organic component ensembles a variety of bony cells which are continuously involved in metabolic modulation of pH regulation, mineral storage, homeostasis, bone remodelling and other functions, causing bone to be a biologically active and dynamic entity (12). The adult human skeleton possesses around of 213 bones.

2.1.1 - MACROSTRUCTURE

Macroscopically, bones of the skeletal system are white coloured and usually classified individually according to their shape in long, short, flat, sesamoid and irregular bones (figure 2.1a). Long bones are characterized for being longer than wider and this category includes the majority of the bones of limbs such as femurs, tibiae and humeri. They are specifically designed for rigidity, possessing some elasticity and great hardness, and attachment of muscles and ligaments. The majority of long bones present morphological similarities (figure 2.1b) as they are constituted by three common components: (1) the diaphysis (or shaft), the body of long bones being mainly made up of compact bone organized in a long tubular structure; (2) the epiphyses, the long bones' ends in which the joints with adjacent bones are established, being predominantly composed by cancellous bone; (3) the epiphyseal plate (or growth plate), a hyaline cartilage plate located in the metaphysis in the long bone's ends. Short bones are those bones that are almost as wider as longer and commonly exhibit a cuboidal shape. These bones include smaller bones and they are found only in the ankle and wrist (e.g. tarsus and carpus). Flat bones are usually associated with protection functions due to their morphology thinner and flatted which provides broad section for protection or muscular attachment (e.g. ribs, sternum and cranial bones). Sesamoid bones are usually found in locations where tendons intersect the ends of long bones, being responsible for protection of these tendons from an excessive mechanical load (e.g. patella and knee cap). Just like the vertebrae of the spine or the facial bones, the irregular bones are characterized by their peculiar morphology, which cannot be included in none of previous classifications (12).

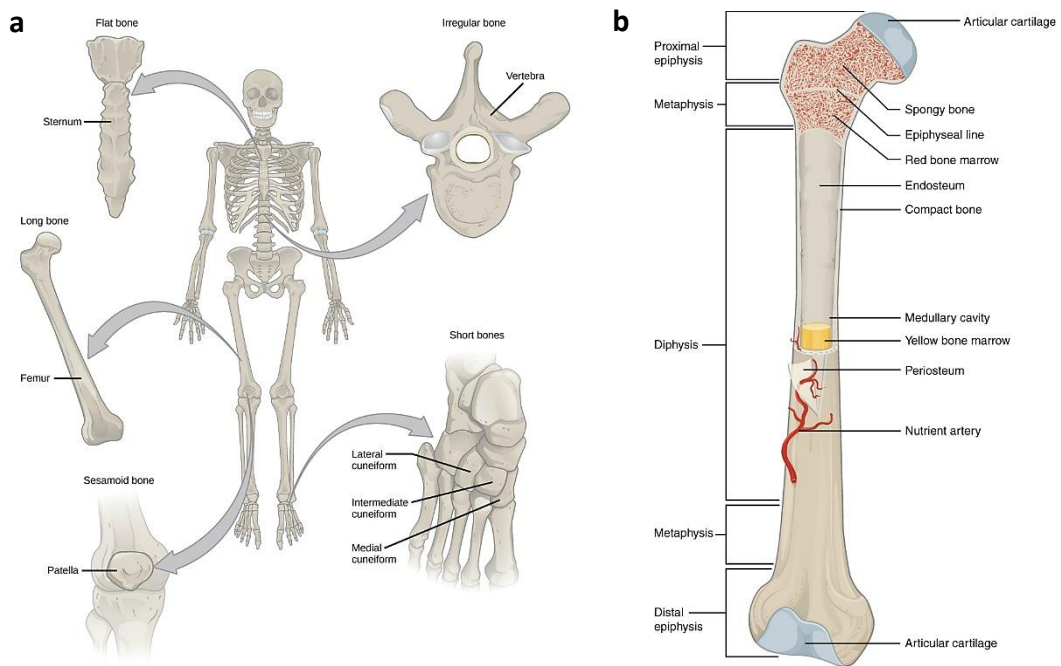


Figure 2.1 - (a) Different types of bone morphology: long, short, flat, sesamoid and irregular; (b) Adult long bone structure, adapted (13).

Despite these different morphologies, all bones are macrostructurally identical in that densely packed or compact bone – that is more external and the principal responsible for bone strength, whilst the inner bone tissue is commonly composed by a tridimensional structure of trabecular bone with metabolic and homeostasis functions. Although both compact and trabecular bone are made up of the same kind of extracellular matrix (ECM) and cell types, they differ in which regards to their structure and functions (14). Thereby, compact bone is mostly associated with biomechanical and

protective functions, whereas the majority of metabolic functions are due to the trabecular bone (table 2.1), such that it is more responsive to disturbances in metabolic homeostasis (12).

Table 2.1 - Differences between human cortical and cancellous bone. Adapted from (15).

Attributes	Cortical	Trabecular
Skeletal mass	80%	20%
Bone surface	33%	67%
Surface/volume ratio (mm⁻¹)	2.5	20
Soft tissue	10%	65%
Adult tissue	Secondary osteon (Haversian systems) Interstitial lamellae Circumferential lamellae	Curved plates, rods Bone structural units Interstitial lamellae
Porosity	Low	High
Marrow	Fat	Hematopoietic
Main soft tissue	Viscera	Marrow
Developmental	Intramembranous ossification	Endochondral ossification
Turnover	Slow	Rapid
Function	Mainly biomechanical, also supportive and protective	Mainly mineral haemostasis, also supportive

Compact bone, also known as cortical or dense bone, is found on the outer layer of all individual bones surrounding the trabecular structure and exhibit an ivory-like compact shape. It represents approximately 80% of the total bone mass and it is mainly composed of bony mineral and ECM providing the adequate strength to perform its functions. Structurally, cortical bone is made up of a collection of cylindrical units named Harvesian systems, or osteons, which run parallel to the bone axis. The Harvesian system represents the cortical bone fundamental unit and it combines a central canal – through which blood vessels, lymphatic nodes, connective tissue and poorly myelinated fibers pass – with its surrounding concentric bony tissue lamellae and respective osteocytes (14). The lamellae constitute a more external surface of the cortical bone and they are interspersed by small voids known as lacunae, which are interconnected by smaller channels – canaliculi (16). The osteocytes are found within the lacunae and they are interconnected with one another and with the osteoblasts on the surface of the bone by extending cytoplasmatic processes into the canaliculi. This communication with external osteoblasts allows the process of osteocytic osteolysis, which comprises the transference of Ca^{2+} from the interior of the bone to the surface (17). Additionally to cell-to-cell interaction, canaliculi enable the nutritional support and oxygenation of the whole cellular constituents and also permit the removal of waste products resultant from metabolic activities. The gaps between the osteons are filled with a tissue similar to lamellar bone although with a less organized pattern. The interstitial lamellae separate each Harvesian system from its neighbouring structures by forming a strongly basophilic cement line constituted essentially by inorganic matrix content (16). The superficial layer of compact bone is mainly constituted by osteoblastic and osteoclastic

precursor cells which are continuously renewing the cortical bone by producing new osteoid (figure 2.2) (18, 19).

Trabecular bone, synonymous to cancellous or medullar bone, constitutes about 20% of the remaining total bone mass and it is located in the inner layer of individual bones. Structurally, cancellous bone presents a honeycombed shape and is considerably less dense and resistant than compact bone, being committed essentially to metabolic and mineral homeostatic functions. It has a higher surface area reaching about 67% of the total and its structure consists of an irregular network of calcified spicules extended from the cortex to the inner canal – trabeculae – made up of osteon fragments. The trabecular structure is classified as being rod-like or plate-like and the portion of each type depends on the magnitude and distribution of loading. Its thickness commonly ranges from 50 to 400 μm and it is formed by bone lamellae. Furthermore, trabeculae structural organization is not random, rather the structures run according to the mechanical stress guidance and they are continuously able to adapt to mechanical tension solicitations (20). Similarly to the cortical bone, the most external layer is mostly coated by osteoblasts and osteoclasts responsible for constant renewal of cancellous bone. The cavities between trabeculae are filled with hematopoietic marrow, in which the majority of metabolic supportive functions of bone occur (16).

2.1.2 - MICROSTRUCTURE

Independently from being cortical or cancellous, the microscopical structure of bone can be categorized in two major forms: woven bone or lamellar bone. Woven bone, also designated as primary bone, is broadly found during the embryonic stages, as well as in newborns and it is later resorbed and replaced by lamellar bone (21). Primary bone may also be found in locations where fast bone formation takes place, like in growth plates and during processes of bone healing of fractures, closure of cranial sutures or in pathological conditions, such as in Paget's disease. Comparing to lamellar bone tissue, woven possesses a higher metabolic rate which substantiates an enhanced turnover during the remodelling phase. Woven bone is also characterized by an anisotropic distribution of cells and collagen fibers, which explains its diffused and irregular display, as well as its biomechanical fragility (21). After woven bone is laid down, it can undergo remodelling processes to become lamellar. Lamellar bone, or secondary bone (figure 2.2), commonly appears firstly during the third foetal trimester and it is produced much more slowly, being characterized by a highly and ordered arrangement whereas the cells are broadly uniform in size, shape and orientation, supporting a more resilient biomechanical performance than woven bone (21).

2.1.2.1 - EXTRACELLULAR MATRIX

Regarding its composition, the mature bone tissue may be considered a composite material constituted by a tough organic matrix (approximately 35%), which is greatly

strengthened by inorganic minerals (60 to 70% bone weight) and cells. The remainder ECM is filled with a homogenous gelatinous medium, named ground substance, that is composed of extracellular fluids and proteoglycans (e.g., chondroitin sulfate and hyaluronic acid), which are thought to assist on the regulation of calcium salts deposition. The proportions of these components vary with age, location and metabolic status (20).

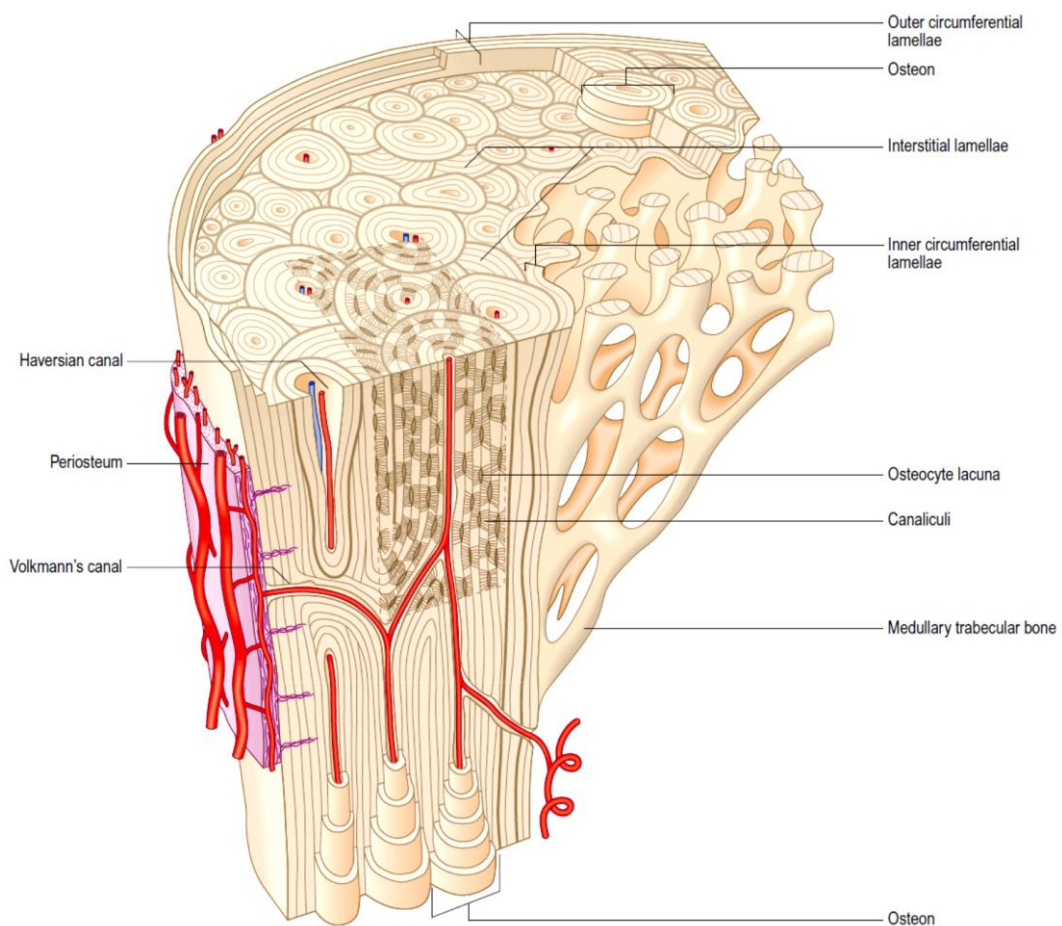


Figure 2.2 - Microstructural organization of mature lamellar bone comprising areas of compact and cancellous bone (20).

2.1.2.2 - BONE COLLAGEN

The overall extracellular structure of the bone acts as an interconnected network for cells, in close interaction. The organic part of this matrix is 90 to 95 per cent constituted by collagen fibers, which closely resemble those of many other connective tissues and it is predominately composed by collagen type I fibers, combined with a very small amount of collagen type V, which is thought to regulate fibrillogenesis (20). Nevertheless, the molecular structure of collagen is unique in which regards its organization, which displays internal covalent cross-linkages, and larger transverse spacing, within its fibrils (figure 2.3). The cross-links make it stronger and chemically more inert while the internal gaps enable deposition of minerals. The adequate and ordered deposition of collagen in sufficient amounts is required to accomplish the formation of optimal bone mass and mineral density during the skeletal development, since bone mineral crystals deposition is aligned with the long axis parallel to the collagen axis. As so, collagen contributes largely to the mechanical strength of bone as well as to the tensile strength, compressive resistance and elasticity, which enhances the resistance to fractures during mechanical loading (20).

Collagen is produced by osteoblastic cells which synthesize tropocollagen, which is lately polymerized in the ECM and gradually increases its cross-links with maturation. Collagen fibres from the periosteum, also designated as extrinsic fibres, are incorporated in cortical bone and anchor the fibrocellular layer, at their surface. Terminal collagen fibres of tendons and ligaments are incorporated deep into the matrix of cortical bone. The fibres may be interrupted by new osteons during cortical bone

modelling and turnover or remodelling, and remain as islands of interstitial lamellae or trabeculae (20).

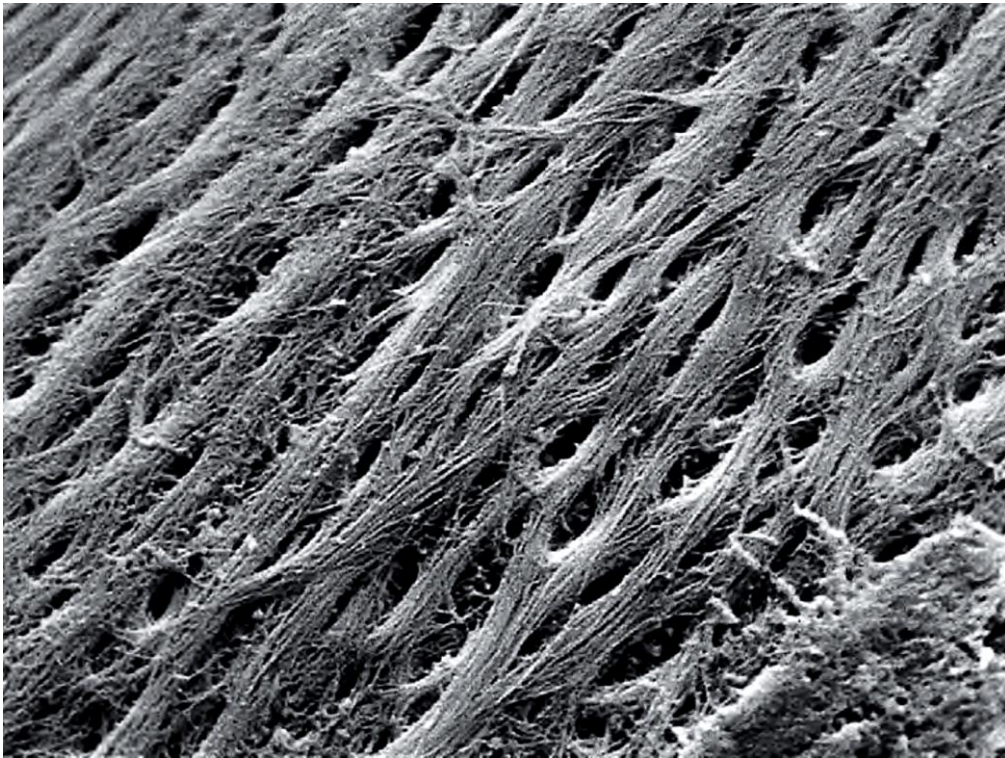


Figure 2.3 - Scanning electron microscopy image of collagen fibers of human cancellous bone (20).

2.1.2.3 - NON-COLLAGENOUS ORGANIC COMPONENTS

Several non-collagenous proteins can also be found among the extracellular organic component attached to collagen fibers or surrounding bone crystals. They are

essentially secreted by osteocytes and osteoblastic cells and they include among the several, osteopontin (or bone sialoprotein-1, BSP-1) (OPN), bone sialoprotein-2 (BSP-2), osteocalcin (OC) and osteonectin. Despite their exact biological role is far from being completely fulfilled these components play important role in bone metabolic functions as well as in osteoblastic and osteoclastic cell function and interaction (16).

Bone matrix also contains proteoglycans (e.g. decorin and biglycan, which seem to modulate cell activity, especially the collagen fibrillogenesis process), glycoproteins (e.g., fibronectin and vitronectin, with a distinctive role in cell signalling), many growth factors (e.g. transforming growth factor β (TGF- β), bone morphogenic protein (BMP), insulin-like growth factor (IGF-9 among other), proteases and proteases inhibitors (16, 20).

2.1.3 - BONE MINERALS

The inorganic constituents of the extracellular matrix play an important role, conferring strength, rigidity and allowing ion storing. This component is the main reason why the bone may be recorded on radiographs since it needs to be at least 50% mineralized to be visible on radiographs produced by a standard X-ray unit. With the mineral removal with calcium chelators, such as ethylene diamine tetra-acetic acid (EDTA), the bone keeps its shape but becomes highly flexible (20).

The crystalline salts deposited in the organic matrix are constituted essentially by calcium and phosphate. The substance which largely makes up these crystals is commonly referred as hydroxyapatite, although with an important carbonate content and a lower Ca/P ratio than the pure hydroxyapatite, $\text{Ca}_{10}(\text{PO}_4)_6(\text{OH})_2$. Bone crystals are thin plates or leaf-like structures that possess a broad surface area despite the small size. These structures range in size up to 150 nm long, per 80 nm wide, per 5 nm thick; however most of them are broadly half this size (20).

Ionic substituents, such as magnesium, strontium, carbonate, citrate, and fluoride are broadly present among the bone salts. It is thought they are conjugated with hydroxyapatite rather than organized separately. Additionally, these ions seem to modulate the biological response in the local microenvironment (16).

2.1.4 - BONE CELLS

Bone tissue exhibits four main types of cells among its organic matrix including osteoclasts, osteoblasts, osteocytes and bone lining cells. Bony cells may be generally classified attending to their functional activity into bone forming and bone resorbing cells, or according to its differentiation or maturation state.

The cell-to-cell and cell-to-matrix interactions are critical in order to maintain bone mass balanced and bone tissue homeostasis. For instance, osteoblasts are known to bind bone matrix through integrins which recognize RGD among other bone-specific protein sequences, such as osteopontin, collagen and bone sialoproteins. Moreover, osteoclasts interaction with bone matrix and osteoblastic-secreted factors are essential for the osteoclastic function and bone renewal to occur correctly (18).

2.1.4.1 - OSTEOCLASTS

Osteoclasts are the only cells known to be able of absorb or breakdown bone tissue. These large (ranging 40 μm and higher) and multi-nucleated cells (normally 3 to 20 nuclei) are derived from circulating hematopoietic stem cells that differentiate along the monocyte/macrophage lineage (see figure 2.4a). Since their differentiation pathway is common to macrophages and dendritic cells, osteoclastic differentiation depends directly on precursor cell exposition to several specific factors such as the macrophage colony-stimulating factor (M-CSF) and the receptor activator of nuclear factor kappa- β ligand (RANKL), both secreted by osteoblastic cells (22). Both cytokines are crucial not

only for differentiation but are also required for proliferation, survival and differentiation of osteoclastic precursor cells (20). The M-CSF binds to its receptors in osteoclastic precursors, stimulating their proliferation and disrupting apoptosis, while RANKL binds to its ligand (RANK), triggering osteoclastogenesis (23, 24). Along with these two factors, osteoprotegerin (OPG) was found to bind RANK preventing RANK-to-RANKL interaction, leading to inhibition of osteoclastogenesis (24). This three-way system works as a key regulator of bone resorption.

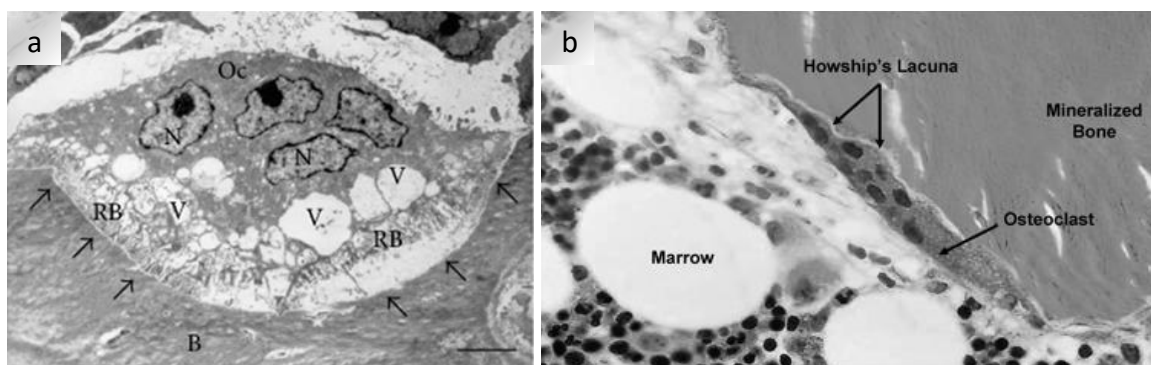


Figure 2.4 - (a) Rat multinucleated osteoclast (Oc) revealing some nucleus (N) and vacuoles (V) and the organization of a ruffle border (RB) next to bone surface (B) undergoing resorption, adapted from (18); (b) Histological analysis of human bone revealing multinucleated osteoclasts forming Howship's lacunae (25).

Osteoclastic cells are commonly found in areas undergoing bone resorption (figure 2.4b) and reveal high mobility. These cells mediate the resorption process via the release

of powerful lysosomal enzymes and acids, which digest protein and mineral components of the bone matrix, respectively. The key family of proteinases involved in this degradation process of bony tissue are the cathepsins and matrix metalloproteinases (26).

2.1.4.2 - OSTEOLASTS

Osteoblasts are derived from undifferentiated stem cells of mesenchymal origin, which can be found in bone marrow, endosteum, and periosteum, among other locations (see figure 2.5). These osteoblastic progenitor cells, also referred as “preosteoblasts”, can migrate from neighbouring tissues or through the vascular system to the target area. Commonly, osteoblasts comprise 4 to 6% of the total resident bone cells and are located in bone outer layers and in bone cavities undergoing bone remodelling events (i.e. trabeculae). These are the unique cells known to be able of promote new bone formation by deposition of extracellular matrix rich in collagenous and non-collagenous proteins, being further responsible for the subsequent mineralization process. Morphologically, mature and active osteoblasts are mononucleated cells with plump cuboidal-like shape, with a prominent Golgi apparatus and endoplasmic reticula, both related with their high secretory activity (18, 27). With the decreasing of the metabolic level, the osteoblasts shape becomes progressively flattened out with the decreasing of the metabolic index.

The synthesis of new bone tissue takes place in two main steps. In the first step, osteoblastic cells secrete the most of bone remodelling modulators and bone matrix

molecules such as type 1 collagen, non-collagenous proteins (such as osteonectin, bone sialoprotein 2, osteocalcin and osteopontin), proteoglycans (including decorin and biglycan) which promotes the matrix formation (16). The second step, focuses on the matrix mineralization and takes place into two phases namely, the vesicular (i) and the fibrillar phase (ii). In vesicular phase, numerous matrix vesicles (ranging from 30 to 200 nm) are released into the newly formed bone matrix binding to the previously secreted components (28). These vesicles were described to contain a phosphatase, active at neutral pH, which has strong specificity and promote further hydrolyse of a variety of nucleotide and metabolite. Additionally, matrix vesicles were found to up ^{45}Ca , even in the presence of low levels of Ca (29). Following, the fibrillary phase occurs with the rupture of the vesicles leading to the spreading of hydroxyapatite crystals on the surrounding matrix as the vesicles' content contact with phosphate-containing substrates in the presence of ATP (29, 30).

Osteoblasts cytoplasmic membrane is rich in alkaline phosphatase (ALP), an important enzyme for ECM mineralization. The increasing of ALP expression is intimately bounded with a shift to a more differentiated state of the osteoblastic cells and generally determines the occurrence of the mineralization process, at least within *in vitro* systems (31). Furthermore, ALP is responsible for the degradation of matrix vesicles leading to the release of phosphate and calcium ions, allowing the subsequent formation of hydroxyapatite crystals (18).

Osteocalcin and osteonectin (ON) are both products of osteoblasts which play crucial roles in new bone mineralization. The first is a 6-kDa protein, synthesized at the locations undergoing bone remodelling and binds to hydroxyapatite, thus suggesting a

participation of OC in nucleation of the bone mineralization. The 35-kDa protein osteonectin also binds to hydroxyapatite and to collagen fibres, facilitating extracellular mineralization (17).

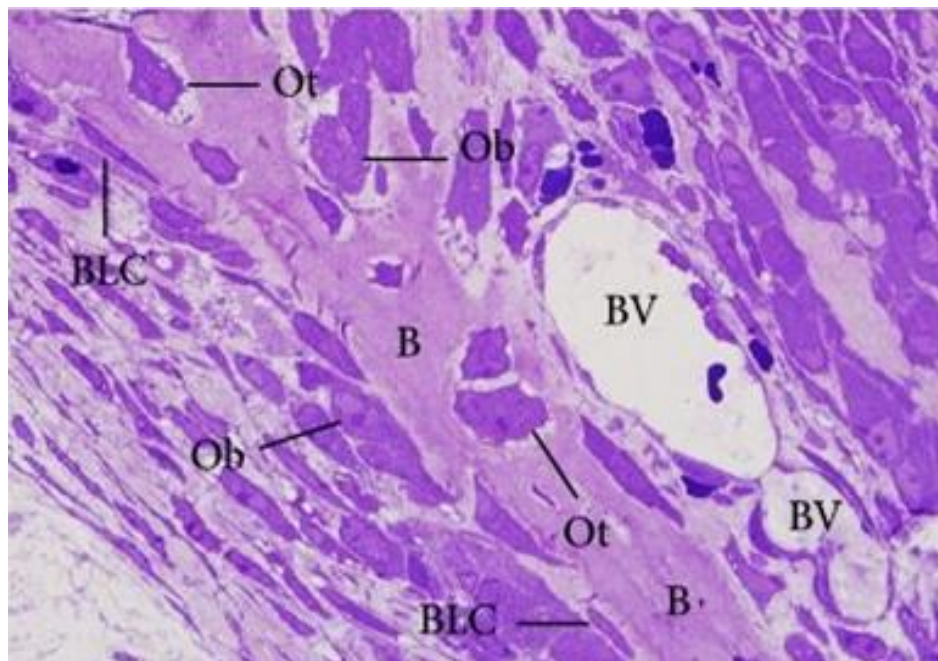


Figure 2.5 - Histological analysis of rat bone section stained with toluidine blue. The image reveals osteoblasts (Ob) and bone lining cells (BLC) present on bone surfaces and the osteocytes (Ot) trapped into the bone matrix along the bony trabecula (B). BV refers to blood vessels (18).

Osteoblastic activity continues in living bone through life time span, allowing a continuous renewal of bony tissue. Once the remodelling cycle is finished, osteoblasts cease the production of bone matrix and become committed to one of three pathways:

(1) become embedded by new mineralized bone matrix and differentiate in osteocytes, (2) shift their shape turning into flattened lining cells covering the bone surface, or (3) become relatively inactive or undergo apoptosis (18, 32).

2.1.4.3 - OSTEOCYTES

Osteocytes comprise around 90 to 95% of bone cells in the adult skeleton. When osteoblasts become entrapped in the newly formed bone matrix (figure 2.5), a subpopulation differentiate into osteocytes which are more mature cells and mainly responsible for bone matrix maintenance (33). This differentiation process comprises also conspicuous morphological and ultrastructural changes including osteoblast size reduction, decreasing number of organelles such as rough endoplasmic reticulum and Golgi apparatus, and decreasing nucleus-to-cytoplasm ratio resulting in a diminished protein synthesis (34). Despite that fully-matured osteocytes are relatively inactive when compared to active osteoblasts downregulating the expression of osteoblastic markers such as OC, BSP-2, collagen type 1 and ALP, they still can produce several factors, essential for bone matrix support, including dentine matrix protein 1 and sclerostin (18, 35). Osteocytes may be found in bone lacunae of 1 to 2 μm wide, surrounded by collagen fibrils, which support cytoplasmic process responsible for the intercellular communication through canaliculi channels and gap junctions (20). Additionally to cell-mediated exchanges of minerals, this network also act as mechanosensor, as it has the capacity to detect mechanical deformation within bone, thus modulating processes such as bone formation or bone resorption (36). The specific

mechanical stimuli to which bone cells respond *in vivo* may be connected with strain changes itself, as well as strain-generated changes to their fluid environment, which consequently affects the release of signalling molecules and growth factors, that seem to regulate cell proliferation and differentiation (37).

2.1.4.4 - BONE LINING CELLS

Bone lining cells derive from osteoblastic cells which cease the production of new bone matrix, becoming partially inactive. They exhibit an elongated shape (see figure 2.5 and 2.6) with a flat nuclei and usually are located over bone surfaces where neither bone resorption nor bone formation occur (38). Due to their abridged metabolic activity, they possess fewer organelles than osteoblasts.

Bone lining cells are compactly associated and connect each other via gap junctions and communicate with internal bone cells, such as osteocytes, by cytoplasmic extensions or thigh junctions made through surface canaliculi (39). Since the activation of bone remodelling process takes place at inactive bone surfaces, bone lining cells are thought to interfere in bone metabolism in two possible ways: (1) building a microenvironment suitable for bone resorption mediated by osteoclasts, as well as by producing OPG and the receptor activator of nuclear factor kappa- β ligand; and (2) regulating new bone matrix deposition and mineralization, enrolling osteoblast-like functions (39).

Also, bone lining cells showed to play an important role in the maintenance of the bone fluids and the fluxes of ions between the bone fluid and interstitial fluid compartments, interfering deeply into mineral homeostasis (20).

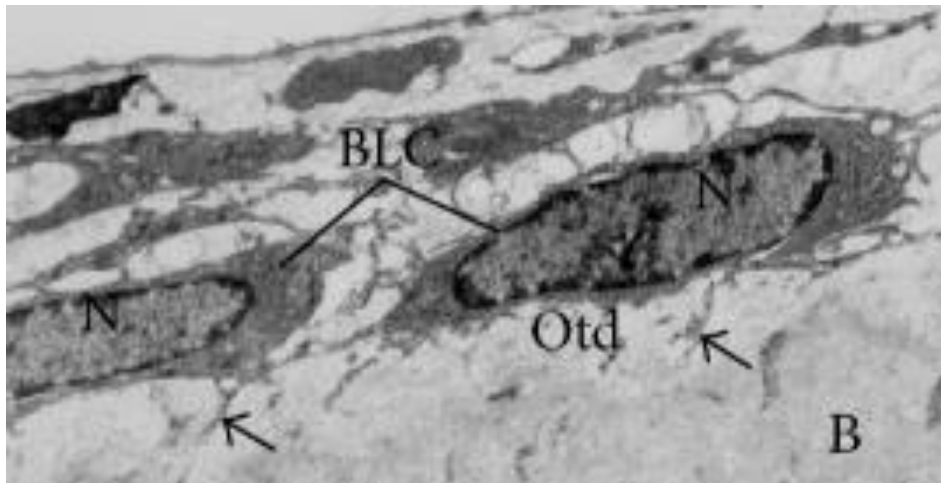


Figure 2.6 - Bone lining cells (BLC) exhibiting flat shape with scarce cytoplasm, located on the osteoid (Otd) surface. B refers to calcified bone surface and N to the nucleus. Adapted from (18).

2.1.5 - BONE REMODELLING

Bone remodelling is a natural process whereby bone tissue renews itself throughout lifespan. Due to its cellular components and functions, bone has been described as a highly dynamic and metabolically active specialized connective tissue. These cellular components are the main responsible for this remarkable ability and highly regulated process of bone renewal in which older bone is continually being absorbed by osteoclastic cells while new bone is being continually deposited by osteoblastic cells. Thus, the bone renewal process is dependent upon the stringent interaction between osteoclasts and osteoblasts, which are further modulated by specific bio-molecular factors. Generally, with the exception of growing bones, each cycle of bone remodelling is balanced such that the bone resorption rate and the new bone deposition rate are equal to each other, preserving the loss of bone mass. Usually, in the adult bone, this cycle lasts about 90 to 130 days (40).

Bone remodelling process aims to preserve bone strength and mineral homeostasis, preventing skeleton weakening derived from the accumulation of fatigue and microdamage. Once under the specific environmental stimulus, bone remodelling occurs following four phases (see figure 2.7): osteoclast activation, old bone resorption, reversal phase, and new bone formation (41).

In the earliest phase, several factors induce osteoblasts to produce molecules that will give rise to osteoclastic precursor cells differentiation and osteoclast activation. Among the factors involved in this activation stage vitamin D and parathyroid hormone (PTH) play a critical role. Vitamin D is a known enhancer of calcium absorption in the intestinal tract and it is also an important agent, modulator of both bone resorption and

deposition. After being converted to 1,25-dihydroxycholecalciferol in liver and kidneys with PTH interference, vitamin D is able to modulate bone remodelling process. Accordingly, high doses of functional vitamin D increase bone resorption rate, nevertheless the reduction of vitamin D or its absence, interferes with PTH causing a sharp decrease of bone absorption and increased bone calcification (17). The cellular mechanisms behind these effects carried out by functional vitamin D are not completely cleared, although it is thought to be related with the ability of 1,25-dihydroxycholecalciferol to increase calcium ions transport through cell membranes.

The secretion of PTH is dependent on both ionized plasma calcium and vitamin D concentrations. The diminished blood calcium levels lead to an increased PTH production. This augmentation of PTH modulates osteoblasts and stromal cells inducing them to produce other important molecules for osteoclast activation: the macrophage colony-stimulating factor and the receptor activator of nuclear factor kappa- β ligand (17). As mentioned before, the M-CSF, also known as CSF-1, is an important factor for osteoclast development. Additionally, it was showed that cell-to-cell contacts between osteoblastic and osteoclastic cells were crucial for M-CSF signalling and osteoclast activation (18). With the increasing of PTH, osteoblasts initiate the expression of surface receptors RANKL, which are specific receptors for RANK, present in the membrane of osteoclast progenitor cells. Once this link occurs, osteoclastics progenitor cells are stimulated to differentiate in mature osteoclasts. RANKL together with M-CSF are able to differentiate osteoclasts and activate them for bone resorption, begging another bone remodelling cycle.

Once osteoclasts are activated, a resorption phase of limited duration (second phase) begins, in which osteoclasts give rise to bone resorption, following a two-step mechanism. Firstly, osteoclasts bind to bone matrix *via* integrin receptors and become polarized. Accordingly, four types of osteoclastic membrane domains can be observed: upon the contact with the bone matrix, the fibrillary actin cytoskeleton organizes into an actin ring promoting the formation of the sealing zone (i) - the bone resorption cavity. Then, osteoclast continues to rearrange its cell membrane forming a ruffled border (ii) that contacts with bone surface. The remaining domains of osteoclasts membrane are basolateral (iii) and functional secretory domain (iv) which are not in contact with the bone matrix (42, 43). Posteriorly to the establishment of ruffle border structure, two types of substances are produced and excreted to the microenvironment: proteases and acids. The acids secretion is mediated through an H⁺ pump at the ruffle border and aims to acidify the resorption lacuna and to enable dissolution of hydroxyapatite crystals (17, 42). The proteases digest the majority of bone matrix proteins by hydrolysis. Another important hormone playing an important role in bone remodelling is calcitonin. It is produced by the thyroid gland in response to a certain rising of calcium level and its role include the inhibition of osteoclastic activity by inducing loss of ruffle borders and cells' dislocation from the underlying bone (17).

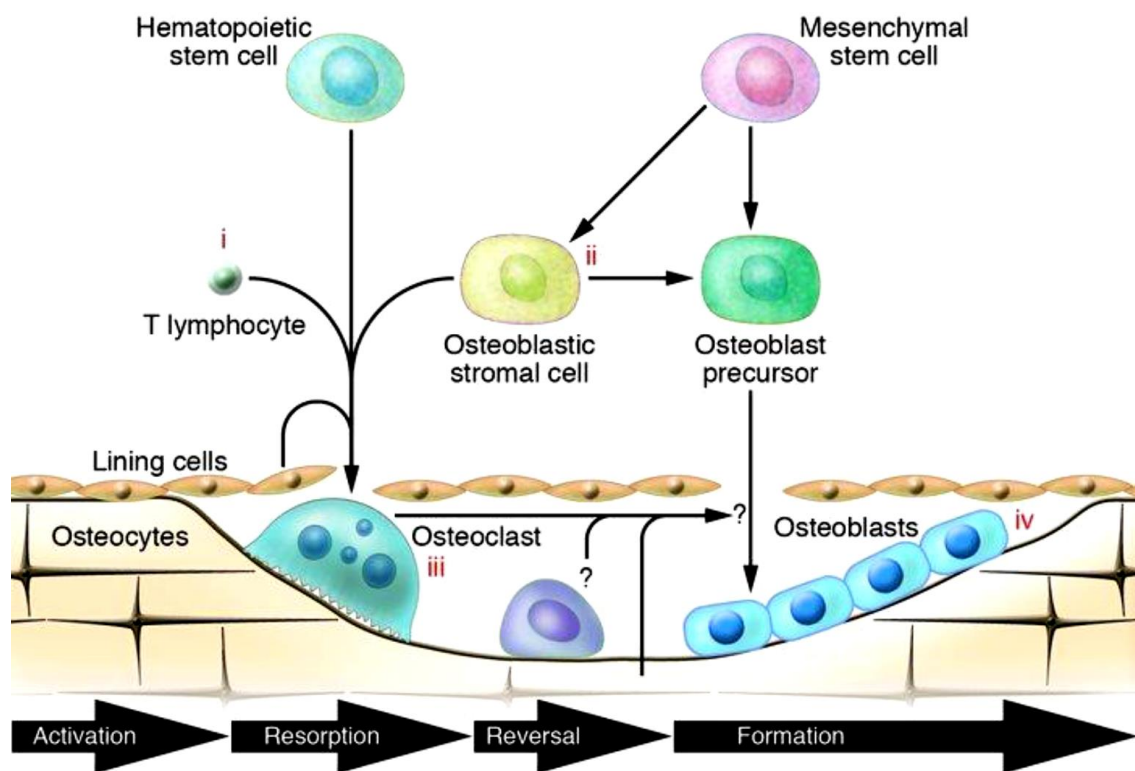


Figure 2.7 - Schematic representation of the four stages of bone remodelling cycle

(41).

After the end of bone resorption, a reversal phase (third phase), representing the transition from bone resorption to bone formation, occurs. In this phase, several markers produced by osteoclasts and preosteoblasts are thought to induce osteoblastic maturation and activation. Then, osteoclasts leave the area undergoing remodelling and resorption cavities are filled with functional osteoblasts. The formation of new bone begins (fourth phase), with the synthesis of new collagenous matrix by osteoblasts, followed by the matrix mineralization (19). Once the new bone formation is completed, osteoblasts embedded in new matrix become osteocytes, and remaining functional

osteoblastic cells become flat lining cells or undergo apoptosis. Several matrix-derived markers were reported to be involved in bone turnover and homeostasis. Thus, osteoclast formation and activation is broadly regulated not only by RANKL and M-CSF but also by OPG, 1,25-dihydroxyvitamin D3, calcitonin and others (19). Factors such as growth hormone (GH) thyroxine, estrogens, androgens, glucocorticoids, as well as mechanical stress, have also influence in bone metabolism. These factors are particularly significant as they exert their effects on the bone by producing local growth factors. Further, bone metabolism is also directly mediated by several cytokines and growth factors, which are produced by bone cells, where other cells in the microenvironment act in an autocrine or paracrine way to regulate the proliferation and differentiation of bone cell precursors (44).

2.1.6 - BONE HEALING

Bone tissue is characterized by an adequate capacity to regenerate itself upon the establishment of a lesion or small defects. This healing process aims to generate new bone tissue to stabilize the damaged bone parts with minimal alterations of bone anatomy and function. Ordinarily, bone healing occurs following four main stages (see Figure 2.8). Primarily, after an injury such as a fracture, the damaged bone zone undergoes an inflammatory phase (a) in which the necrotic tissue is cleaned; following, a repair phase (b) is initiated with the formation of a cartilage tissue – soft callus – replacing the lost bone. Simultaneously, osteoclasts continue the resorption of remaining bone debris and new blood vessel formation occurs. Also during this stage, new collagen fibers are produced by fibroblasts leading to the formation of a denser fibrous net, which will consolidate new bone tissue; in a third phase, the newly formed cartilage is replaced by trabecular bone (c) in a process similar to endochondral ossification; finally, fracture healing is completed by a remodelling phase (d) that may last for more than a year and in which the morphology is mended to ensure a perfect bone recover (45).

This ability, however, is limited since it may prevent only low magnitude fractures or small defects. When bone defects or fractures exceed a critical size, additional therapeutic solutions are required in order to attain fully structural repair and normal functionality (46). Also, circumstances that impair the physiological tissue healing, such as local infections, may decrease the correct healing capability of the damaged bone. Several pathological conditions encompassing diabetes mellitus, osteoarthritis, osteopenia, osteoporosis, among other, are known to decrease cellular function and to

impair the formation of the bone mineralized matrix, leading to severe bone weakening and bone remodelling unbalancing (47).

These situations represent major complications in therapeutic strategies for bone tissue healing and require alternative therapeutic solutions.

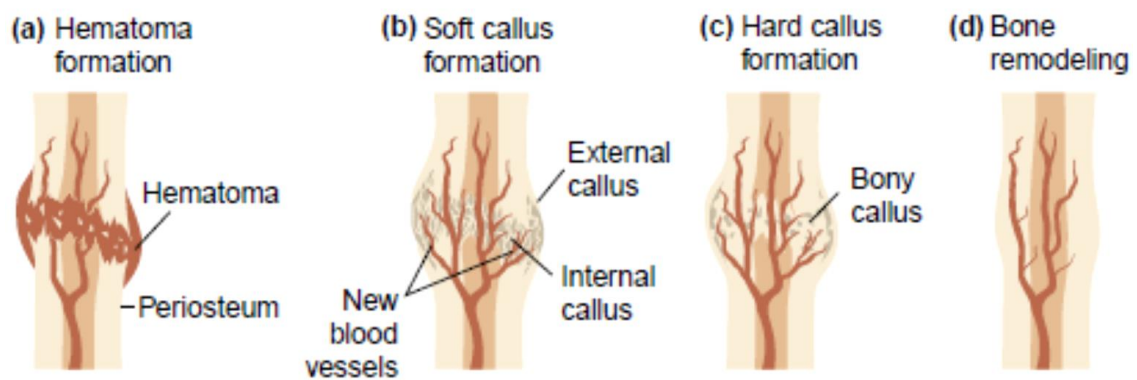


Figure 2.8 - Schematic representation of the four stages of bone fracture repair (45).

2.2 - DIABETES MELLITUS

Diabetes mellitus (DM) is not a single pathological entity but rather a group of metabolic disorders which are globally characterized by a chronic hyperglycaemia, as well as by impaired carbohydrate, fat and protein metabolism (48). These metabolic modifications arising from a persistent hyperglycaemic state seem to be caused by abnormal insulin production or decreased sensitive of the tissues to insulin, or most commonly, both (48). Accordingly, it may be difficult to identify which of mechanisms, if either alone, is the major cause of hyperglycaemia (49).

The chronic hyperglycaemia or the lack of control of glucose concentration in the organism, together with the protracted depleted action of insulin on its target organs, is associated with long-term damage and consequent dysfunction, or even failure, of various organs, especially the eyes, kidneys, blood vessels and nerves (2). The most well-known factors behind DM development include the genetic factors, pathologic triggering (i.e. viruses) and environmental factors, including increased sedentary life styles and poor eating habits (1, 50).

Despite being a common metabolic disorder, DM triggering and developmental processes are not completely understood as they apparently range from immuno-mediated events of autoimmune destruction of insulin-producer cells, to organ-specific dysfunctional uptake of functional insulin or abnormal resistance to insulin action (48, 51). Following the establishment of the hyperglycaemic state, a few physiological changes occur leading to the emergence of several clinical symptoms, which are considered typical of the diabetic condition. The common symptoms associated to

diabetic patients include polyuria, polydipsia, weight loss, and blurred vision. In several cases, susceptibility to certain infections and delayed growth may also keep up with chronic hyperglycaemia (51). Acute, life-threatening consequences of uncontrolled diabetes are hyperglycaemia associated with ketoacidosis or the nonketotic hyperosmolar syndrome, which may progress to coma and, if not treated, death (51).

Long-term exposure to hyperglycaemia and non-attenuated insulin production and uptake impairment result in severe damage of several organs leading to retinopathy, nephropathy, peripheral and autonomic neuropathy, which may further induce gastrointestinal, genitourinary, and cardiovascular symptoms. Diabetic patients also tend to develop hypertension, and abnormalities of lipoprotein metabolism (49).

2.2.1 - DIABETES CLASSIFICATION

Typically, diabetes mellitus is classified into two broad categories: type 1 diabetes mellitus (T1D) and type 2 diabetes mellitus (T2D). Although, more recently literature describing glucose metabolic disorders uses a more complex classification considering four main groups: type 1 diabetes; type 2 diabetes; other forms of diabetes mellitus; and gestational diabetes mellitus (GDM) (1). Similarly to other autoimmune disorders, T1D involves chronic inflammatory infiltration and massive destruction of insulin-producing β -cells of the pancreatic islets of Langerhans, leading consequently to the absolute deficiency of insulin secretion (52). In contrast, T2D is characterized by the combination of abnormal resistance to insulin uptake and action, which promotes an inadequate compensatory insulin secretion. In this category, a degree of hyperglycaemia sufficient to cause pathologic and functional changes in various target tissues, but without clinical symptoms, may prevail for an extended period of time before clinical detection (51). Other variants of diabetes mellitus were found to arise from genetic abnormalities or specific pathological or clinical conditions, in which insulin action is negatively affected (see table 2.2).

2.2.1.1 - TYPE 1 DIABETES

Type 1 diabetes mellitus accounts for around 5-10% of diabetes-affected individuals and it is also known as insulin-dependent diabetes mellitus, or juvenile-onset diabetes, as its onset usually occurs during childhood (53).

persistent anti-islet autoantibodies and 60% risk for diabetes onset at age 15 (56). A less prominent association was found between the HLA class I genes, such as HLA-A and HLA-B, and T1D (55). Despite the autoimmunity seems to be the predominant mechanism of T1D, associated primary causes are not yet fully established. In fact, even before T1D clinical onset, autoantibodies reacting against β -cells are spotted suggesting a sequence of inciting events preceding hyperglycaemia.

The most studied pathological agents contributing to T1D incidence comprises viral, bacterial and other infections. Enteroviruses, specifically coxsachievirus, were earlier described by Yoon et al. to be involved in β -cells infection, precipitating insulin-dependent diabetic state (57). Further studies reported the presence of enteroviruses in recent onset patients (58). Among the discoveries of the intestinal bacterial composition, few information was achieved regarding T1D. The presence of *Mycobacterium avium subspecies paratuberculosis* (MAP) were described to be a major risk factor. Accordingly, clinical significant humoral responses to MAP antigens and whole cell lysates were detected in patients with juvenile-onset diabetes (59).

Regarding the immune events taking place before the emergence of clinical symptoms, the most critical encompass the production of autoantibodies following the activation of self-reactive lymphocytes. The core-targeted antigens by the autoantibodies comprise the insulinoma-associated antigen-2 (I-A2 and ICA512), insulin (micro IAA), glutamic acid decarboxylase 65 (GAD65) and zinc transporter 8 (ZnT8) (53, 60). Consequently, the insulin-producing β -cells are persistently targeted and destroyed in a continuous autoimmune process, which may take several years before the clinical symptoms arise. Following the pronounced reduction of insulin production, the clinical

symptoms emerge. While some patients may firstly develop ketoacidosis (particularly children and adolescents), others experience modest fasting hyperglycaemia which may rapidly evolve to severe hyperglycaemia accompanied (or not) by ketoacidosis associated with infection or other stresses (61). Yet, few other patients may retain a residual number of functional β -cells sufficient to prevent ketoacidosis for several years. Notwithstanding, some forms of T1D have no known etiology since these patients suffer a permanent insulinopenia and are likely to develop ketoacidosis, without evidence of autoimmunity (51).

2.2.1.2 - TYPE 2 DIABETES

Type 2 diabetes mellitus is also referred as non-insulin-dependent diabetes mellitus, or adult-onset diabetes, and represents around 90% of those patients affected by diabetes (62).

T2D develops mainly due to genetic factors associated with sedentary life style which, together, lead to deficient insulin production, impaired insulin action or both, simultaneously. The specific etiology associated to this form of DM is not completely understood. However, in contrast with T1D, autoimmune destruction of pancreatic β -cells does not seem to occur in these patients (51). Instead, in the majority of cases, insulin metabolism disorders are the result of prone lifestyle habits, lack of practice of physical exercise, and consequent obesity, which itself causes some degree of insulin resistance (51, 63). Additionally, T2D is rarely associated with ketoacidosis despite that this complication may occur temporarily, caused by associated infections (51).

Due to the gradual development of hyperglycaemia, which may not be severe enough to trigger any of the classic symptoms, T2D may remain underdiagnosed for many years. Commonly β -cell function is still sufficient to avoid the need for insulin administration. However, with time, the insulin secretion may get progressively decreased, becoming insufficient to compensate the insulin resistance, which may also accentuate (51).

The abnormal insulin uptake and the resistance to insulin normal functionality may be improved with weight reduction, practice of physical exercise, and pharmacological treatment of hyperglycaemia nonetheless, it is rarely restored to normal (51, 64). The risk of T2D incidence is strongly associated with the ageing, obesity or history of obesity, and lack of physical activity; yet, it seems to show greater occurrence in individuals with hypertension and/or dyslipidaemia, and its frequency varies in different racial/ethnic subgroups (65).

Although, type 2 diabetes onset is often associated with patients of middle age or later, recently, it was noticed an increase of T2D incidence in children and young people (66).

2.2.1.3 - OTHER FORMS OF DIABETES MELLITUS

Apart from the most common type 1 and type 2 diabetes mellitus, other forms of diabetes have been identified and classified independently according to their specific

etiology, into two main categories: (1) diabetes mellitus derived from genetic defects; and (2) diabetes mellitus associated with particular disorders or conditions.

The variant forms of diabetes associated with genetic defects have its causes in identified genetic abnormalities which interfere with pancreatic β -cells or insulin action physiological mechanisms. A kind of genetic abnormalities includes defects in the insulin gene leading to a condition commonly referred as maturity onset diabetes of the young (MODY), or monogenic diabetes, which results in an impaired insulin production (51). These types of defects are generally hereditary and inherited in an autosomal dominant pattern (67). Another kind of genetic defects are associated with insulin action and usually related with insulin receptors, which may induce a variety of conditions ranging from hyperinsulinemia and moderate hyperglycaemia to severe diabetes (67).

Other variants of DM may have their etiology connected with primary diseases or other conditions. For instance, severe diseases of the exocrine pancreas such as pancreatitis, infections, pancreatic carcinoma, traumas or pancreatectomy may lead to a significant loss in β -cell mass and subsequently to the establishment of a diabetic state (68). Attending to its origin, either accompanying a syndrome or a specific pathological condition, the types, of diabetes encompassing these group is conventionally labelled as secondary diabetes. This variant may also be triggered by several endocrinopathies, which are strongly associated with an increased level of hormones that antagonize insulin action. This is the case of Cushing's syndrome, glucagonoma, acromegaly, pheochromocytoma in which the cortisol, glucagon, growth hormone and epinephrine, respectively, are secreted in excess (69).

Additionally to the previously mentioned causes of diabetes, several drugs (e.g. pyriminil and pentamidine) are known to interfere negatively in the production, uptake and normal function of insulin and thereby, may precipitate a diabetic-like state (69).

2.2.1.4 - GESTATIONAL DIABETES

Gestational diabetes mellitus (GDM) was known, for many years, as a group of disorders associated with glucose metabolism or any degree of glucose intolerance condition, with its onset or first recognition during pregnancy (51). This DM variant shares several symptoms with T1D and T2D. However, some patients may not be clearly classified as having one particular form of the two main types of the disease. Further, this definition applies independently on the need of insulin administration, or specific diet modification treatment, or even if the condition persists after pregnancy (51). This kind of DM may be detected in the second or third trimester of pregnancy through a screening for clinical risk factors and testing abnormal glucose tolerance, which is usually mild and asymptomatic (70). Pregnancy itself impairs the normal glucose metabolism thus a special attention is required regarding both diagnosis and control, especially since it was demonstrated that the risk of adverse maternal, foetal and neonatal outcomes, continuously increase as a function of maternal glucose at 24-28 weeks (71).

Besides sharing symptoms, GDM etiology also shares common background of physiological and genetic abnormalities that characterized diabetes mellitus outside pregnancy. Commonly, glucose metabolism returns to normal after delivery; however, women developing GDM are more likely to develop diabetes posteriorly (72).

2.2.1.5 - NEONATAL DIABETES

Neonatal diabetes (ND) represents another form of diabetes which should be highlighted, since it differs from the main types previously described. ND may be diagnosed in the first 6 months after birth and similarly to GDM, it may be temporary or permanent (51).

Among the main causes leading to a temporary form of this neonatal disorder, the most common genetic defect is an abnormality on ZAC/HYAMI. On the other hand, defects on the gene encoding the Kir6.2 subunit of β -cell K_{ATP} channel represents the most common alteration responsible for a permanent ND (51).

2.2.2 - DIABETES DIAGNOSIS

The diagnosis of diabetes mellitus aims not only to detect evidence of altered glucose metabolism, but also to understand the etiology, stage of development and degree of both glucose metabolism and associated complications.

Diabetes may be diagnosed through three well-known clinical tests: (1) the fasting plasma glucose (FPG); (2) the 2-h plasma glucose value after 75g of oral glucose administration – the oral glucose tolerance test (OGTT); being both focused on plasma glucose criteria; and (3) the A1C-based test (1).

The FPG must be conducted under fasting and since the plasma glucose levels may be affected by situations of severe stress such as infections, myocardial infarction, surgeries, among other, this information needs to be taken in account (73). The temporal relation of diet-to-blood sampling time is not considered in the casual FPG. The second test, the OGTT, is the most sensitive technique to provide solid information about the diabetic disorder by measuring the rate of glucose disposal after a particular and significant oral administration of glucose (73).

The A1C Test has been recommended more recently by international organizations in order to diagnose diabetes with a threshold of $\geq 6.5\%$, which is referred as A1C (haemoglobin A_{1c}). Further, this test was reported to be clinically useful since A1C parameter is broadly relevant reflecting chronic hyperglycaemia as well as it is a specific pointer of glycaemic control, used as guide for diabetes treatment (1). Additionally, in comparison with the remaining tests, A1C possess several advantages including greater convenience (since it does not require a specific diet condition nor fasting), evidence to suggest greater preanalytical stability, and less interference by

factors such as day-to-day unbalances due to additional stress or illness (74). Nevertheless, A1C alone is unable to allow for the diagnose of diabetes, being necessary a complementary evaluation with one of those previously mentioned tests. The main reason for this limitation lies in the fact of A1C results being conditioned by erythrocytes renewal in addition to plasma glucose levels (73). Furthermore, when compared with FGP or OGTT tests, A1C is significantly more expensive and the final correlation between A1C and glucose may be incomplete for several individuals (1, 74).

The currently accepted criteria for the diagnosis of diabetes are showed on table 2.3.

Table 2.3 - Criteria for the diagnosis of diabetes mellitus. Adapted from (51).

FPG \geq 126 mg/dL (7.0 mmol/L). Fasting is defined as no caloric intake for at least 8 h.*
OR
2-h PG \geq 200 mg/dL (11.1 mmol/L) during an OGTT. The test should be performed as described by the WHO, using a glucose load containing the equivalent of 75 g anhydrous glucose dissolved in water.*
OR
A1C \geq 6.5% (48 mmol/mol). The test should be performed in a laboratory using a method that is NGSP certified and standardized to the DCCT assay.*
OR
In a patient with classic symptoms of hyperglycemia or hyperglycemic crisis, a random plasma glucose \geq 200 mg/dL (11.1 mmol/L).
*In the absence of unequivocal hyperglycemia, results should be confirmed by repeat testing.

2.2.3 - DIABETES AND BONE

Diabetic osteopenia (DO) is among the variety of complications that may arise from diabetes mellitus development, which regard tissue and organ damage or function impairment.

Indeed, diabetes mellitus is known to broadly affect bone metabolism leading to abnormal conditions such as mineral loss conducting to an osteopenic state, which worsens due to chronic hyperglycaemia and latterly, osteoporosis (3, 75-77). Following, DO is tightly associated with bone fractures which are considered the major causes of morbidity and premature mortality and thus the relation between diabetes and bone healing and metabolism has been extensively reviewed (3, 76, 78).

Despite this focused studies, the processes involving the risk for osteoporosis development and low- and high-trauma fractures remains unclear since reports became contradictory at times, depending upon the type of diabetes, the metabolic control, the onset of the disease, the clinical trials or experimental animal models, the gender, and the time points selected for the evaluation, among other factors (3, 79, 80).

For instance, type 1 diabetes was reported to have a greater tendency to cause bone mineral loss and consequently fracture risk due to a fragile bone structure. On the contrary, type 2 diabetes was described as a multidimensional condition, therefore specific experimental models available to mimic this condition are far from the real representation of the disorder increasing the contradictory and poor accurate information.

2.2.3.1 - EFFECTS OF TYPE 1 DIABETES ON BONE

Type 1 diabetes mellitus is strongly associated with severe bone tissue comorbidities, comprising the modest reduction of bone mineral density (BMD), decreased linear bone growth during puberty, and early development of osteopenia and later osteoporosis (6, 79, 81, 82).

The overall research focused in T1D was consistent in that this diabetes type tends to be associated with a diminished bone mass (83). Accordingly, several data shown that about 20% of T1D patients, between ages 20-65, are osteoporotic and up to 40% are osteopenic (78, 84, 85). Further, clinical evaluation has demonstrated a substantially increased risk of hip fracture. This was supported by *in vivo* studies using rodent models, which reported an abnormal bone turnover process in which osteoblastic function is impaired, while osteoclastic activity seems to be enhanced (75, 77, 86). Additionally, an induction of apoptosis of bone lining cells was noticed which, together with impaired bone turnover, seems to lead to an unbalanced cycle with greater bone suppression than new bone formation (87).

Systemic interferences may also elicit a response in bone tissue, namely diabetic-mediated acidosis, leading to renal complications which, by themselves, lead to a decreasing blood and extracellular pH (88). Despite the verified pH alterations, this does not imply an increased osteoclast activity. In fact, several studies report increased bone destruction under hyperglycaemic conditions, despite the fact that there is a significant amount of evidence showing a normal or even decreased osteoclastic activity in experimental diabetes (75, 87).

In contrast with bone resorption, bone formation is considerably affected by T1D and this outcome derives from impaired function of osteoblastic cells which, in physiological conditions, would express receptors for insulin and insulin-like growth factor-1 (IGF-1), known growth factors able to stimulate the activity, maturation and proliferation of osteoblastic-lineage cells. Further, hyperglycaemia itself reduces osteoblast replication and function. Numerous reports regarding bone histology in studies involving animals showed diminished osteoblast, number together with a reduced osteoid volume and mineral apposition, moreover, lower levels of important bone formation-related factors in plasma such as OC, IGF-1 and ALP, were also reported in both spontaneously diabetic and chemical-induced diabetic rats (83, 89).

More recently, a study conducted on diabetic mice showed a relation between T1D hyperglycaemia and the decreasing expression of osteoblastic master regulator runt-related transcription factor 2 (RUNX2), as well as of some of its target genes such as matrix metalloproteinase-9 (MMP-9) and OC. Given its importance at the regulation of osteoblastic differentiation, RUNX2 down-regulation points to an impaired osteoblastogenesis and consequent impaired new bone formation. In which regards OC and MMP-9 diminished secretion along with deficient expression of critical factors such as DMP-1, MMP-13 and others, these were found to affect mineral homeostasis and new bone tissue mineralization (90, 91).

Several reports pointed to a negatively affected mineralization in diabetes, together with a lowered torsional strength, angular deformation and energy absorption, even with soft reductions in BMD. Despite this reduction in mineral density, this unbalanced process is accompanied by an increasing glomerular filtration rate (+70%)

and calcium output (+568%), as well as a reduced calcium reabsorption (92). These comes in line with histological and radiographic evaluations which showed significant decreased trabecular connectivity density of tibiae, combined with an increased trabeculae separation, even under diabetic conditions with insulin treatment (93).

2.2.3.2 - EFFECTS OF TYPE 2 DIABETES ON BONE

In contrast to type 1 diabetes, type 2 diabetes is known as a multidimensional condition reported to exert a variety of adverse and sometimes contradictory effects in bone metabolism and regeneration.

While some studies reported a reduced bone density in T2D patients (94, 95), other approaches registered an increased bone mineral density (76, 96) or even no changes, as comparing with physiological conditions (97, 98). Despite this variability, T2D is broadly associated with BMD increase rather than an osteopenic condition. Additionally, studies regarding the fracture risk within T2D also point to divergent conclusions however the majority indubitably suggests a higher risk of fracture which is thought to be strongly associated with obesity, since complications occur mainly in the hips, ankles, proximal humeri and feet. Other works, such as the Rotterdam study, detected changes in the fracture risk, specifically in women (5). In this case, a decreased risk of fracture of wrist and forearm in older women affected by T2D was reported (99, 100). These results may indicate a site-specific relation between type 2 diabetes and bone fracture as well as an age correlation.

Ultimately, the higher BMD and consequent increased fracture risk in type 2 diabetes may be explained by the following causes. Firstly, T2D is associated with an increase of 50 to 60% risk of falling (3, 101, 102). Secondly, long-term hyperglycaemia leads to complications which are considered prevalent risk factors for falls, including retinopathy and peripheral neuropathy (3). At last, despite the increased BMD and larger bone volume, diabetes is associated with a poor bone quality and, which is not detected in cross-sectional BMD measurements (3).

2.2.3.3 - ANIMAL MODELS OF DIABETES MELLITUS

The aiming for a more accurate insight on diabetes mellitus requires complex studies, which enable both the assessment of isolated cell and tissues, as well as systemic modifications and impairments. This need for an improved knowledge about this ensemble of metabolic disorders has led to a continual enhancement of *in vitro* and *in vivo* models. The most frequent experimental animal models of diabetes embrace small animals such as rodents, as these models may share the common properties with the attained outcome of the human disease (103, 104).

While some animal models may spontaneously develop diabetes, such as the non-obese diabetic (NOD) rat, other models may be pharmacologically induced by specific compounds such as streptozotocin (STZ), alloxan, vacor, dithizone and others (104, 105). Alloxan and streptozotocin are the most prominent diabetogenic chemicals, as they are toxic glucose analogues, which preferentially accumulate in pancreatic β -cells, leading

to a massive destruction or malfunction of these cells consequently inducing a diabetic state (105, 106).

Alloxan was firstly discovered by Whöler and Liebig in 1838 (107) as a derivative of pyrimidine and was used as a diabetic inducer by McLetchie (108). This compound was reported to exert two distinct pathological effects: (1) inhibition of glucose-induced insulin secretion by a specific inhibition of glucokinases; and (2) induce the formation of reactive oxygen species (ROS) leading to a selective necrosis of pancreatic β -cells and consequent insulin-dependent state. Biochemically, alloxan is known to have a short half-life and it also decomposes spontaneously into non-diabetogenic alloxanic acid, when in aqueous solutions. Thus, alloxan uptake through glucose transporter 2 (GLUT2) must be fast in order to achieve a representative model of type 1 diabetes. In other hand, higher concentrations of alloxan may inhibit a variety of functionally important enzymes and proteins, as well as the cellular functions leading to undesired metabolic changes beyond the diabetic state.

Streptozotocin is a nitrosurea derived from *Streptomyces achromogenes* and was firstly introduced as a broad-spectrum antibiotic, and a drug for cancer treatment (106, 109). However, years later, STZ was reported by Rakietyen and co-workers to exert a diabetogenic effect additionally to its antimicrobial action (110). Similarly to alloxan, following absorption, STZ enters pancreatic β -cells through GLUT2 channels in plasma membrane and starts a cascade of biological responses that ultimately lead to hypoinsulinemia and hyperglycaemia, in animals (106). When injected, STZ alkylates DNA by transferring its methyl group to the 6th oxygen of the guanine base, damaging the molecule. Following, poly(ADP)-ribose polymerase is over-activated to offset the

STZ-caused DNA breaks, resulting in the depletion of NAD⁺, and subsequently ATP, within cells. Thus, the unbalances in these molecules' metabolism may result in the inhibition of several cell functions, namely regarding insulin production (105, 106).

In rodents, STZ-induced diabetes exhibits several hallmarks representative of the verified chronic complications commonly associated with human DM (103). Furthermore, the pathologies development may be controlled depending on the length of the study and the time for which the animals are hyperglycaemic (92, 109).

After STZ administration, blood glucose follows a well described triphasic pattern of hyperglycaemia (105, 106). The first phase begins as early as 1 hour following STZ administration and lasts 2-4 hours, during which an inhibition of insulin production originates a hypoinsulinemia, leading to the hyperglycaemia development. This stage is associated with morphological changes in the pancreatic β -cells, such intracellular vacuolisation, swelling of the mitochondria and decrease in Golgi body area (105). Approximately 4 to 8 hours after STZ injection, hypoglycaemia sets in. This second phase commonly lasts several hours, is irreversible, and may be severe enough to cause convulsions and death, particularly following the depletion of glycogen stores in liver (105, 109). This state is mainly caused by an extreme release of insulin into circulation upon explosion of vesicles and bursting of the cell membranes (105). The last phase occurs 12-48 hours after STZ administration and it is characterized by degranulated and destroyed β -cells, which debris are posteriorly cleaned by non-activated macrophages. No β -cells remain intact, further demonstrating the specificity of this drug (105, 106).

The streptozotocin-induced diabetes model has been extensively used and is highly reproducible, being particularly useful for building upon and data comparison.

2.2.4 - DIABETES AND BIOMATERIALS IMPLANTATION

The increasing incidence of DM has led to a higher occurrence of complications associated with hyperglycaemia and consequent severe damage to tissues and organs (111). Accordingly, as the number of diabetic patients increase, the requirement of specific therapies and/or the implantation of biomedical devices to support tissue healing, is increasing as well. The most common implants used by DM patients include orthopaedic implants and glucose sensors. In particular, the glucose sensors have been especially designed for use in diabetic patients (11).

The acceptance and performance of an implant highly depends on fibrosis, infections and integration on the damaged tissues. Implant-associated infections represent a major cause of implant's failure and rejection (112). A variety of factors may contribute to the occurrence of these infections, including factors related with the surgery aseptis, the quality of the host tissues (e.g. bone and soft tissues around the wound), and even the complexity of the operation (11, 112). Further, infections associated with biomaterial implantation are generally more difficult to overcome as they usually require longer period of antibiotic therapy and additional surgical procedures, including prostheses removal and wound cleanse (113, 114).

Diabetes mellitus, along with other pathological disorders, such as rheumatoid arthritis, and immunocompromising diseases, for instance, are known to alter wound healing as well as an increase in the risk of infection (115, 116). Further, compared with the general population, a higher implant failure and rejection rate has been registered in diabetic patients even in those with adequate metabolic control (117). Despite a number of studies have focused the understanding the diabetes effects on healing

ability (118-121), only few have discussed the infection prevalence and the ability of diabetic patients to receive implants and modulate the associated infections (11). Furthermore, many causes were described to promote infection in DM, including defective immune response, enhanced adherence of several microorganisms to diabetic cells, and higher amount of medical interventions (116), among other.

It is known that in physiological conditions, the presence of a foreign body, such as biomaterial, triggers an inflammatory reaction and eventual fibrotic encapsulation, which can severely reduce the device's performance or resulting in biomaterial rejection (11). For example, regarding the glucose percutaneous implants, some work has been carried out in order to diminish the risk for infection (122). These devices have been coated, aiming not only to reduce bacterial adherence and eradication, but also to minimize foreign-body encapsulation, which is a cause of implant malfunction, since the lack of vascularization and the fibrotic dense barrier blocks the accurate glucose measurement (11).

Regarding orthopaedic implants, several studies have addressed the effects of diabetes on the osseointegration. These works reported higher rate of implant failure among the cases in which the disease was poorly controlled (123). Further, as mentioned previously, diabetes affect bone remodelling and mineralization which contributes to diminished implant osseointegration. Additionally, reduced bone-implant contact area in diabetes was reported, even with similar bone formation and quality in both physiological and diabetic conditions (124, 125).

In which regards the effect of insulin on implant osseointegration, studies are contradictory. Conformably, a study conducted in alloxan-induced diabetic rat,

demonstrated that insulin treatment restored bone formation around endosseous implants (126). The authors found that the ultra-structural characteristics of bone-implant interface was similar in both healthy and diabetic-insulin-treated animals. These results are endorsed by other reports which strongly suggest that metabolic control is essential to achieve successful implant osseointegration (126-128). In contrast, Fiorelli et al. have shown that, despite that insulin treatment and normoglycaemia maintenance seem to enhance bone formation around the implant, it is not enough to equally the bone-implant contact attained in non-diabetic animals (129).

2.3 - TETRACYCLINES

Tetracyclines (TCs) are a family of broad-spectrum anti-microbial agents that are widely used in human and veterinary medicine. The range of TCs anti-microbial activity includes aerobic and anaerobic Gram-positive (e.g. *Staphylococcus* spp., *Streptococcus* spp., *Bacillus* spp.) and Gram-negative bacteria (e.g. *Haemophilus*, *Escherichia*, *Salmonella* spp.), and other organisms such as *Rickettsia*, *Plasmodium* and *Chlamydia* spp., *Mycoplasma pneumoniae*, and some protozoa (such as amoebae) (10, 130).

In early 1948, due to the failure of most used antibiotics to improve his condition, the young Toby Hockett was the first patient treated with “the yellow-colored compound” developed by the Lederle Laboratories, under the name of aureomycin, or chlortetracycline (131). This active principle was discovered in the early 1940’s by Duggar and co-workers, as a natural fermentation product of the soil bacterium *Streptomyces aureofaciens* and it drew special attention due to the inhibitory effects on growth of all strains, in an initial panel of bacteria (9, 131). Authors further found that the extract exerted a remarkable antibacterial activity, even against most lethal pathogens at that time (such as typhus and rickettsias) (131). For this reason, researchers labelled aureomycin as a “broad spectrum antibiotic”. Few years later, Alexander Finlay and colleagues at Pfizer gathered various soil samples from around the world and isolated a compound from *Streptomyces rimosus*, which was similar to aureomycin and named Terramycin, also known as oxytetracycline (132). Joint work of Lederle and Pfizer teams led to the understanding of both aureomycin and terramycin preliminary chemical structures (see figure 2.9). Following, the

understanding of chlortetracycline and oxytetracycline led to the preparation of tetracycline through the hydrolysis of chlortetracycline, which showed the same antimicrobial potential of both chlor- and oxytetracycline, and an enhanced stability (133). Following these findings, several TCs' derivatives were later developed and chemically modified in order to attain enhanced efficacy and output, within the management of infectious conditions.

Apart from their generation, tetracyclines are commonly classified according to their origin into natural-derived products (e.g. tetracycline, chlortetracycline, demeclocycline) and semisynthetic compounds or chemically modified tetracyclines (e.g. minocycline and doxycycline) (134, 135); or according to their half-life into short-acting (e.g. chlortetracycline, tetracycline and oxytetracycline) or long-acting (e.g. minocycline and doxycycline).

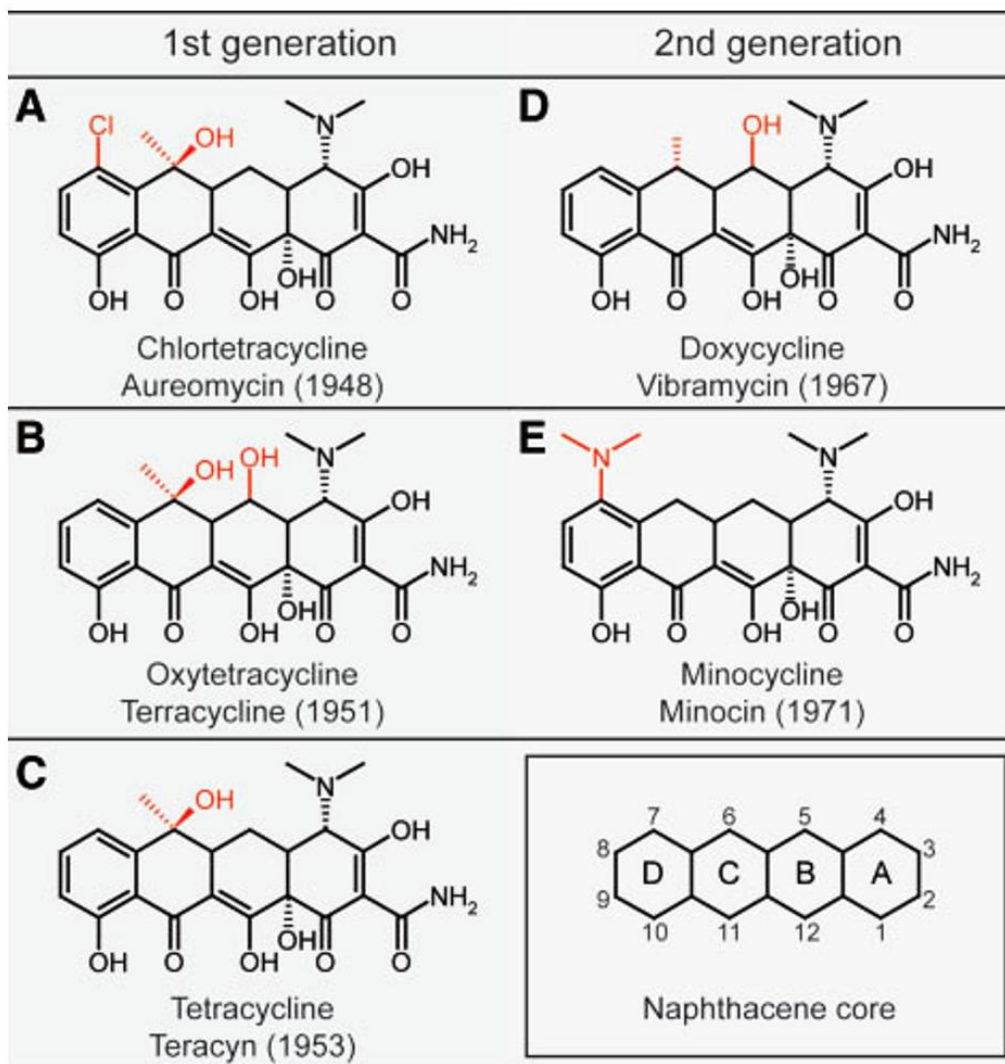


Figure 2.9 - Chemical structure of naphthacene ring system, first-generation antibiotics (chlortetracycline, oxytetracycline and tetracycline), and second generation-antibiotics, followed by the year they were approved by the FDA; Adapted from (136).

2.3.1 - CHEMISTRY AND ANTI-MICROBIAL PROPERTIES

Chemically, tetracyclines from the first generation share a common basic structure. This common chemical structure consists of a tetracyclic naphthacene carboxamide ring system (figure 2.10), with similar functional groups displaying minor differences (131, 137). Second generation, encompassing semisynthetic and chemical modified tetracyclines, share the same basis of naphthacene ring with an A-ring carbon 1 (C1)- carbon 3 (C3) diketo substructure and an exocyclic C2 carbonyl or amine group. Additionally, an active tetracycline requires a C10-phenol group and a C11-C12 keto-enol substructure in conjunction, with a 12a-OH group. The antibiotic function has been associated with the dimethylamine group bound to carbon 4 (C4), in ring A (137). The removal of dimethylamine group from C4 or its replacement may significantly diminish the antibacterial properties.

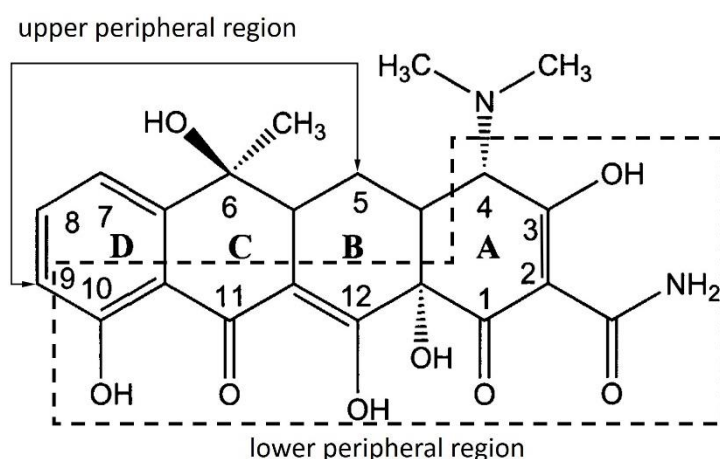


Figure 2.10 – Chemical structure of tetracycline. Adapted from (131).

Both upper and lower peripheral regions are able to bind several functional groups and substituents, of which replacement may significantly affect TC's function. For instance, chemical changes of the lower peripheral regions are strongly associated with sharp reduction of both antibiotic and non-antibiotic effects (135). In contrast, synthetic modifications of C7 and C9, of D ring, have been reported to enhance stability, half-life, as well as the non-antimicrobial activity (137). This was accomplished with some semisynthetic tetracyclines, including minocycline and doxycycline.

The basis of TCs bacteriostatic action relies on their ability to interfere with the normal cellular function of bacteria. It is currently accepted that tetracyclines bind to the 30S subunit, more specifically the 16S particle, of bacterial ribosomes (131, 138). In this specific mechanism of action, the lower region of the A-ring was demonstrated to form an H-bond and bind with ribosomal magnesium and key RNA nucleotide bases (139). Consequently, TCs inhibit the binding of charged tRNA to its receptor on the mRNA-charged ribosome complex, ultimately blocking the protein synthesis processes (140). Tetracyclines were also reported to bind the 40S subunit of eukaryotic ribosomes however, their concentration within eukaryotic cells is not sufficient to disrupt protein synthesis (141).

The inhibition of protein synthesis is considered the key mechanism of tetracyclines bacteriostatic effects however, other mechanisms have been associated with TCs activity. Tetracyclines were reported to affect cell growth through membrane-mediated mechanisms, as in the case of Gram-negative bacteria (131). Accordingly, the most lipophilic tetracyclines were reported to exert an atypical bactericidal effect by

causing membrane perturbations, which interfere with multiple signalling pathways, leading to severe cellular dysfunction (142).

2.3.2 - NON-ANTIBIOTIC PROPERTIES

Around three decades ago, this class of antimicrobial agents was unexpectedly found to modulate cellular behaviour, as well as extracellular factors secretion or inactivation. Tetracyclines and some of semisynthetic derivatives are known to inhibit collagenases and other host-derived metalloproteinases (MMPs), in a mechanism independent of their antimicrobial activity, interfering with biological processes such as proteolysis, inflammation, angiogenesis and apoptosis (143). MMPs are responsible for crucial processes including connective tissue remodelling, wound healing, tumor invasion and metastasis. However, the overexpression of several MMPs due to pathological conditions may lead to a breakdown of collagen fibrils, consequently affecting the basement membrane (9).

Regarding their non-angiogenic properties, TCs were found to disrupt the formation of new blood vessels. Accordingly, TCs and derivatives were described to inhibit the synthesis of MMP-8 and MMP-9 by endothelial cells subsequently affecting the migration of endothelial cells (144). Accordingly, tetracyclines were considered useful for therapies of a wide variety of conditions in which pathologically elevated MMP's activity and concomitant extracellular matrix proteins degradation are the hallmark of the disease pathogenesis (145). The conditions which may represent suitable targets for TCs include periodontitis, corneal ulceration, osteopenia/osteoporosis, rheumatoid arthritis, cancer invasion and metastasis, abdominal aortic aneurysms, inflammatory skin diseases among other immune-inflammatory conditions (145). Further, it is known that collagenases, as well as other MMPs, may be involved in the degradation of type I collagen matrix which is the major

constituent of bone organic matrix. This, together with the destruction of other components of connective tissue leads to impaired bone remodelling or regeneration. Early *in vivo* research has shown that tetracyclines were able to inhibit bone loss by inhibiting osteoclast-mediated bone resorption, but also by enhancing the osteoblastic differentiation and activity, upregulation of type I collagen expression and increased bone formation, essentially in conditions of significant bone loss (146, 147).

Additionally, tetracyclines derivatives have been reported to inhibit caspase-1 functions thus diminishing the apoptotic activity in pathological conditions which cause unbalanced programmed cell death (e.g. cancer and neurodegenerative disorders) (9).

2.3.3 - DOXYCYCLINE

Further studies and synthetic modifications conducted by Lederle and Pfizer led to the development of second generation tetracyclines derivatives. Pfizer researchers opted for a disjunctive approach, modifying the C-ring of oxytetracycline in order to attain a compound with higher stability combined with preserved antimicrobial activity (148). Two years later, Doxycycline ($C_{22}H_{24}N_2O_8$, figure 2.9) was synthesized by Charlie Stephens as an analogue presenting relevant advantages in comparison with the original tetracyclines including, remarkable activity, chemical stability and pharmacological efficacy which was later approved by *Food and Drug Administration* (FDA) (149).

Doxycycline became a long-acting second generation tetracycline-derivative most frequently prescribed to treat a wide variety of infectious agents including Gram-positive pathogens (e.g. *Staphylococcus aureus*, and *Streptococcus pneumoniae*, *Bacillus anthracis*), Gram-negative pathogens (e.g. *Pasteurella multocida*, and *Escherichia coli*) and other such as *Plasmodium falciparum* and rickettsias (131, 150).

In addition to its antibacterial potential, doxycycline was reported to possess non-antibacterial properties, which mechanisms of action were broadly described to minimized host tissue breakdown by inhibiting matrix metalloproteinases specifically collagenases and gelatinases action (145). The compound revealed to be able to disrupt several matrix metalloproteinases, such as MMP-8 and MMP-9, preventing connective tissue degradation and enhancing the treatment of pathological conditions, in which MMPs play a central role, such as rheumatoid arthritis (151, 152), inflammatory skin disease rosacea (153, 154), cancer invasion and metastasis (155), corneal ulceration (156), periodontitis (157), osteopenia and osteoporosis (8, 145, 158).

Doxycycline was reported to act as an osteogenic agent enhancing new bone formation and regeneration by improving type 1 collagen synthesis as well as other osteogenic factors (i.e. bone morphogenetic proteins) (159). The benefits of doxycycline in bone healing were assessed in several conditions. Following, recent work of Walter and co-workers (160) demonstrated the efficiency of doxycycline coating process on a titanium zirconium implant surface and its beneficial effects on osseointegration and bone regeneration. Authors' *in vitro* studies with MC3T3-E1 cell lineage demonstrated enhanced bioactivity as well as good bioavailability of doxycycline coated surfaces. Additionally, the implantation of this doxycycline-coated alloy on rabbits showed positive effects on bone formation markers as well as enhanced bone regeneration when compared with the implant without doxycycline coating (160). Eglence demonstrated that low concentrations of doxycycline induce an osteoblastic differentiation similar to that obtained from cells exposure to bone morphogenic protein-2 (BMP-2). Doxycycline was also reported to modulate positively osteoprogenitor cells from human femoral cancellous bone (161). its efficacy was once more demonstrated *in vivo* with studies of periodontal implantation on dogs (162) and clinically in the repair of bilateral infrabony defects in humans (163). Additionally, regarding clinical application of MMPs inhibitors, doxycycline's non-antibacterial properties have been reported to contribute to their effectiveness in situations as cation-chelation activity with consequent avidity for mineralized tissues, and MMPs inactivation, and long-term clinical safety (7, 164).

Following, low-dose regimens of doxycycline (sub-antimicrobial doxycycline doses SDD) shown to be non-antimicrobial, safe and effective. Further, these regimens were described to preserve doxycycline anti-apoptotic, anti-inflammatory and

immunomodulatory properties over the bone tissue while preventing complications associated with long-term high doses therapies (e.g. hyperpigmentation, increased photosensitivity, hypersensitivity, among other) (157, 165). Within this therapeutic regimen, doxycycline was reported to attain peak plasma levels of around 1 µg/mL, and to maintain mean plasma levels of around 0.5 µg/mL for several hours. Within these concentrations, doxycycline was able to stimulate the proliferation of osteoblastic-induced bone marrow cells (7). Moreover, an extended clinical trial have demonstrated beneficial effects of SDD in postmenopausal women exhibiting both local (periodontitis) and systemic (osteopenia) bone loss (8, 158). These properties made a compelling case for SDD as an attractive option for the management of local, as well as systemic, osteoporosis or osteopenia conditions.

2.3.4 - MINOCYCLINE

The studies focused on tetracyclines, conducted by Lederle scientists, aimed to produce new semisynthetic derivatives which the maintenance of the structure needed for antimicrobial activity, while the remaining functional groups would be removed or replaced to achieve unique non-antimicrobial properties (131). The modifications on C-ring and D-ring functional groups led to the development of a novel compound with a characteristic D7-dimethylamino group (figure 2.9) which was later found to exhibit far greater antibacterial and pharmacological activity, in comparison with first generation tetracycline (10, 131).

Minocycline ($C_{23}H_{27}N_3O_7$) was approved for clinical use by FDA, in 1971, and became one of the most used second-generation, semi-synthetic tetracycline till nowadays (10). It combines the tetracyclines efficacy against gram-positive and gram-negative bacteria and it was also reported to exert a beneficial effect on treatment of acne vulgaris, rheumatoid arthritis and some sexually transmitted diseases (10, 166). Minocycline exhibits enhanced pharmacological properties when compared with first-generation tetracyclines including faster and complete absorption (when administered orally), longer half-life, excellent tissue penetration and bioavailability (167). Additionally, minocycline lipophilicity was studied in order to assess its relation with the pharmacological behaviour. The results showed that, due to its highly lipophilic properties, this molecule was able to cross the blood-brain membrane accumulating on the CNS (168).

Similarly to first-generation tetracyclines and other semi-synthetic compounds, minocycline non-antimicrobial properties were also points of great interest. It was

considered the most effective tetracycline-derivative concerning neuroprotection and this potential was early reported in experimental models of ischaemia (169, 170), brain trauma (171) and neuropathic pain (172), as well as on the modulation of Parkinson's (173), Alzheimer's (174) and Huntington's (175) diseases. Furthermore, minocycline was demonstrated to be a potential promotor of bone regeneration and remodelling. Accordingly, it was considered to be a suitable compound for periodontal disease treatment since it combines antimicrobial, anti-inflammatory and anti-apoptotic properties (10, 176). Additionally, it was found that long-term exposure to minocycline strongly stimulates osteoblastic progenitors to proliferate and differentiate in fully functional osteoblasts, subsequently promoting new bone formation and enhancing mineralization (7, 177).

Minocycline benefits on bone physiology were further reported to improve osteopenic/osteoporotic conditions (178, 179). Following, studies performed on animal models of induced osteoporosis showed that minocycline was able to increase new bone formation and prevent trabecular bone loss (179). Also, it was reported to prevent bone mineral density decrease in pathological conditions at least through three main mechanisms: (1) reduction of the bone resorption by modulating osteoclastic activity; and (2) promotion of the efficiency of bone-marrow derived progenitor cells enhancing osteoblastic differentiation and function (178); (3) inhibition of collagenases, leading to an improved bone regeneration and remodelling, through the increase of bone matrix osteoid and osteoblastic cells organization, favouring the formation of a more adequate collagen matrix (180).

**CHAPTER 3 - THE OSTEOGENIC PRIMING OF
MESENCHYMAL STEM CELLS IS IMPAIRED IN
EXPERIMENTAL DIABETES**

3.1 - INTRODUCTION

Diabetes mellitus includes several metabolic disorders which are ultimately characterized by chronic hyperglycaemia arising from abnormalities in insulin production, action or both (48). Uncontrolled chronic hyperglycaemia leads to severe dysfunction and failure of various tissues and organs including bone (6, 53). Clinically this seems to result in diminished linear bone growth followed by early onset of osteopenia and latterly osteoporosis, and consequent increased risk of fragility fracture, and deficient bone healing (181).

Type 1 diabetes is undoubtedly associated with a significant reduction of bone mineral density, broadly correlated with an increased risk of fragility fractures (76, 182). The most T1D patients have inadequate accrual peak of new bone mass essentially due to abnormalities on bone formation process (79). Indeed, *in vivo* and *in vitro* studies of DM effects on bone tissue reported consistent impaired osteoblastic maturation and function, rather than osteoclastic and bone resorption enhancement (80, 89).

Current knowledge regarding cellular and molecular mechanisms of DM was provided by *in vitro* studies, in which osteogenic-induced precursor cells were cultured in diabetic conditions, such as hyperglycaemic medium (183-187). Despite these models yielded information on the effect of high glucose levels, they provided limited data since they fail to disclose the systemic-modulation of osteogenic precursor cells developing under a full diabetic environment. In an attempt to overcome this limitation, animal models of experimental diabetes became popular especially alloxan- and streptozotocin-induced diabetes. These new approaches allowed data gathering on

diabetic-derived precursors to respond to osteogenic stimuli (188-191). Accordingly, impaired cellular activity was reported specifically regarding the osteogenic responsiveness although the reasons leading to this impairment still unclear.

3.2 - RESEARCH HYPOTHESIS AND OBJECTIVES

Within the previously mentioned context, the present work aimed to characterize the priming capability and functionality of undifferentiated precursor cells developed within the diabetic environment. In order to achieve the main goal, bone marrow-derived mesenchymal stem cells (MSCs), harvested from animals with experimental diabetes chemically induced with STZ, were grown in the absence of any given differentiation factor. Cultures were characterized for cell proliferation, viability/apoptosis, morphology, alkaline phosphatase activity, collagen synthesis and osteogenic and adipogenic gene expression profile, and compared to MSCs cultures harvested from sham animals.

3.3 - MATERIALS AND METHODS

3.3.1 - ANIMALS

The protocols involving animals were performed under the authorization of *Direção Geral de Alimentação e Veterinária* (DGAV) and comprised the standards for the protection of experimental animals, according to the Portuguese (Decree No. 113/2013) and European (Directive 2010/63) legislations.

This study used 12 male Wistar rats (Charles River, Wilmington, MA), 7 to 8 weeks old, with a body weight of around 250-300 g. Animals were allowed to acclimatize for 1 week before the beginning of the study and then, were housed in groups, in conventional type II cages, on a controlled environment of temperature and humidity, in a 12h light/dark cycle. The animals were clearly identified with indelible ink, and received dry food (4RF21 Mucedola, Settimo Milanese, Italy) and water *ad libitum*.

Experimental diabetes was induced by an intraperitoneal injection of STZ, Sigma® (60 mg.kg^{-1} , dissolved freshly in 10 nM citrate buffer, pH 4.5, $n = 6$) – STZ group. Control rats were injected with citrate buffer alone ($n = 6$) – CTRL group. Hyperglycaemia was confirmed by measuring tail vein blood glucose levels with a glucometer (Accu Check GO, Roche Diagnostics, Portugal) 72 hours after streptozotocin or buffer injection, and levels were expressed as milligrams per decilitre. Animals with blood glucose levels $\geq 300 \text{ mg.dl}^{-1}$ were considered to be diabetic.

Six weeks following both STZ and vehicle administration, animals were euthanized by exsanguination under general anaesthesia (intraperitoneal injection of pentobarbital sodium $35 \text{ mg} \cdot \text{kg}^{-1}$).

3.3.2 - DIABETIC BONE ALTERATIONS

Proximal tibial specimens were scanned by microcomputed tomography (μCT). μCT was performed in a μCT 35 (Scanco Medical), with a voxel size of $12 \mu\text{m}$, X-ray tube voltage of 70 kVp, current intensity of 114 mA, and integration time of 600 ms. Microstructural measures, included bone volume per total volume (BV/TV), connective density (CD), trabecular number (Tb.N), trabecular thickness (Tb.Th), and trabecular separation (Tb.Sp) The computation of these structural measures has been previously detailed (192).

3.3.3 - ESTABLISHMENT OF BONE-MARROW CELL CULTURES

Bone marrow-derived MSCs were isolated from Sham and STZ animals using a modification of Dobson (193) and Sekiya (194) methodologies, for bone marrow harvest and MSCs isolation. Accordingly, tibiae and femora were aseptically excised, cleaned of soft tissues and decontaminated in a solution of Rat Mesenchymal Stem Cell Growth Medium (Lonza), with the addition of $1000 \text{ UI} \cdot \text{mL}^{-1}$ penicillin and $1000 \mu\text{g} \cdot \text{mL}^{-1}$ streptomycin, for 30 minutes, plus 30 minutes. Following, long bones epiphyses were

cut off and diaphysis were flushed out with Rat Mesenchymal Stem Cell Growth Medium.

Nucleated cells were isolated with a density gradient (Ficoll-Paque Premium®), re-suspended in culture medium supplemented with 10% heat inactivated fetal bovine serum (FBS, Gicbo), penicillin-streptomycin (100 UI.mL⁻¹ – 100 mg.mL⁻¹, Gibco) and fungizone/amphotericin B (2.5 μ g.ml⁻¹, Gibco), and plated onto conventional 6-well culture microplates and kept in a humidified atmosphere (5% CO₂/air, 37°C).

Culture medium was subsequently renewed every 2 days until around 75% confluence (approximately 15 days), when the cells were enzymatically released with trypsin 0.04% in 0.25% ethylenediaminetetraacetic acid (EDTA) solution, and seeded at 10⁴ cells.cm⁻² in culture microplates.

Cultures were maintained in the previously described conditions for 12 days and assessed for proliferation/viability, morphology, functional activity and differentiation events.

3.3.4 - OPTICAL MICROSCOPY

Cell cultures were regularly monitored by phase contrast optical microscopy, for a qualitative assessment of cell morphology and proliferation.

3.3.5 - CELL PROLIFERATION AND METABOLIC ACTIVITY

Cell proliferation was estimated by the total DNA content, using the Quant-iT™ PicogreenVR DNA assay (Life Technologies) according to the manufacturer's instructions, following cell lysis with Triton X-100 0.1%.

Metabolic activity was determined with MTT assay at days 1, 5, 8 and 12. The method consists of the reduction of the MTT salt [3-(4,5-di-methylthiazol-2-yl)-2,5-diphenyl tetrazolium bromide, Sigma®] by the mitochondrial succinic dehydrogenase of proliferating cells, to a purple formazan product that accumulates in the cytoplasm. Cultures were incubated with MTT solution (0.5 mg.ml⁻¹) at 37°C, in a humidified atmosphere of 95% air and 5% CO₂ for 4 hours. Following, the medium was decanted and the formazan crystals were dissolved in DMSO, and the absorbance was measured at 550 nm (Synergy HT, Biotek).

3.3.6 - CELL MORPHOLOGY

Cell cultures morphology were evaluated by confocal laser scanning microscopy (CLSM) following staining of cytoskeleton and nucleus counterstaining.

For CLSM assessment, the cultures were fixed in 3.7% paraformaldehyde (15 minutes) and permeabilized with Triton 0.1%. Following, cell cultures were incubated with albumin (10 mg.ml⁻¹), in order to reduce non-specific staining. Cell cytoskeleton filamentous actin (F-actin) was visualized by treating cells with Alexa Fluor 488®-conjugated phalloidin (1:20 dilution in phosphate buffered saline (PBS), 20 minutes) and

propidium iodine ($1 \mu\text{g}\cdot\text{ml}^{-1}$, 10 minutes) for cell nuclei labelling. Labelled cultures were mounted in Vectashield® and examined with Leica SP2 AOBS (Leica Microsystems) microscopy.

3.3.7 - ALKALINE PHOSPHATASE ACTIVITY AND TOTAL PROTEIN CONTENT

Alkaline phosphatase (ALP) activity was determined in cell lysates, by the hydrolysis of p-nitrophenyl phosphate into a yellow coloured product, i.e., p-nitrophenyl, which has a maximal absorbance at 405 nm, in an alkaline buffer solution. The rate of the reaction is directly proportional to the enzyme activity.

Cell lysates were obtained by treatment of the cultures with 0.1% Triton in $\text{d}_2\text{H}_2\text{O}$ and then assayed by colorimetric determination of the product p-nitrophenol at $\lambda = 405 \text{ nm}$, in an ELISA reader (Synergy HT, Biotek). The hydrolysis of p-nitrophenyl phosphate (pH 10.3) was carried out for 30 minutes at 37°C then the reaction was ceased by adding NaOH 5M. The ALP activity of each sample was normalized to its protein concentration (measured according to the Lowry method) and the results were expressed as nanomoles of p-nitrophenol produced per minute per μg of protein ($\text{nmol}\cdot\text{min}^{-1}\cdot\mu\text{g}^{-1}$).

The total protein content was determined according to the Lowry method. In this method, the peptide bonds of proteins react with copper, under alkaline conditions, to produce the ionized form of copper (Cu^+), which then reacts with the Folin reagent – a mixture of phosphotungstic acid and phosphomolybdic acid in phenol. The product

becomes reduced molybdenum/tungsten blue by the copper-catalyzed oxidation of aromatic amino acids. The reaction results in a strong blue colour, which depends partially on the tyrosine and tryptophan content, and may be detected colorimetrically, by absorbance, at 705 nm. The protocol for protein determination included the following solutions:

A. 20 g $\text{Na}_2\text{CO}_3 \cdot \text{L}^{-1}$ 0.1 N NaOH

B. 0.1 g Na Tartrate + 0.05 g $\text{CuSO}_4 \cdot 5 \text{H}_2\text{O}$ + 10 ml dH_2O + H_2SO_4

C. 50 ml reagent A + 1 ml reagent B

D. Phenol Reagent – 1 part Folin-Ciocalteu 2 N: 1 part dH_2O

Cultures were washed with PBS and incubated with 0.1% Triton in water (15 minutes at room temperature). 200 μl of the cell lysates were treated with 1.5 ml of reagent C, vortexed and incubated for 10 minutes. Following, 150 μl of reagent D was added and the samples were vortexed and incubated in dark, for 1 hour, at room temperature. Finally, the absorbance was measured at 750 nm in 1 cm cuvettes, in a spectrophotometer (Jenway 6405).

A series of dilutions of 0.5 $\text{mg} \cdot \text{ml}^{-1}$ bovine serum albumin in 0.1% Triton were used as standard. Results were expressed as micrograms per square centimetres ($\mu\text{g} \cdot \text{cm}^{-2}$).

3.3.8 - PROGRAMMED CELL DEATH

Apoptotic activity was quantified by assessing caspase-3 activity with the EnzCheck® Caspase-3 Assay Kit #2 (Molecular Probes), according to manufacturer's instructions.

3.3.9 - COLLAGEN SYNTHESIS

Assessment of the total collagen synthesis was conducted by *in situ* determination with Sirius red dye.

Briefly, previously fixed cell cultures were incubated with 100 µL/well of 0.1% Sirius red F3BA solution (BDH, UK) in saturated picric acid for 1 hour, at room temperature, under mild shaking. Thereafter, the dye solution was removed by suction and the stained cell layers extensively washed with 0.01 N hydrochloric acid, to remove all non-bound dye. The cell morphology was photodocumented before dissolving the stain. Following, the stained material was dissolved in 200 µL of 0.1 N sodium hydroxide using a microplate shaker, for 30 minutes, at room temperature. The absorbance was measured at 500 nm on an ELISA reader (Synergy HT, Biotek) against 0.1 N sodium hydroxide blank.

Results were presented as percentage of staining compared to control.

3.3.10 - GENE EXPRESSION

Cell cultures of both control and STZ-induced groups were analysed by qPCR, at days 5 and 12, for the expression of housekeeping gene glyceraldehyde 3-phosphate dehydrogenase (GAPDH), ALP, RUNX2, collagen type 1 alpha 1 (Col1 α 1), OPN, OC, OPG, insulin receptor substrate 1 (IRS1), insulin receptor substrate 2 (IRS2), peroxisome proliferator-activated receptor gamma (PPAR γ), and adipocyte protein 2 (AP2).

Total RNA was extracted using the NucleoSpin[®] RNA II kit (Macherey-Nagel), according to the manufacturer's instructions. Total RNA concentration and purity were assessed by UV spectrophotometry at 260 nm, and by calculating the A260 nm/ A280nm ratio, respectively. RNA was reverse transcribed to cDNA using the SuperScript III First-Strand Synthesis (Invitrogen). cDNA was amplified by real-time quantitative PCR using the SYBR Green RT-PCR kit (Applied Biosystems, Foster City, CA) in a Bio-Rad iCycler. Relative RNA levels were calculated using the iCycler software and normalized using GAPDH levels. The reaction was followed by melting curve analysis to verify specificity. The expression of each gene was evaluated using the $2^{-\Delta\Delta C_T}$ method and dilution curves were used to test the PCR efficiency.

Results were expressed as the percentage variation from control, corresponding to 100% at each time point. The primers used are listed on table 3.1.

Table 3.1 - Forward and reverse sequences of the primers used for the qPCR analysis.

GENE	FORWARD SEQUENCE	REVERSE SEQUENCE
GAPH	AAATGGTGAAGGTCGGTGTG	CCCATACCCACCATCACACC
ALP	GGCTCTGCCGTTGTTTC	GGGTTGGGTTGAGGGACT
RUNX2	ATCCAGCCACCTTCACTTACACC	GGGACCATTGGGAACTGATAG
COLLAGEN 1 A1	TGGCAAGAACGGAGATGA	AGCTGTTCCAGGCAATCC
OSTEOPONTIN	AAAAATGCTCACCATCACTGC	AATTGCCCACTGACTTCCAC
OSTEOCALCIN	GCCCTGACTGCATTCTGCCTCT	TCACCACCTTACTGCCCTCCTG
OSTEOPROTEGERIN	ATTGGCTGAGTGTTCTGGT	CTGGTCTCTGTTTTGATGC
IRS-1	TGTGCCAAGCAACAAGAAAG	ACGGTTTCAGAGCAGAGGAA
IRS-2	GAGCCTTCAGTAGCCACAGG	CAGGCGTGGTTAGGGAGTAA
PPARγ	GCGGAGATCTCCAGTGATATC	TCAGCGACTGGGACTTTTTCT
AP2	ATGTGTCATGAAAGGCGTGA	AAACCACCAAATCCCATCA

3.3.11 - OSTEOGENIC INDUCTION AND CULTURE CHARACTERIZATION

Bone marrow mesenchymal stem cells were isolated from Sham and STZ animals, following the previously described methods. In order to assess the capability of osteogenic induction of these populations, first passage cells were grown in osteogenic inducing conditions for 12 days. To attain these conditions, alpha-modified minimum essential medium (α MEM) supplemented with 10% foetal bovine serum, penicillin-

streptomycin ($100 \text{ UI}\cdot\text{mL}^{-1} - 100 \text{ mg}\cdot\text{mL}^{-1}$, Gibco), fungizone amphotericine B ($2.5 \text{ }\mu\text{g}\cdot\text{mL}^{-1}$, Gibco), ascorbic acid ($50 \text{ mg}\cdot\text{mL}^{-1}$, Sigma-Aldrich), beta-glycerophosphate ($4 \text{ mmol}\cdot\text{L}^{-1}$, Sigma-Aldrich), and dexamethasone ($10 \text{ nmol}\cdot\text{L}^{-1}$, Sigma-Aldrich), was used and changed every 2 days.

Cell cultures were characterized at days 5 and 12 for the expression of osteogenic-specific genes ALP, RUNX2, Col1 α 1, OPN, OC, OPG, as previously described, and normalized using GAPDH levels. Results were expressed as the percentage variation from control.

The Alizarin Red histochemical assay was further conducted to address the mineralization of the ECM of the grown cultures, at day 12, through the identification of calcium deposits within the matrix. Briefly, fixed cultures were covered with 1% Alizarin Red S solution (0.028% in NH_4OH , Sigma-Aldrich), pH 6.4, for 2 minutes, and were rinsed with distilled water and acid ethanol (ethanol, 0.01% HCl). Stained cultures were photo-documented with an inverted microscope (Nikon TMS) and digital imaging system (Nikon DN 100).

3.3.12 - ACTIVATION OF SPECIFIC SIGNALING PATHWAYS IN STZ-DERIVED CULTURES

The activation of specific signalling pathways was evaluated in cultures growing in the presence of specific inhibitors. At day 8, established MSCs cultures were treated with

10 mM of the ERK inhibitor PD 98059 (Sigma-Aldrich), 10 mM of the WNT inhibitor ICG-001 (R&D Systems), or 20 mM of the p38-inhibitor SB 203580 (Sigma-Aldrich), for at least 6 hours of the culture. These were characterized for metabolic activity and gene expression analysis, as described above. The expression levels of ALP, RUNX2 and PPAR γ were assayed. Results were presented as percentage of variation from control.

3.3.13 - STATISTICAL ANALYSIS

Three independent experiments were performed with the cell cultures established from different animals. In biochemical assays, each point represents the mean \pm standard error of six replicates. Statistical analysis was done by two-way analysis of variance (ANOVA) followed by Tukey range test post hoc analysis. P values $\leq 0.05\%$ were considered significant.

3.4 - RESULTS

3.4.1 - DIABETIC EXPERIMENTAL MODEL

Diabetes mellitus was chemically induced by a single intraperitoneal injection of streptozotocin. Animals of control group revealed the normal course of body weight increase ($6.41\% \pm 3.45$), while animals of STZ group lost weight ($37.57\% \pm 8.65$), during the experimental period. At euthanasia, STZ group had a significantly higher glycaemia in comparison to control ($\leq 125 \text{ mg. dl}^{-1}$).

3.4.2 - DIABETIC BONE ALTERATIONS

Bone structure of proximal tibia of both control and STZ groups were addressed by microcomputed tomography. The results of μ CT evaluation showed a significant reduction of trabecular content in STZ animals (figure 3.1, right) in comparison with control (figure 3.1, left). Decreased trabecular interconnectivity was also verified at the bone's proximal metaphysis, in diabetic bone. Additionally, morphometric indexes of the trabecular structure revealed a significant decrease in BV/TV and in trabecular thickness, combined with a tendency for connective density reduction. Despite the overall reduction of trabecular bone mass, no significant differences were found regarding trabeculae number and separation. Resulting measurements are shown in table of figure 3.1.

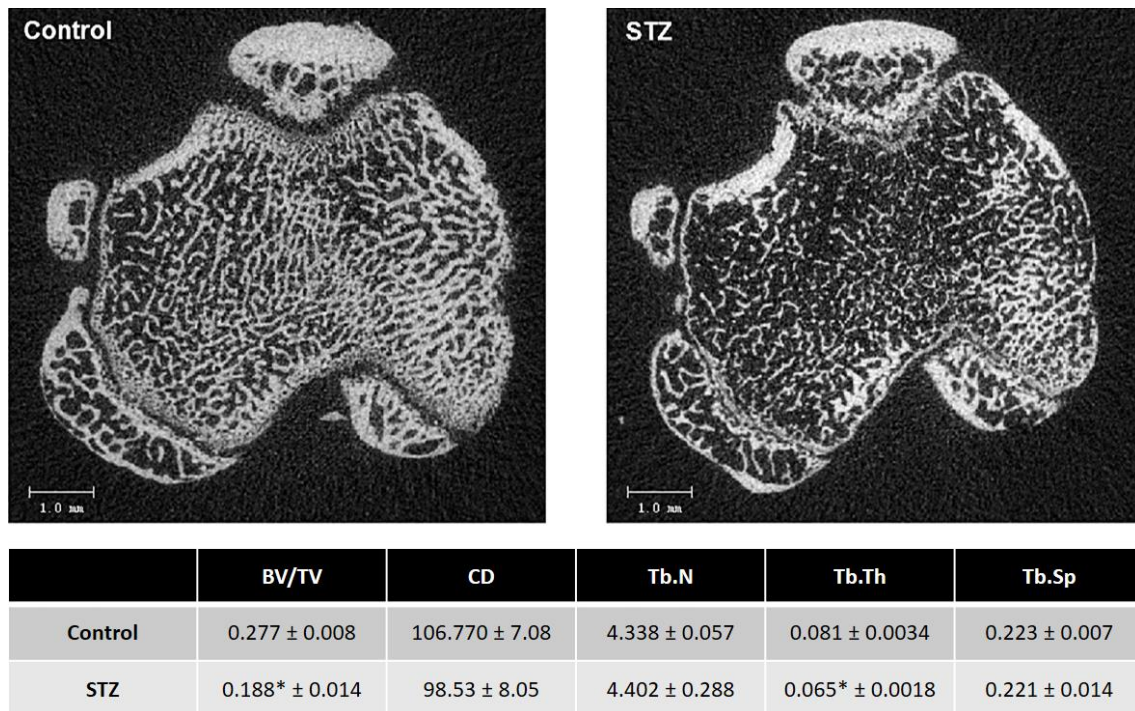


Figure 3.1 - Top: representative 2D microtomographic images of the proximal tibia metaphysis, in control and STZ animals ($n = 6$). Bottom: table of microstructural parameters of the trabecula structure of the proximal tibia. The addressed variables included BV/TV (bone volume per total volume), CD (connective density), Tb.N (trabecular number), Tb.Th (trabecular thickness), and Tb.Sp (trabecular separation). * - significantly different from control ($P \leq 0.05$).

3.4.3 - CELL PROLIFERATION AND METABOLIC ACTIVITY

The figure 3.2 shows the results of cell proliferation assessment with DNA quantification assay, along the culture time points. Accordingly, STZ-derived cell cultures

presented reduced total DNA content values from day 5 onwards, in comparison with control cultures. At days 8 and 12, significant differences were achieved with a reduction in diabetic-derived cells proliferation, higher than 20%, when compared with control.

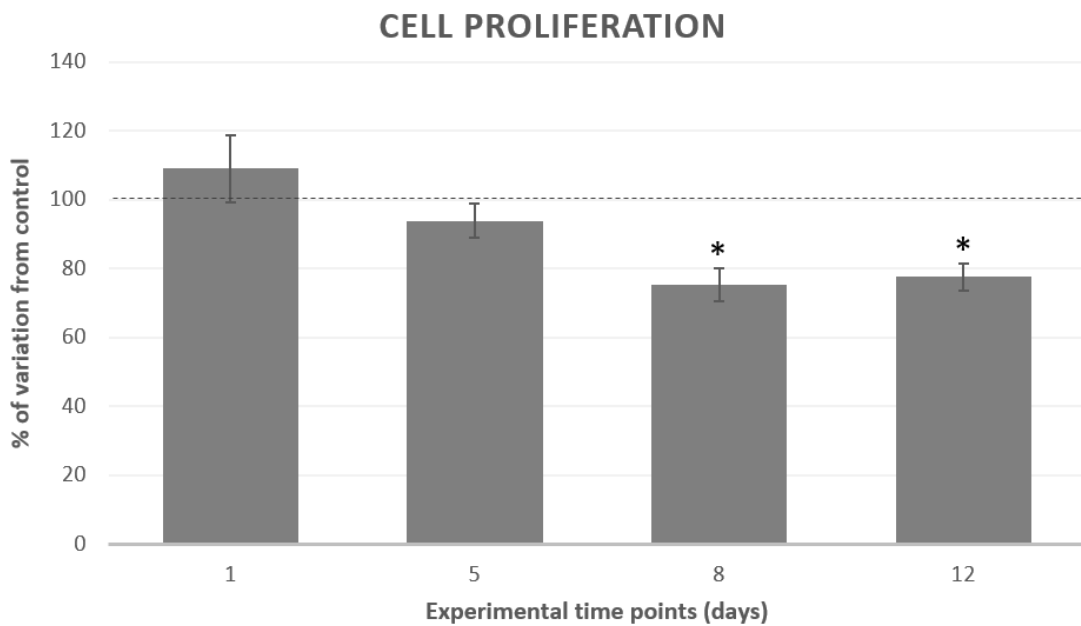


Figure 3.2 - Cell proliferation (DNA assay) of STZ-derived bone marrow mesenchymal stem cell cultures, established for 12 days. Percentage of variation from control at each time point. * - significantly different from control ($P \leq 0.05$).

The MTT assay was the method used to assess the metabolic activity of the cultures (figure 3.3). Cultures established from control animals presented an increasing of metabolic activity from the first day till around day 8, remaining stable afterwards, with a slight decrease of MTT values. Cultures established from diabetic animals

followed a similar growth pattern, with the MTT values increasing during the first week and diminishing softly subsequently. STZ-derived cultures showed higher MTT reduction values at early culture time points (days 1 and 5), comparing to control cultures, although without significant differences. At day 8 and 12, metabolic activity values attained for STZ were significantly lower than those achieved with control cultures.

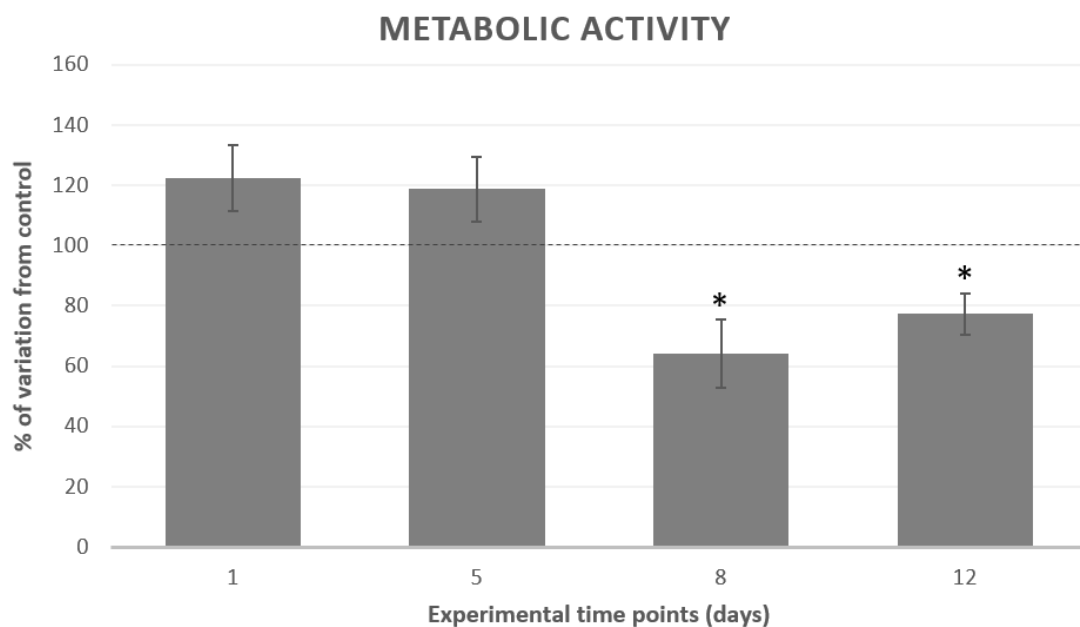


Figure 3.3 - Cell viability/metabolic activity (MTT assay) of STZ-derived bone marrow mesenchymal stem cell cultures, established for 12 days. Percentage of variation from control at each time point. * - significantly different from control ($P \leq 0.05$).

3.4.4 - CELL MORPHOLOGY

Cell colony morphology was addressed by confocal laser scanning microscopy (CLSM) and representative images are shown in figure 3.4. Control cultures, at day 3, presented a fibroblastic-like morphology, characteristic of osteoblastic cells in culture, with elongated cytoplasm, adequate nuclear organization, and a dense network of microfilaments and stress fibers. Strong labelling was often observed along cellular edge and within the extended cellular filopodia. Moreover, culture exhibited intense cell-to-cell contacts establishment, typical of nodular growth pattern. Cells proliferated adequately and, at day 5, a large area of the culture plate surface was already covered by a cell monolayer. At day 8, an organized flattened sheet of continuous cell multilayers was observed, similarly to the organization achieved at day 12.

The STZ-derived cultures showed a similar behaviour in this time course. However, at day 3, fewer stress fibers were visible on proliferating cells and the intense labelling at the cellular edge, broadly observed in control, was more rarely identified.

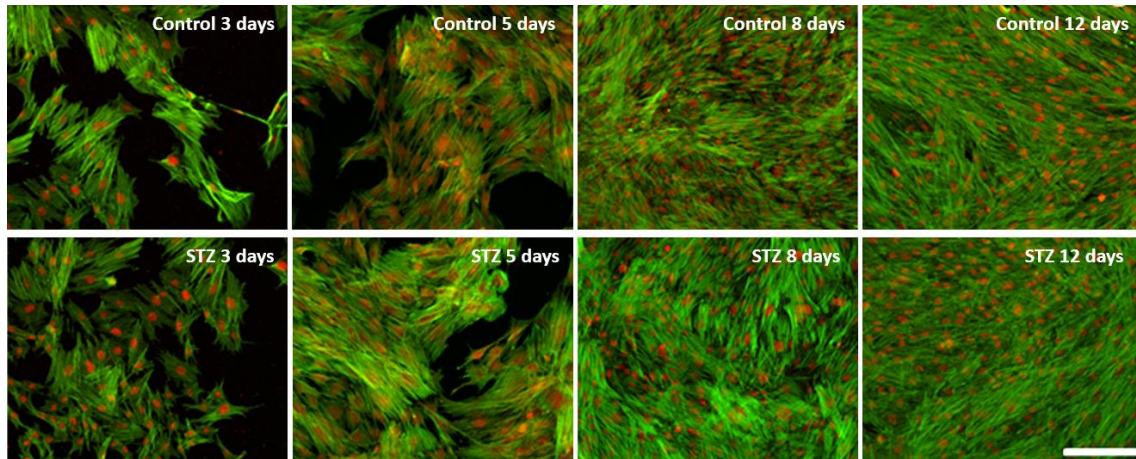


Figure 3.4 - Confocal laser scanning microscopy imaging of rat bone marrow-derived mesenchymal stem cell cultures, established for 12 days, from control and STZ-induced diabetic animals. Cytoskeleton was stained in green and nucleus counterstained in red. Scale bar corresponds to 200 μm .

3.4.5 - ALKALINE PHOSPHATASE ACTIVITY

The results regarding ALP activity were normalized by total protein content, determined by the Lowry method, and are shown in the figure 3.5 below. ALP activity showed a gradual increase with the culture time in both experimental conditions. Despite the similar pattern of increasing activity, STZ-derived cultures revealed a significantly higher ALP activity at days 8 and 12, as compared with the one attained within control cultures.

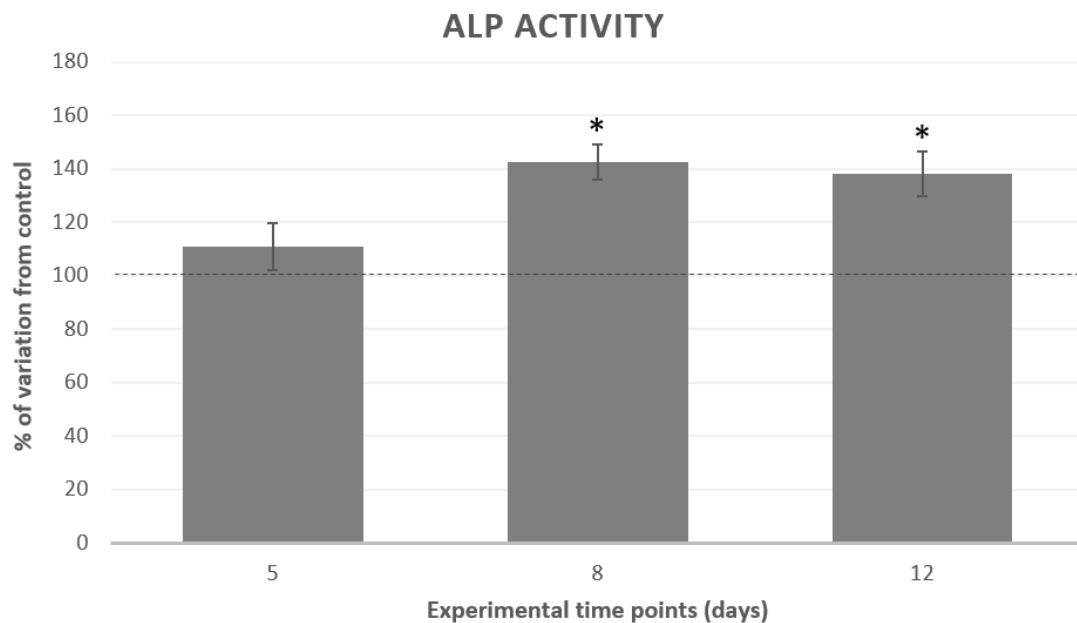


Figure 3.5 - Alkaline phosphatase activity (ALP per total protein content) of STZ-derived bone marrow mesenchymal stem cell cultures established for 12 days. Percentage of variation from control at each time point. * - significantly different from control ($P \leq 0.05$).

3.4.6 - PROGRAMMED CELL DEATH

Apoptosis was estimated by the determination of caspase-3 activity at experimental days 1, 5, 8 and 12 (figure 3.6 below). Concerning programmed cell death, in comparison to control cultures, STZ-derived cultures demonstrated significant higher caspase-3 activity at later culture time points.

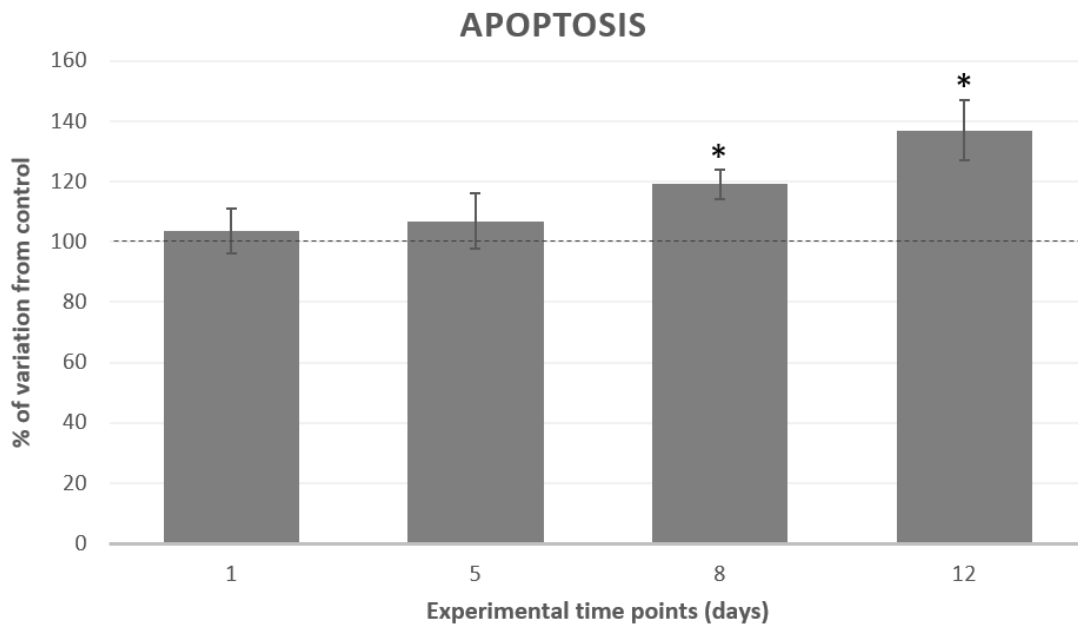


Figure 3.6 - Apoptotic analysis (caspase-3 activity assay) of STZ-derived bone marrow mesenchymal cell cultures established for 12 days. Percentage of variation from control at each time point. * - significantly different from control ($P \leq 0.05$).

3.4.7 - COLLAGEN SYNTHESIS

Total collagen synthesis was evaluated qualitatively (Sirius red dye histochemical staining) and then, following, quantified. Representative imaging of histochemical staining is presented on figure 3.7. Accordingly, in control cultures, an increasing staining intensity was verified throughout the culture time points. At earlier time points, control cultures exhibited a cluster-like organization. Until day 12, an increasing intensity of staining was observed, combined with a re-organization of the cultures into multilayers.

The same pattern of collagen synthesis was verified in STZ-derived cell cultures however, with no evidences of cluster organization, and with slighter less intense coloration, suggesting lower levels of collagen synthesis.

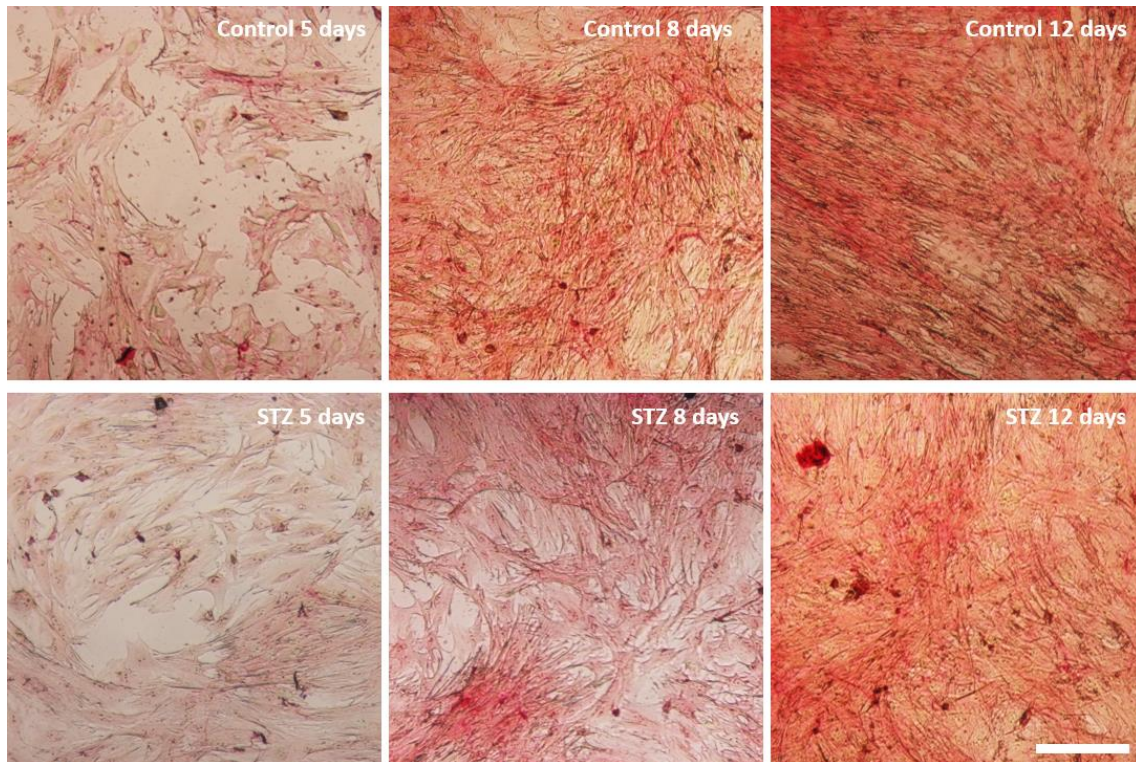


Figure 3.7 - Total collagen staining of STZ-derived bone marrow mesenchymal stem cell cultures established for 12 days, from control and STZ-induced diabetic animals ($n = 6$). The scale bar corresponds to 750 μm .

The quantitative determination of staining products was consistent with the histochemical analysis. Conformably, quantitative data revealed a similar collagen

content for both control and STZ cultures at days 5, and a tendency for a reducing collagen production afterwards, for STZ-derived cell cultures, in comparison with control. This reduction attained statistical significance at day 12. The results for collagen quantitative determination are presented on figure 3.8 below.

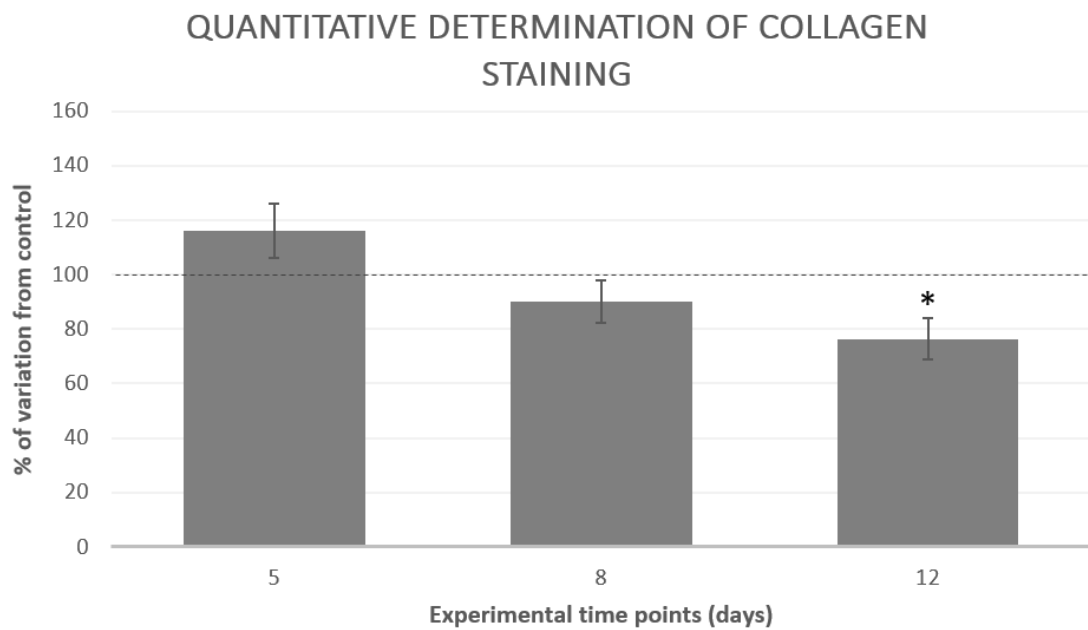


Figure 3.8 - Colorimetric determination of the total collagen stained product within the established STZ-derived bone marrow mesenchymal stem cell cultures. Results were expressed as the percentage variation from control corresponding to 100% at each time point. * - significantly different from control ($P \leq 0.05$).

3.4.8 – GENE EXPRESSION IN STANDARD CONDITIONS AND IN OSTEOGENIC-INDUCING CONDITIONS

qPCR analysis showed the expression of significant osteogenic and adipogenic markers, from both control and STZ-derived cell cultures. The results are shown in figure 3.9 and 3.10. The results addressing the osteogenic gene expression (figure 3.9) demonstrated that in undifferentiating conditions, STZ-derived cell cultures were able to express significantly higher levels of ALP, while the expression of remaining osteogenic genes (RUNX2, COL1 α 1, OPN, OC and OPG) were hindered, both at day 5 and 12, as compared to control.

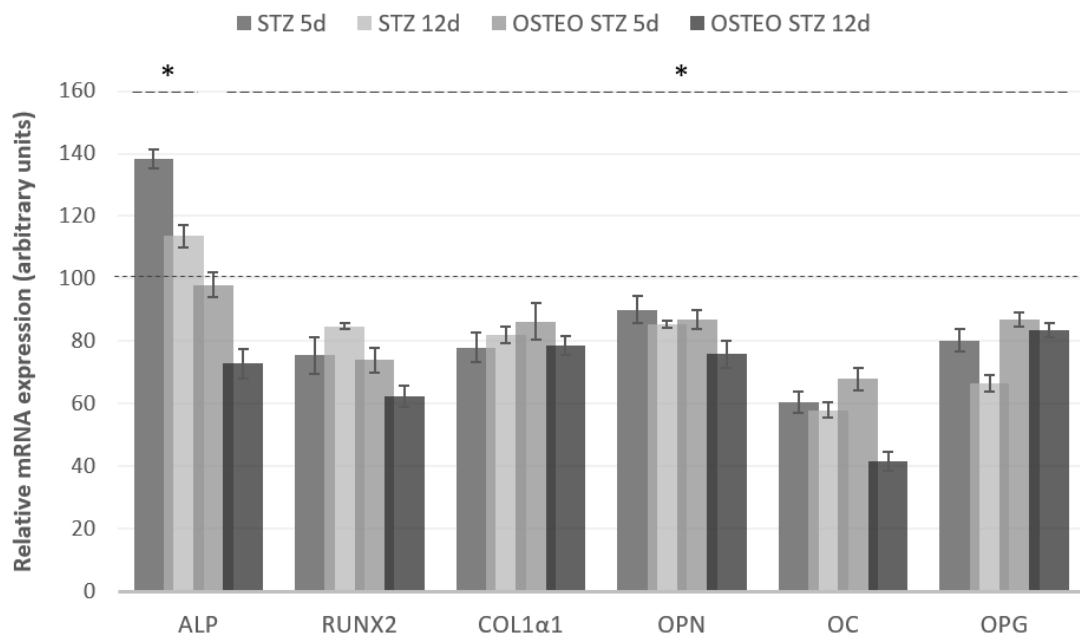


Figure 3.9 - qPCR gene expression analysis of ALP, RUNX2, Col1 α 1, osteopontin, osteocalcin, and osteoprotegerin in MSCs cultures, established for days 5 and 12, from control and STZ-induced diabetic animals ($n = 6$). Cultures were grown in

undifferentiating (STZ) and osteogenic-differentiating (Osteo STZ) conditions. Results were expressed as the percentage variation from control corresponding to 100% at each time point. * - significantly different from control ($P \leq 0.05$).

The results concerning adipogenic gene expression are presented in figure 3.10. According to the assay, STZ-derived cell cultures, grown in undifferentiating conditions, showed significantly increased expression of PPAR γ , IRS1, and IRS2, at both days 5 and 12 of the culture. In the other hand, AP2 expression was not affected.

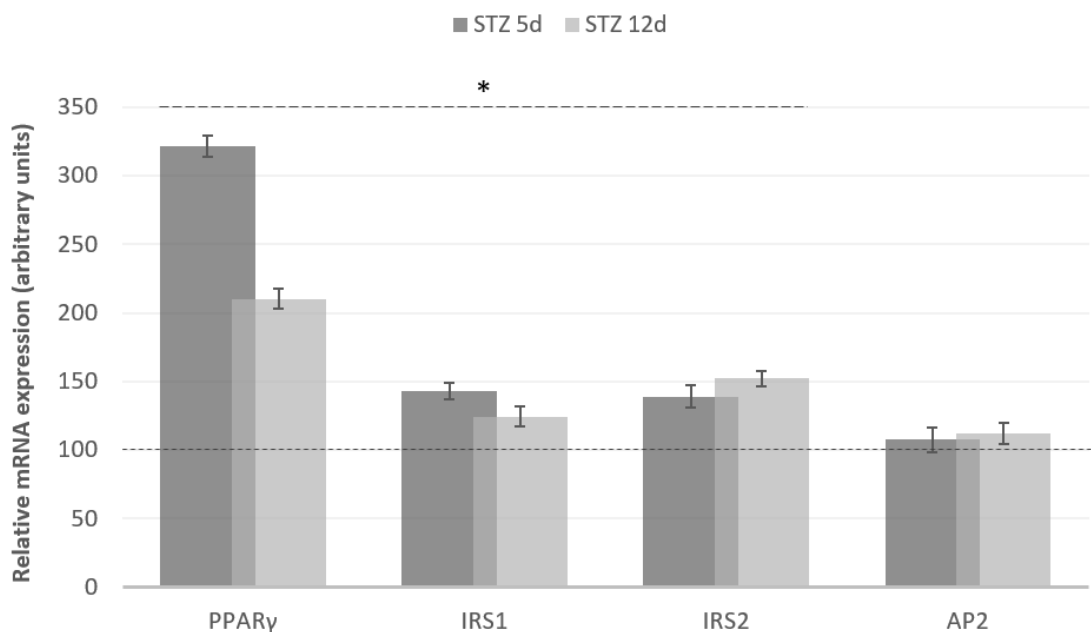


Figure 3.10 - qPCR gene expression assessment of adipogenic genes PPAR γ , IRS1, IRS2, and AP2, in undifferentiated STZ-derived MSCs cultures, established for 5 and 12 days. Results were expressed as the percentage variation from control corresponding to 100% at each time point. * - significantly different from control ($P \leq 0.05$).

3.4.9 – MINERALIZATION ASSESSMENT IN OSTEOGENIC- AND STZ-INDUCED CONDITIONS

The ability of MSCs to promote mineralization was evaluated by the Alizarin Red assay and the attained micrographs are shown at figure 3.11. According to the staining, at day 12 of the cultures, a significant mineralization of the extracellular matrix, as assessed by Alizarin Red assay, was verified in STZ-derived cultures

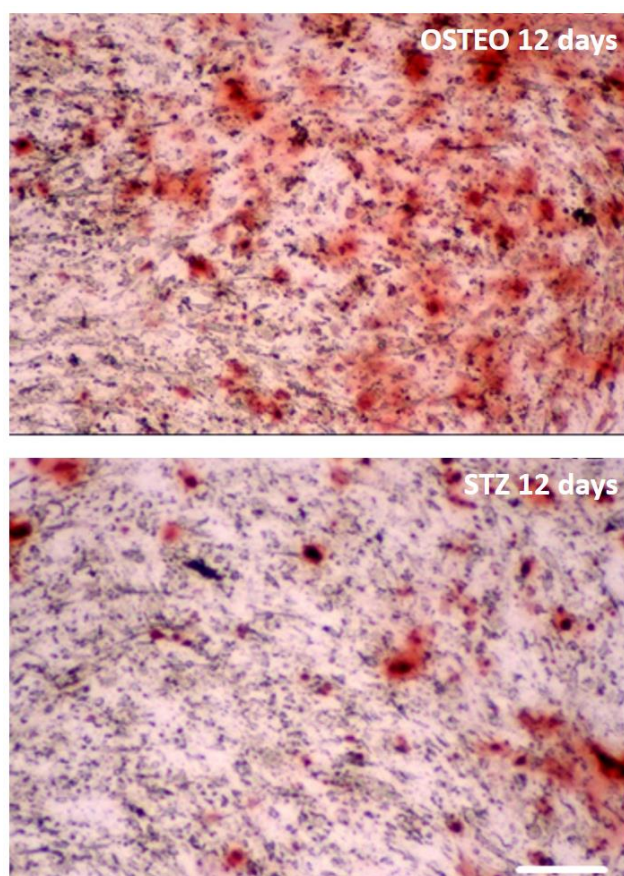


Figure 3.11 - Colorimetric determination of the mineralization nodules within the established control- and STZ-derived bone marrow mesenchymal stem cell cultures, at day 12.

3.4.10 – EVALUATION OF SPECIFIC SIGNALING PATHWAYS

The data concerning the activation of specific signalling pathways are showed in figure 3.12. Accordingly, inhibition assays with specific inhibitors demonstrated that, comparing to control, STZ-derived cell cultures exhibited diminished metabolic activity regarding ERK and WNT activation. In contrast, increased metabolic activity was verified within p38 assessment.

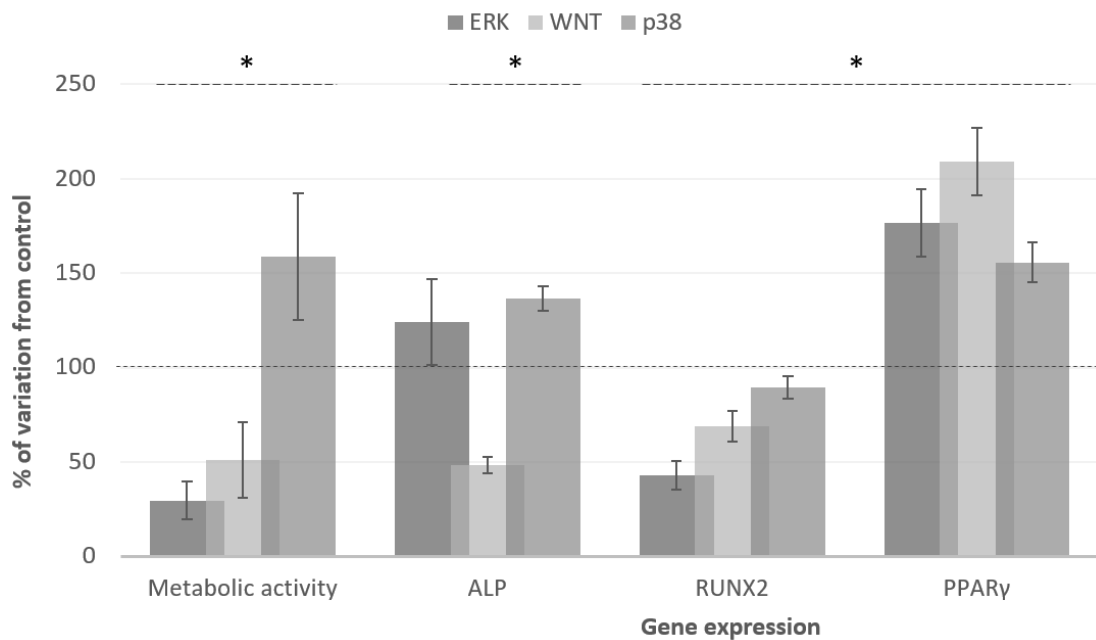


Figure 3.12 - Metabolic activity and gene expression analysis (of ALP, RUNX2, and PPAR γ) of MSCs cultures, grown for 8 days. Cultures were incubated with specific inhibitors of the ERK (PD 98059), p38 (SB203580), and WNT (ICG-001) signalling pathways for the last 6 hours of culture (n=6). Results were expressed as the percentage

variation from control corresponding to 100%. * - significantly different from control ($P \leq 0.05$).

Concerning ALP expression in STZ group, increased levels were found to be associated with ERK and p38 pathways while a significant reduced expression was found to be bound with WNT pathway. A reduced expression of RUNX2 and increased expression of PPAR γ were verified within the experimental conditions conducted to evaluate the three assayed pathways.

3.5 - DISCUSSION

Diabetic conditions seem to play a negative role on bone tissue metabolism and regeneration, even though little is known regarding the determinant molecular and cellular mechanisms, affecting the maturation and functional activity of osteoblastic precursor populations. This study focused on the characterization of the behaviour of unstimulated MSCs developed within a diabetic environment, an issue that was not addressed before. MSCs were harvested from the bone marrow of diabetic animals and allowed to adhere and expand *in vitro*, under undifferentiating conditions (i.e., in the absence of supplemented lineage-specific growth factors or diabetic-simulated conditions). Attained results support the notion that bone marrow-derived MSCs, developed under the diabetic microenvironment, display an impaired viability/proliferation, increased apoptosis, and diminished osteogenic and increased adipogenic priming. Furthermore, osteogenic induction of these cells, further confirmed the impaired osteogenic commitment, in comparison to those grown from non-diabetic animals.

Within the used animal model, diabetic induction with STZ allowed the development of hyperglycaemia (plasma glucose $\geq 300 \text{ mg.dl}^{-1}$), with associated body weight decrease, and changes in the bone structure. Microtomographic evaluation of the proximal tibia showed significant morphological alterations and reduced morphometric indexes (i.e., decreased BV/TV and trabecular thickness), supporting the development of a hyperglycaemia-mediated osteopenic condition (82).

MSCs cultures from diabetic animals, at late culture time points, revealed an increased apoptotic rate, impaired proliferation - reduced total DNA content - and a reduced metabolic activity, which may be related with the reduced number of active cells in STZ-derived cultures. This behaviour was similar to the one verified within *in vitro* models mimicking the diabetic microenvironment, such as hyperglycaemia and hypoinsulinemia (185, 186, 188, 195), reporting an impaired proliferation of osteoblastic populations. Also, an increased apoptosis was verified in dexamethasone-induced osteoblastic differentiating MSCs, from diabetic animals (191). These alterations may be related to a deficient insulin receptor activation by insulin, which induces a mitogenic stimulation, coupled with the inhibition of apoptosis, in a process probably mediated by the downregulation of p27 (a cyclin-dependent kinase inhibitor that seems to attenuate cell proliferation) (93). Other osteotropic factors produced by pancreatic β cells, such as islet amyloid polypeptide and preptin (which are absent or significantly reduced in diabetic conditions), also seem to favor osteoblastic proliferation and to reduce the frequency of apoptotic events (196).

In terms of cytoskeleton organization, at 3 days, STZ-derived cultures presented a reduced number of stress fibers and decreased F-actin labelling at the cell border. This is line with previous observations in MSCs grown from diabetic mice, revealing a decreased adhesion to substrate, and a disturbed distribution and expression of F-actin, leading to abnormal stress fibers formation (189). The cytoskeleton organization is critical for cell morphology and homeostasis, notwithstanding its involvement in other cellular processes, such as intracellular transport and differentiation (197). Osteoblastic function is highly dependent upon cell adhesion and cytoskeletal organization, as

extracellular cues seem to direct MSCs functionality and, particularly, the osteogenic differentiation (198).

Grown MSCs from STZ animals revealed an increased ALP activity and an impaired collagen production at late culture time points. Increased ALP activity was previously described in osteoblastic cells grown *in vitro*, in chronic hyperglycemic conditions (184, 185), and in the serum of diabetic patients (80, 199). Nonetheless, it has been suggested that ALP within the diabetic environment presents an altered kinetic profile, supposedly in a process related to changes in metal-binding properties (200, 201). Regarding collagen expression in diabetic conditions, a significant reduction of total collagen was verified in the bone of diabetic rats (202). Furthermore, collagen synthesis of human osteoblasts was significantly reduced in the presence of human diabetic serum (187). The high level of pro-inflammatory cytokines verified within the diabetic environment (203) may contribute to the altered ALP/collagen expression, as tumour necrosis factor α and interleukin 1β were found to stimulate ALP activity and lessen collagen expression in human MSCs (204).

Regarding MSCs gene expression profile, normally, this population expresses a genetic signature of its potential multilineage differentiation capacity, even at early differentiating stages (205). In the present work, MSCs harvested from diabetic animals presented an altered gene expression profile. In STZ-derived cultures, the osteogenic-related gene expression revealed an increased ALP expression, and a decreased expression of RUNX2 - the master regulator of the osteogenic differentiation - and, as well, a decreased expression of several of its downstream targets (i.e., Col1a1, osteopontin, osteocalcin, osteoprotegerin). This is an interesting finding supporting that

the diabetic microenvironment may hinder RUNX2 activity and downregulate the expression of its downstream targets. ALP expression, found to be increased in STZ cultures, and thus sustaining its acknowledged increased activity, seems to be independently regulated from RUNX2 activation. This comes in line with previous data on the inhibition of RUNX2, with either small interfering RNA (206), or overexpression of a dominant negative (204), which were found not to alter ALP expression, and suggested that it may be unrelated to this transcription factor regulation. Additionally, gene expression analyses were also conducted on osteogenic-induced MSCs. Cultures from STZ-derived animals revealed an impaired osteogenic induction, both at days 5 and 12, with significantly reduced expression of both ALP and RUNX2, as well as its assayed downstream targets, thus validating the compromised osteogenic priming of undifferentiated precursors. In accordance, a reduced mineralization of the extracellular matrix - the summit of the osteogenic differentiation process - was further verified in STZ-derived cultures through Alizarin Red staining. The impaired osteogenic capability of differentiating diabetic MSCs has been previously established in both *in vitro* (207) and *in vivo* (90, 91) models.

Additionally, in undifferentiated MSCs from diabetic animals, expression of the adipogenic markers PPAR γ , IRS1, and IRS2 was significantly upregulated, while the expression of AP2 was not affected. PPAR γ is a key regulator of adipogenic differentiation and shifts the balance of MSCs fate by favoring adipocyte differentiation and thus, inhibiting osteoblast differentiation (208). An increased expression of PPAR γ has been verified in osteoblastic cells grown in hyperglycaemic conditions (183) and in growing osteoblasts from diabetic animals (190). Results on the present work suggest that the enhanced adipogenic priming might be related to the upregulation of IRS-1 and

IRS-2, since the activation of these adapter proteins and associated PI 3-kinase pathway were found to be determinant for the activation of PPAR γ , resulting in the induction of adipogenic differentiation (209). Most interestingly, the expression of AP2, abundantly synthesized in the late phase of developing adipocytes (209), was found not to differ significantly between growing STZ and control-derived MSCs cultures. This seems to support an increased priming of the adipogenic trigger by diabetic-derived MSCs, without an effective progression into this differentiation pathway.

The assessment of significant signalling pathways revealed a reduced metabolic activity associated with ERK and WNT signalling, in STZ-derived MSCs cultures. Furthermore, a different regulation on the assayed osteogenic markers was verified in diabetic-derived cultures, as ALP expression was found to be enhanced by p38 pathway and diminished by WNT pathway; while ERK, WNT, and p38 pathways converged to a decreased expression of RUNX2. Contrariwise, PPAR γ levels were found to be increased in STZ-derived cultures, in close association with the three assayed pathways.

These results are in accordance with previous literature data on the activity of the different signalling pathways. ERK pathway activation was shown to be crucial for the regulation of cell proliferation, and also to play a determining role in the differentiation of MSCs (210). Briefly, the specific inhibition of this pathway was found to block the osteogenic differentiation of human MSCs and to induce the adipogenic differentiation of these cells (211). ERK activation was thus found to stimulate osteoblastic-specific gene expression through RUNX2 activation (212). Of additional relevance, insulin and insulin-like growth factor 1, known to be reduced on the diabetic milieu, was found to induce osteoblast proliferation and differentiation via ERK activation (213).

WNT signalling has also been associated with the osteogenic commitment and adipogenic repression of precursor cells, namely by the stimulation of RUNX2 and downregulation of PPAR γ , respectively (214). In this work, the expression of both osteogenic markers, ALP, and RUNX2, was downregulated in association with WNT signalling, while the expression of PPAR γ was enhanced, in STZ-derived cultures, thus sustaining an impaired activation of this signalling pathway. In type 1 diabetes, a decreased osteoblastogenesis was found to be associated with the inhibition of WNT pathway (215); while hyperglycaemia was found to target distinct components of the WNT pathway in osteoblasts, leading to its inhibition (216), in a process mediated, at least in part, by the increased activation of p38 pathway (217).

In the present study, the metabolic activity of the STZ-derived cultures was found to be enhanced through p38 activation, which was also associated with an increased ALP and PPAR γ expression. p38 activation was previously found to specifically increase ALP expression in osteoblastic populations, despite its negative association with the osteoblastic differentiation process (217, 218). This correlates with the findings of the present research in which an increased ALP expression and activity were verified in STZ-derived MSCs cultures, regardless of the reduced RUNX2 activity and impaired osteogenic priming. Furthermore, within the diabetic milieu, an increased activation of p38 has been verified, through different signalling approaches and cellular populations (219), thus supporting an increased p38 activity within STZ-derived cultures.

Generally, MSCs developed within a diabetic microenvironment, and cultured in undifferentiating conditions, displayed an impaired functionality, with diminished cell proliferation and increased apoptosis. Furthermore, an altered cytoskeleton

organization, increased ALP activity, and decreased collagen synthesis were verified. In terms of gene expression, altered osteogenic gene profile was verified, with decreased expression of RUNX2 and several of its downstream targets; while increased adipogenic gene expression was attained. Furthermore, the osteogenic-induction of cultured STZ-derived MSCs confirmed the impaired osteogenic phenotype, through gene expression analysis and assessment of the extracellular mineralization process. Overall, this behaviour is consistent with an impaired osteogenic priming of bone marrow-derived undifferentiated MSCs, that can be associated with the maintenance of a less mature phenotype of this population (220). In agreement, a deficiency in the conversion of immature mesenchymal cells to mature osteoblasts was verified in a marrow ablation model of diabetic mice (91). Assessment of relevant signalling pathways revealed a decreased activity of ERK and WNT, and an increased signalling through p38, which may determine, at least in part, the verified functional hindrances.

3.6 - CONCLUSION

The present study revealed that diabetic environment may affect MSCs signalling and functionality in an intrinsic and long-lasting way. These alterations may contribute to the diabetic-derived bone alterations, as verified by the impaired behaviour of osteogenic-induced cell populations acquired from diabetic animals, within the bone tissue of animal models of experimental diabetes and in clinical trials with diabetic patients.

Thereby, is possible that local or systemic strategies, specially targeted to modulate the verified hindrances, may improve the functionality of MSCs in diabetic conditions and subsequently enhance the metabolism and regeneration of the bone tissue in diabetic conditions.

**CHAPTER 4 – DOXYCYCLINE ENHANCES THE
OSTEOGENIC FUNCTIONALITY OF DIABETIC-
DERIVED MESENCHYMAL STEM CELLS**

4.1 – INTRODUCTION

Diabetes mellitus is a common metabolic disorder associated with hyperglycemia and hyperlipidemia, due to lack of insulin production or peripheral insulin resistance (221).

DM affects bone metabolism, as a close and complex association between fragility fracture risk and DM, of both type 1 and type 2 diabetes, have been established in clinical trials (182, 221, 222). Insulinopenia as occurs in T1D, or resistance to the metabolic actions of insulin, as occurs in T2D, are both associated with several deleterious consequences for skeletal health (223). Despite the emerging clinical evidences, the mechanisms underlying the diabetes-induced skeletal alterations are not completely understood. *In vitro* studies with relevant cell populations developed under diabetic-stimulated conditions support a decreased activation of osteogenic transcription factors and a reduced expression of osteoblastic markers (186, 224).

In this context, our group has recently demonstrated that bone marrow-derived mesenchymal stem cells developed within the diabetic environment have impaired osteoblastic priming, with an increased activation of the adipogenic pathway (224). Furthermore, data from *in vivo* studies with experimental diabetic models and clinical trials with diabetic patients sustain an impaired bone metabolic activity, as biochemical markers of bone formation and histomorphometric indices of both trabecular and cortical bone seem to be significantly impaired (80, 82). Accordingly, the development of therapies involving anabolic agents for bone have been particular regarded.

Tetracyclines, by their non-antibacterial properties, were earlier found to be effective in the reduction of distinct diabetes-induced abnormalities in the diabetic rat model. For instance, a decreased weight loss was verified, as well as a substantial reduction in the activity of several matrix metalloproteinases. MMPs are members of a family of zinc-dependent proteases that can cleave native collagens, playing an important role in the extracellular regulation of cell growth, migration, and extracellular matrix remodeling (225). In the diabetic environment, MMPs levels are found to be pathologically elevated, which may account for the increased degradation and altered collagen content of the bone's ECM. Tetracyclines administration was found to suppress MMPs-mediated catabolic processes, resulting in the regularization of the collagen synthesis and structure, and in the improvement of the compromised bone remodeling. In a diabetic animal model, TCs were found to increase the procollagen and collagen synthesis, and to enhance osteoblast activity, regarding the production and mineralization of bone matrix. Moreover, in bone and cartilage, MMPs play an important function during embryonic endochondral ossification, modeling/remodeling of bone postnatally, and during physiological bone repair/regeneration (226, 227). Furthermore, MMP's relation with collagen synthesis and structural organization was broadly verified as the subsequently effects on bone remodeling (159).

In animal models of both low-turnover bone loss (osteopenic diabetic rat), as well as in high-turnover bone loss (ovariectomized rat), tetracyclines administration was found to increase the bone formation. Accordingly, the use of second generation tetracyclines, such as the administration of doxycycline in either local or systemic sub-antimicrobial doses (SDD), have been widely studied with the aim to decrease host tissue breakdown (8, 228). Within these doses ranging from 0.5 µg/mL to 1 µg/mL,

doxycycline was found to exert beneficial modulatory effects in both physiological and pathological conditions in several tissues including bone (7, 158). Apart from the inactivation of MMPs, TCs were also found to have a direct anabolic effect in bone metabolism. Briefly, in experimental pathological conditions, TCs increased the procollagen and collagen synthesis, enhanced osteoblast activity in the formation and mineralization of bone matrix formation during disease (diabetes); and increased the number of active osteoblasts relatively to inactive (7, 158).

4.2 – RESEARCH HYPOTHESIS AND OBJECTIVES

In this module we aim to conduct a detailed characterization of the molecular events developing within mesenchymal stem cell cultures, derived from STZ diabetic-induced and control animals, in presence and absence of a low dosage regimen of doxycycline. Grown cultures will be characterized regarding proliferation, functional activity and differentiation, and evaluation of the osteogenic priming. In addition, the effect of the low dosage regimen of doxycycline within the bone remodelling and regeneration, will be further addressed, with the *ex vivo* model of the neonatal rat calvarial bone defect regeneration.

4.3 – MATERIALS AND METHODS

4.3.1 – ANIMALS

This study was conducted in accordance with accepted standards for the humane animal care and manipulation. Procedures were approved by *Direção Geral de Alimentação e Veterinária* and encompassed the standards for the protection of experimental animals, according to the Portuguese and European legislations. Briefly, 12 male Wistar rats (7 to 8 weeks old), acquired from a certified vendor, were housed in groups of 2, in conventional type II cages, and allowed standard rat pelleted diet (4RF21 Mucedola, Settimo Milanese, Italy) and water *ad libitum*, in accordance to home office regulations.

Experimental diabetes was induced in 6 animals, by a single intraperitoneal (IP) injection of streptozotocin, Sigma®, ($60 \text{ mg} \cdot \text{kg}^{-1}$, in 10 mM citrate buffer, pH 4.5) – STZ group (n=6). Control animals were injected with vehicle alone – control group (n=6). Glycemic levels were confirmed 3 days after administration with a glucometer (Accu Check GO, Roche Diagnostics). Animals with blood glucose levels $\geq 300 \text{ mg} \cdot \text{dl}^{-1}$ were considered to be diabetic and enrolled into the STZ group.

4.3.2 – CHARACTERIZATION OF THE EXPERIMENTAL GROUPS

Six weeks following STZ or control administration, glycemic levels were determined in the peripheral blood. Following, animals were euthanized by exsanguination under general anesthesia (intraperitoneal injection of pentobarbital sodium 35 mg.kg^{-1}). Femurs and left tibias were harvested and processed for cell culture establishment. Right tibias were harvested, fixed in ethanol 70% and scanned by microcomputed tomography. Analysis were performed in a μ CT 35 (Scanco Medical), with a voxel size of $12 \mu\text{m}$, X-ray tube voltage of 70 kVp, current intensity of $114 \mu\text{A}$, and integration time of 600 ms. Quantitative histomorphometrical data of the trabecular content were conducted with the Scanco Medical software, version 6.0. Measured variables included bone volume per total volume (BV/TV), connective density (CD), trabecular number (Tb.N), trabecular thickness (Tb.Th) and trabecular separation (Tb.Sp).

4.3.3 – CELL CULTURES

Bone marrow-derived MSCs were isolated using a modification of the protocols previously described by Dobson (193) and Sekiya (194), for bone marrow harvest and MSCs isolation. Briefly, left and right femurs and left tibias were carefully excised, cleaned of soft tissues and decontaminated. Following, epiphyses were cut off and diaphyses were flushed out with Rat-Mesenchymal Stem Cell Growth Medium (Lonza). Nucleated cells were isolated with a density gradient (Ficoll-Paque Premium®),

resuspended in culture medium with 10% heat inactivated fetal bovine serum (FBS, Gibco), penicillin-streptomycin ($100 \text{ UI}\cdot\text{mL}^{-1} - 100 \text{ mg}\cdot\text{mL}^{-1}$, Gibco) and fungizone® amphotericin B ($2.5 \mu\text{g}\cdot\text{mL}^{-1}$, Gibco), plated and maintained in a humidified atmosphere (5% CO_2 /air, 37 °C) until around 70% confluence (approximately 15 days). Cells were enzymatically released (trypsin 0.04% and 0.25% EDTA solution), and seeded at a concentration of $10^4 \text{ cells}\cdot\text{cm}^{-2}$. Where noted, cultures were grown in the presence of doxycycline $1 \mu\text{m}\cdot\text{mL}^{-1}$ (Sigma-Aldrich). The culture medium was changed every 2-3 days and cultures were maintained for 12 days, and characterized as follows.

4.3.4 – CELL PROLIFERATION AND METABOLIC ACTIVITY

Metabolic activity of the cultures was estimated by the MTT assay. Briefly, cultures were incubated with MTT ($0.5 \text{ mg}\cdot\text{mL}^{-1}$, 4 hours). Formazan crystals were following dissolved and the absorbance was measured at 550 nm in an ELISA reader (Synergy HT, Biotek).

4.3.5 – CELL MORPHOLOGY

Fixed cultures (3.7% paraformaldehyde, 15 minutes) were stained for F-actin cytoskeleton and nucleus counterstaining. Cells were permeabilized (0.1% Triton, 5 minutes), incubated with albumin ($10 \text{ mg}\cdot\text{mL}^{-1}$), and treated with Alexa Fluor 488®-conjugated phalloidin (1:20 dilution, 20 minutes) and propidium iodide ($1 \mu\text{g}\cdot\text{mL}^{-1}$, 10

minutes). Cultures were observed in a confocal laser scanning microscope (Leica SP2 AOBS, Leica Microsystems).

4.3.6 – ALKALINE PHOSPHATASE ACTIVITY

Alkaline phosphatase (ALP) activity was determined in cell lysates by the hydrolysis of p-nitrophenyl phosphate into p-nitrophenol (30 minutes, 37 °C), assessed at 405 nm in an ELISA reader (Synergy HT, Biotek). ALP activity was normalized to total protein content (measured according to the Lowry method).

4.3.7 – APOPTOTIC BEHAVIOUR

Apoptosis was quantified by measuring caspase-3 activity with the EnzCheck® Caspase-3 Assay Kit #2 (Molecular Probes), according to manufacturer's instructions.

4.3.8 – COLLAGEN SYNTHESIS

Fixed cultures were stained with 0.1% Sirius red solution (BDH, UK) in saturated picric acid (1 hour), followed by rinsing with HCl (0.01N). Collagen matrix was photodocumented before stain dissolution in 0.1N NaOH, 30 minutes. The absorbance

was measured at 550 nm (Synergy HT, Biotek) and results were presented as % of staining compared to control.

4.3.9 – GENE EXPRESSION

Cell cultures were analyzed by qPCR for the expression of housekeeping beta-actin (β -actin), alkaline phosphatase (ALP), bone morphogenic protein-2 (BMP-2), collagen type I (COL I), osteopontin (OPN), osteocalcin (OC), osteoprotegerin (OPG), and lipoprotein receptor-related protein 5 (LRP5). Total RNA was extracted using the NucleoSpin® RNA II Kit (Macherey-Nagel), according to the manufacturer's instructions. Total RNA concentration and purity were assessed by UV spectrophotometry by calculating A260nm/A280nm ratio. qPCR was conducted using the Bio-Rad iQ5 real-time PCR system (Bio-Rad, Hercules, CA, USA) using SYBR Premix Ex Taq kit (Takara).

The relative gene expression level was normalized to the internal control (β -actin) based on the $2^{-\Delta\Delta C_T}$ method.

Results were expressed as the percentage variation from control, corresponding to 100% at each time point. The primers used are listed on table 4.1.

Table 4.1 – Forward and reverse sequences of the primers used for the qPCR analysis.

GENE	FORWARD SEQUENCE	REVERSE SEQUENCE
B-ACTIN	AGTACCCCATTTGAACACGGC	TTTTCACGGTTAGCCTTAGG
ALP	GGCTCTGCCGTTGTTTC	GGGTTGGGTTGAGGGACT
BMP-2	AGTGACTTTTGGCCACGACG	CGCTCCGCTGTTTGTGTTT
COLLAGEN 1	TGGCAAGAACGGAGATGA	AGCTGTTCCAGGCAATCC
OSTEOPONTIN	AAAAATGCTCACCATCACTGC	AATTGCCACACTGACTTCCAC
OSTEOCALCIN	GCCCTGACTGCATTCTGCCTCT	TCACCACCTTACTGCCCTCCTG
OSTEOPROTEGERIN	ATTGGCTGAGTGTTCTGGT	CTGGTCTCTGTTTTGATGC
LRP5	TGCCACTGGTGAGATTGAC	ACTGCTGCTTGATGAGGAC

4.3.10 – NEONATAL CALVARIA DEFECT EX VIVO MODEL

In this protocol 10 new-born rats were used from 2 different litters. The protocol was conducted as previously described by Wu and co-workers (229) with several modifications. Briefly, the animals were euthanized at third day after birth by decapitation and the heads were disinfected with 70% ethanol. Following, the skin was carefully removed to expose the calvaria, and the parietal bones were dissected out and cleaned of remnant soft tissues. Full-thickness circular defects of 0.8 mm diameter were created through the parietal bones using a surgical instrument.

Bones were cultured concave-side down in 48-well cell culture microplates in α MEM supplemented according to experimental conditions. Accordingly, four experimental groups were established: (1) Control group (CTRL), supplemented with 10% FBS, penicillin-streptomycin ($100 \text{ UI.mL}^{-1} - 100 \text{ mg.mL}^{-1}$), fungizone ($2.5 \mu\text{g.ml}^{-1}$); (2) Diabetic group (GLC), supplemented with 10% FBS, penicillin-streptomycin ($100 \text{ UI.mL}^{-1} - 100 \text{ mg.mL}^{-1}$), fungizone ($2.5 \mu\text{g.ml}^{-1}$), and glucose (20 mM) in order to mimic blood glucose concentrations in diabetic condition; (3) Control with doxycycline group (CTRL Doxy), supplemented with 10% FBS, penicillin-streptomycin ($100 \text{ UI.mL}^{-1} - 100 \text{ mg.mL}^{-1}$) and fungizone ($2.5 \mu\text{g.ml}^{-1}$), and doxycycline ($1\mu\text{g.ml}^{-1}$); and (4) Diabetic with doxycycline group (GLC Doxy), supplemented with 10% heat inactivated foetal bovine serum (FBS, Gibco), penicillin-streptomycin ($100 \text{ UI.mL}^{-1} - 100 \text{ mg.mL}^{-1}$, Gibco) and fungizone/amphotericin B ($2.5 \mu\text{g.ml}^{-1}$, Gibco), glucose (20 mM, Sigma-Aldrich), and doxycycline ($1\mu\text{g.ml}^{-1}$, Sigma-Aldrich). Bones were maintained in a humidified atmosphere (5% CO_2 /air, 37 °C) for 15 days.

4.3.10.1 – OPTICAL MICROSCOPY

Newborn rat bones in culture were monitored regularly by phase contrast optical microscopy to assess qualitatively bone regeneration and remodeling over the 15 days of organ culture.

4.3.10.2 – SCANNING ELECTRON MICROSCOPY

At day 15, bones were rinsed with PBS and fixed with 1.5% glutaraldehyde (Fluka, Germany) in 0.14 M sodium cacodylate buffer (Sigma-Aldrich) for 20 minutes at room temperature. The samples were then dehydrated in a sequence of ethanol-water solutions, for 10 minutes each, using increasing concentrations of ethanol up from 50% to 100%. The samples were then fixed with hexamethyldisilazane (Sigma-Aldrich) at the same increasing concentration sequence and left to dry overnight inside the laminar flow cabinet. Subsequently, samples were sputter-coated (SPI-Module) with a thin gold/palladium film and observed in SEM (FEI Quanta 400FEG). Mineralization nodules were evaluated by energy-dispersive X-ray spectroscopy (EDS) analysis of the calcium phosphates deposits on cell layer surface. The percentage of regenerated area was calculated using the ImageJ software to address the defects area.

4.3.11 – STATISTICAL ANALYSIS

Three independent experiments were performed, with the cell cultures established from different animals. In quantitative assays, each point represents the mean \pm standard error of 6 replicates. Statistical analysis was done by one-way analysis of variance (ANOVA). p values ≤ 0.05 were considered significant.

4.4 RESULTS

4.4.1 – ESTABLISHMENT OF A DIABETES EXPERIMENTAL MODEL

All animals, of both control and STZ groups, survived throughout the duration of the experimental protocol. Whether no significant differences were found on the initial weight (control, 339.5 ± 23.1 ; STZ, 317.0 ± 33.8), 6 weeks following diabetic induction, animals of the control group increased in weight (396.7 ± 37.3), while animals of the STZ group loss weight (228.1 ± 26.41). Further, at euthanasia, all diabetic animals had glycemic levels over 300 mg. dl^{-1} , while animals from the control group had a mean glycemia of $\pm 120 \text{ mg. dl}^{-1}$.

4.4.2 – EVALUATION OF DIABETES EFFECTS ON BONE

The microtomographic analysis of the proximal tibia also revealed significant differences between control (figure 4.1, right) and STZ group (figure 4.1, left). Comparatively, a decreased BV/TV and CD were verified. Furthermore, in terms of the characterization of the trabecular structure, diabetic animals reported a significant reduced Tb.N and Tb.Th, as well as in creased Tb.Sp. The resulting morphometric indexes are shown in table of figure 4.1.

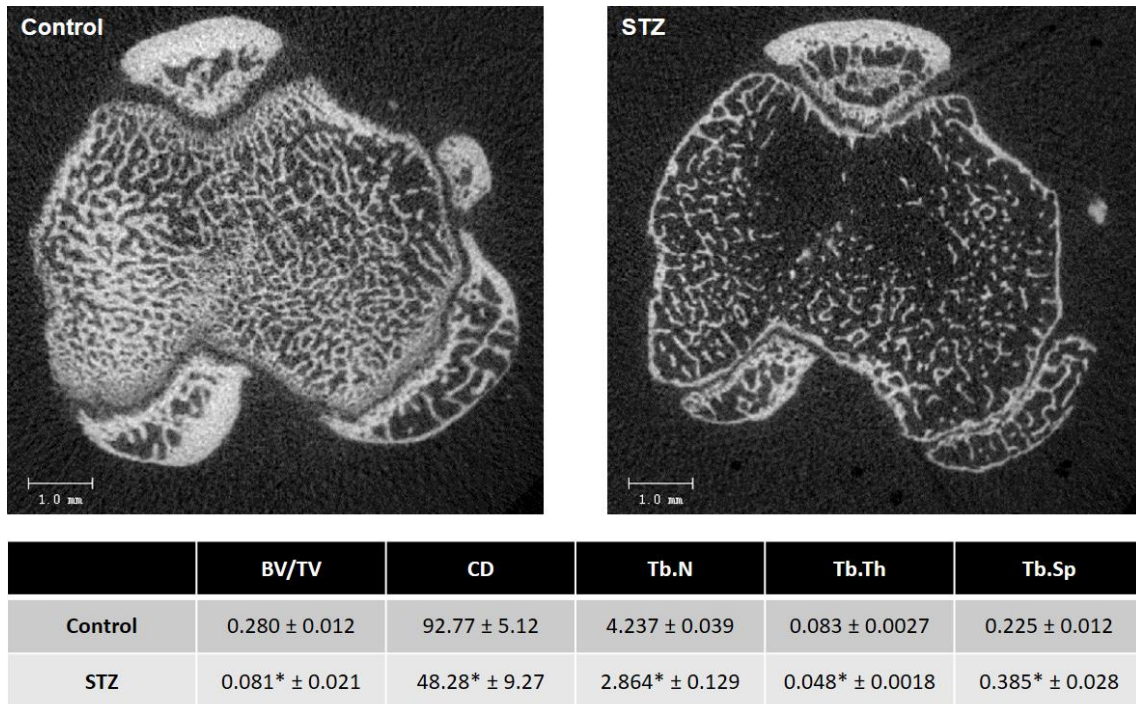


Figure 4.1 – Top: representative 2D microtomographic images of the proximal tibia metaphysis, in control (right) and STZ (left) animals ($n = 6$). Bottom: table of microstructural parameters of the trabecula structure of the proximal tibia. The addressed variables included BV/TV (bone volume per total volume), CD (connective density), Tb.N (trabecular number), Tb.Th (trabecular thickness), and Tb.Sp (trabecular separation). * - significantly different from control ($P \leq 0.05$).

4.4.3 – CHARACTERIZATION OF MSCS CULTURES GROWN IN THE PRESENCE OF DOXYCYCLINE

MSCs cultures were established from the bone marrow of control and STZ-induced diabetic animals. In order to disclose the effect of a low dosage doxycycline regimen on the behaviour of diabetic MSCs, STZ-derived cultures were grown in the absence and in the presence of doxycycline, at a concentration of $1 \mu\text{g}\cdot\text{ml}^{-1}$. The antibiotic was renewed at every medium change that occurred 2 times a week.

4.4.3.1 – METABOLIC ACTIVITY AND CELL PROLIFERATION

The results concerning MTT assessment of cells viability and proliferation are shown in figure 4.2. MSCs cultures from control animals presented an increased metabolic activity until day 8, diminishing afterwards. STZ-derived cultures followed a similar pattern despite that, comparatively to control, a decreased metabolic activity was attained at day 8 and 12. The addition of doxycycline increased the metabolic activity of the STZ cultures from day 5 onwards. At this time point (day 5), the metabolic activity of STZ-derived cultures grown in the presence of doxycycline was significant higher than that of the controls. At late culture time points, i.e., days 8 and 12, no significant differences were found between doxycycline-treated STZ cultures and control.

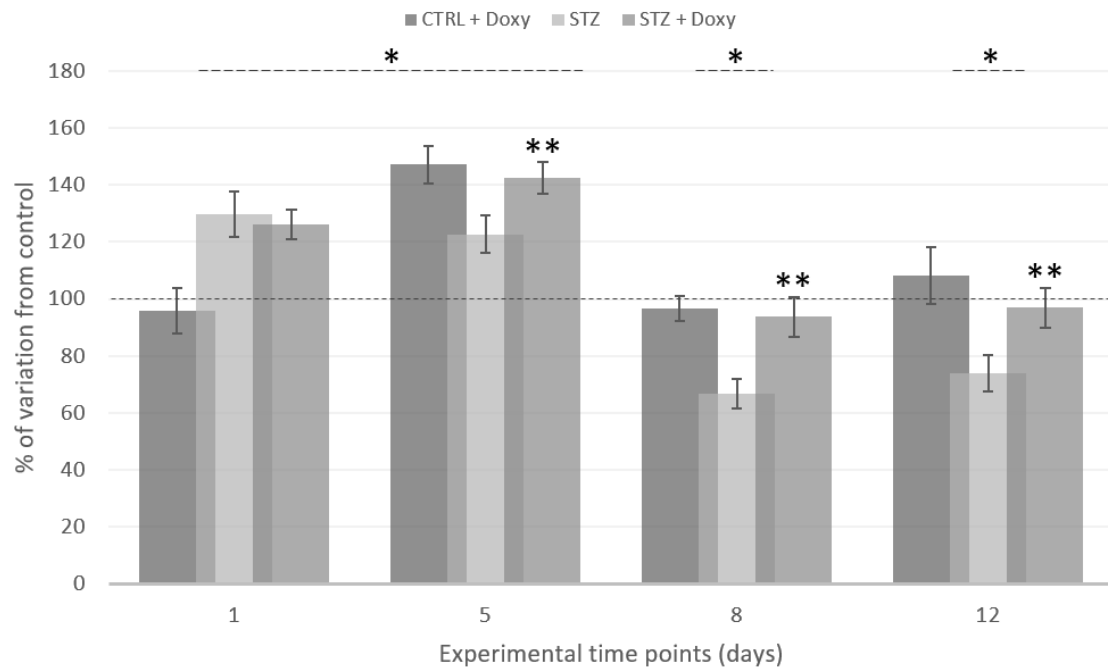


Figure 4.2 – Cell viability/metabolic activity (MTT assay) of rat bone marrow-derived cells cultured in presence and absence of doxycycline ($1 \mu\text{g.ml}^{-1}$) from both control and STZ-induced animals, for 12 days. Percentage of variation from control at each time point. * - significantly different from control ($P \leq 0.05$). ** - significantly different from STZ ($P \leq 0.05$).

4.4.3.2 – CELL MORPHOLOGY ANALYSIS

The morphology of established cultures was detailed with confocal laser scanning microscopy (CLSM), following staining of the actin cytoskeleton and nucleus counterstaining. Representative images are shown in figure 4.3. Control cultures, at day 3, presented the characteristic fibroblastic-like morphology, with elongated and polygonal cytoplasm. Numerous microfilaments could be identified in a dense network, with evidence of stress fibers formation. Strong labelling was often observed along cellular edge and within the extended cellular filopodia. Cells were found to proliferate actively and, at day 12, cells organized into a flattened sheet of a continuous cell layer. The addition of doxycycline to the culture system was found to increase actin cytoskeletal staining, with great evidence of stress fibers formation. At day 12, no significant differences were found between conditions.

The STZ-derived cultures showed a similar behaviour in this time course. However, at day 3, fewer stress fibers were visible on proliferating cells and the intense labelling at the cellular edge, broadly observed in control, was more rarely identified. The addition of doxycycline was found to increase cytoskeletal staining and stress fibers formation, particularly at early time points, i.e., day 3 of the culture.

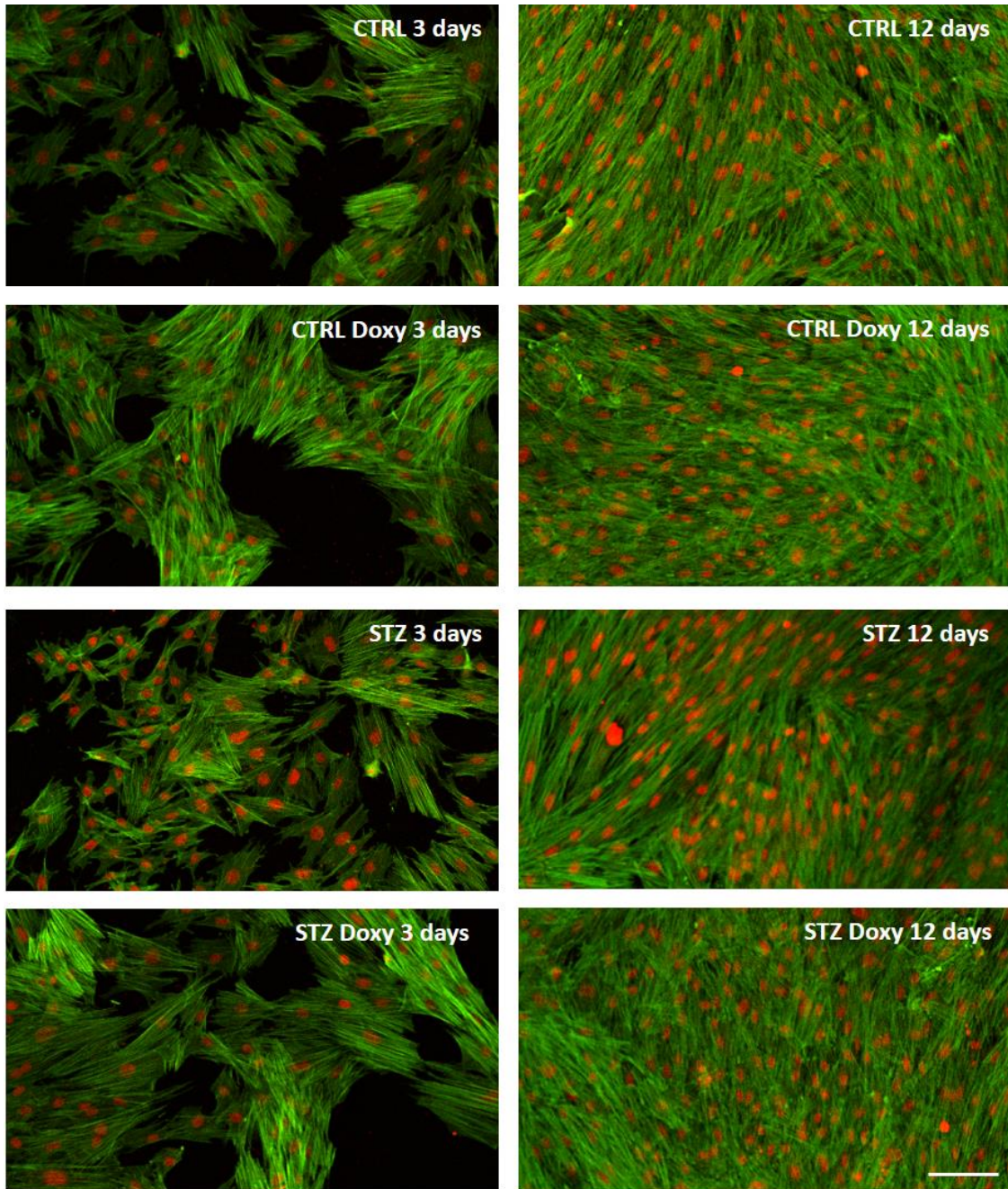


Figure 4.3 – Confocal laser scanning microscopy imaging of rat bone marrow-derived cell cultures, from control and STZ-induced diabetic animals in presence and absence of doxycycline, established for 12 days. Cytoskeleton was stained in green and nucleus counterstained in red. Scale bar corresponds to 200 μm .

4.4.3.3 – ALKALINE PHOSPHATASE ACTIVITY

ALP activity increased throughout the experimental period for both cultures established in the absence and presence of doxycycline (figure 4.4). The addition of doxycycline significantly increased the activity of this enzyme at day 8 of the culture and forward.

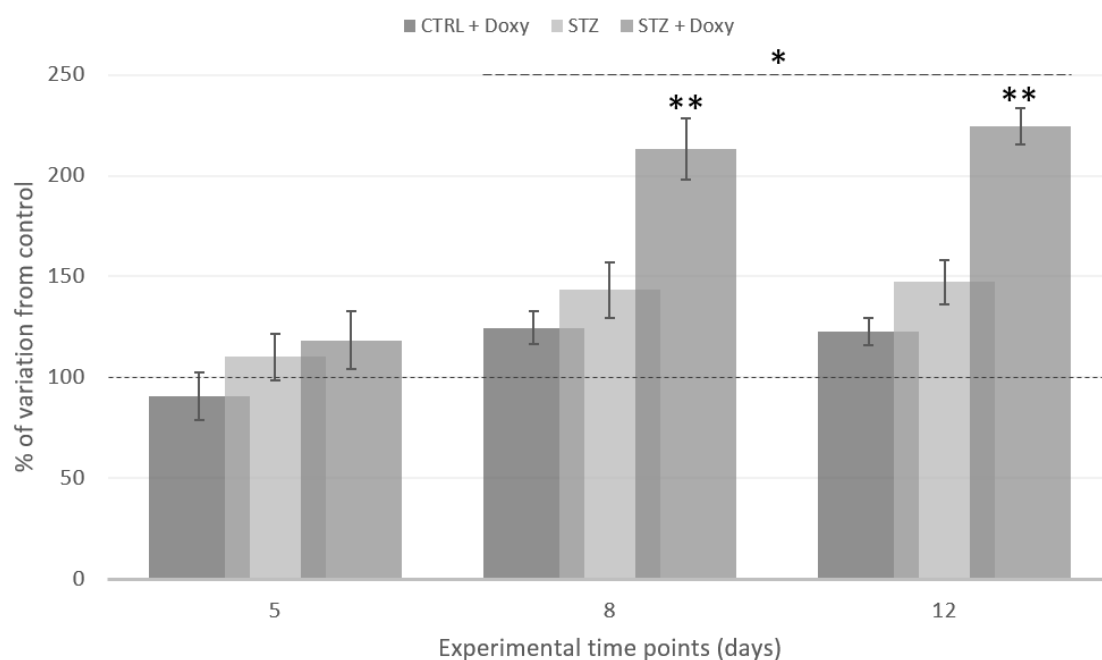


Figure 4.4 – Alkaline phosphatase activity (ALP per total protein content) of rat bone marrow-derived cells cultured in presence and absence of doxycycline ($1 \mu\text{g} \cdot \text{ml}^{-1}$) from both control and STZ-induced animals, for 12 days. Percentage of variation from control at each time point. * - significantly different from control ($P \leq 0.05$). ** - significantly different from STZ ($P \leq 0.05$).

Histochemical assessment of ALP confirmed biochemical data, revealing an increased staining of the cultures grown in the presence of doxycycline (figure 4.5).

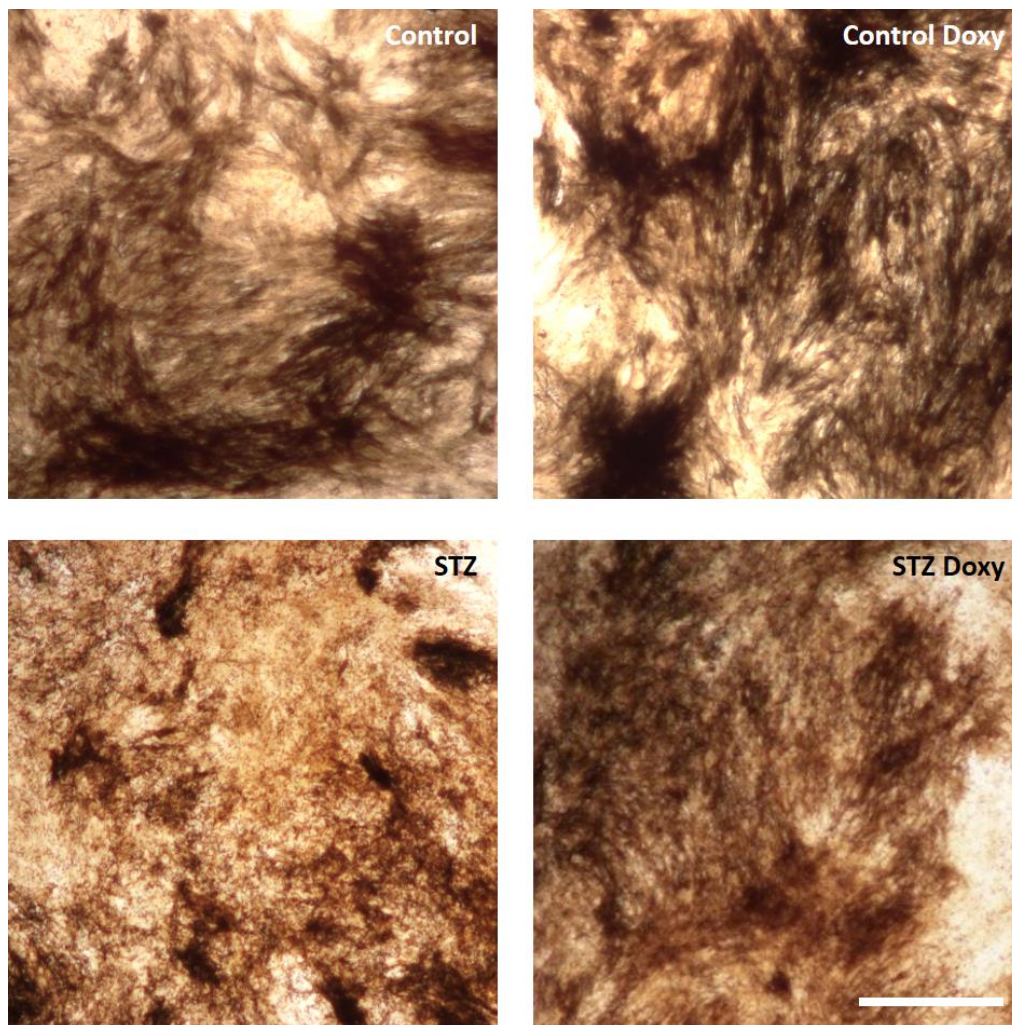


Figure 4.5 – Alkaline phosphatase staining of rat bone marrow-derived cell cultures, established for 12 days, from control and STZ-induced diabetic animals in presence and in absence of doxycycline. Scale bar corresponds to 300 μm .

4.4.3.4 – APOPTOTIC BEHAVIOUR

Results regarding the caspase 3 activity assay to apoptosis evaluation are shown in figure 4.6 below. STZ-derived cultures presented an increased apoptosis, as comparing to control. Significant higher levels of caspase-3 activity were verified at days 8 and 12 of the STZ cultures. The addition of doxycycline did not significantly increase the apoptotic index of the cultures.

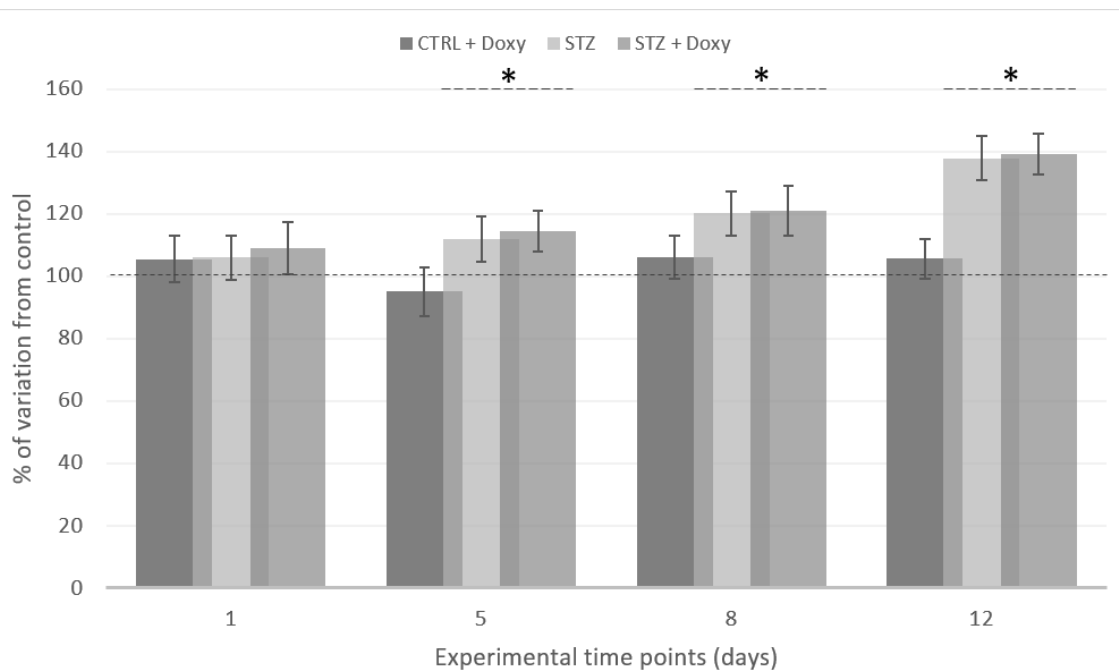


Figure 4.6 – Apoptotic analysis (caspase-3 activity assay) of rat bone marrow-derived cells cultured in presence and in absence of doxycycline ($1 \mu\text{g. ml}^{-1}$) from both control and STZ-induced animals, for 12 days. Percentage of variation from control at each time point. * - significantly different from control ($P \leq 0.05$).

4.4.3.5 – COLLAGEN SYNTHESIS

Total collagen synthesis was addressed by the Sirius red histochemical staining technique (figure 4.7 below).

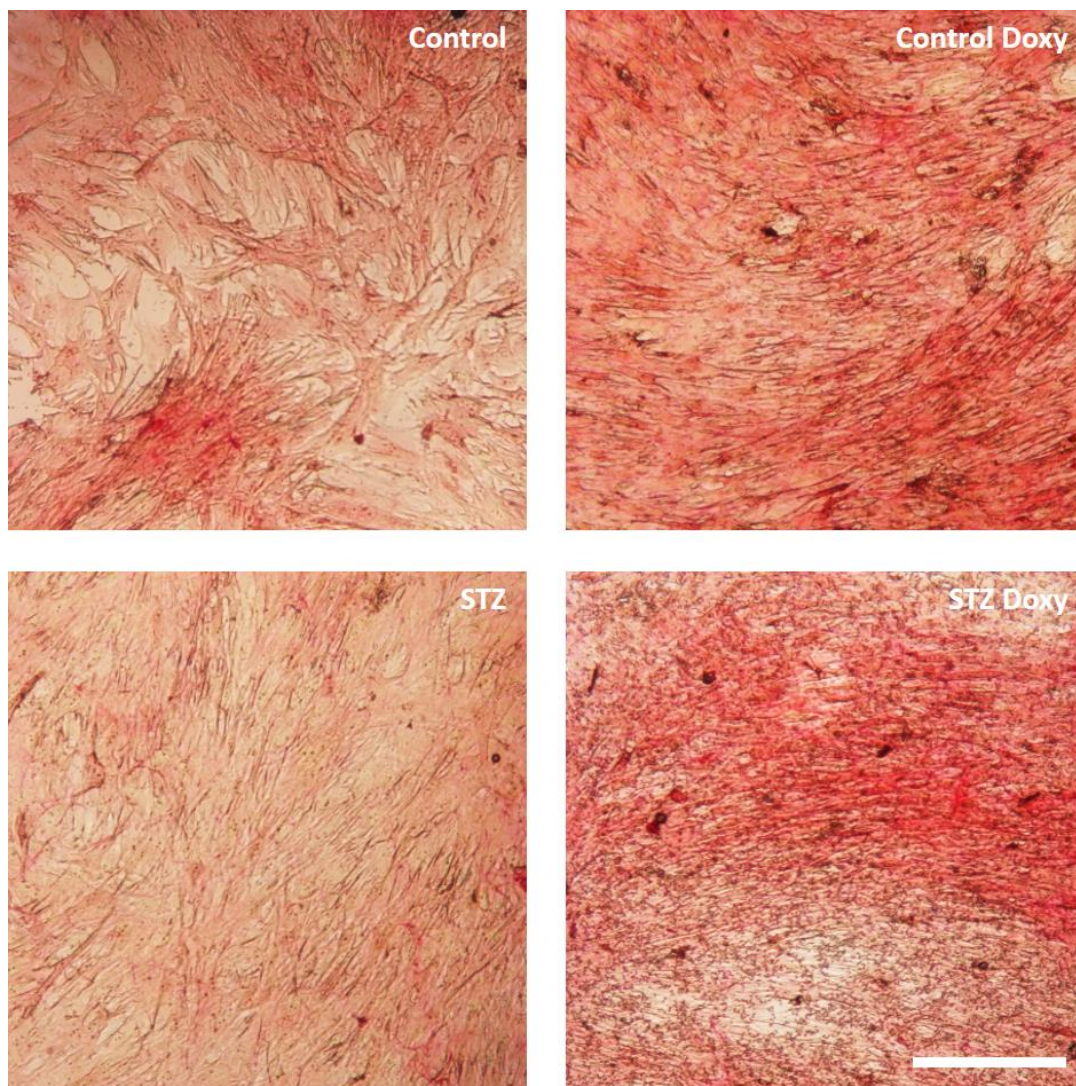


Figure 4.7 – Total type 1 collagen staining of rat bone marrow-derived cell cultures, established for 12 days, from control and STZ-induced diabetic animals in presence and in absence of doxycycline. Scale bar corresponds to 750 μm .

A qualitative analyze was conducted on stained micrographs of the cultures, while a quantitative determination of the stained products was conducted and prone to statistical analysis. In control cultures, an increased collagen synthesis was verified by the increased staining intensity of the cultures. Comparatively, STZ-derived cultures revealed a decreased collagen synthesis, which was found to be significant at day 12 of the culture period. The addition of doxycycline to the STZ culture environment significantly increased total collagen synthesis. Comparatively, a significantly higher staining intensity was found in doxycycline treated-cultures, at day 12. Quantitative colorimetric determination of the stained products supported the qualitative histochemical evaluation (figure 4.8).

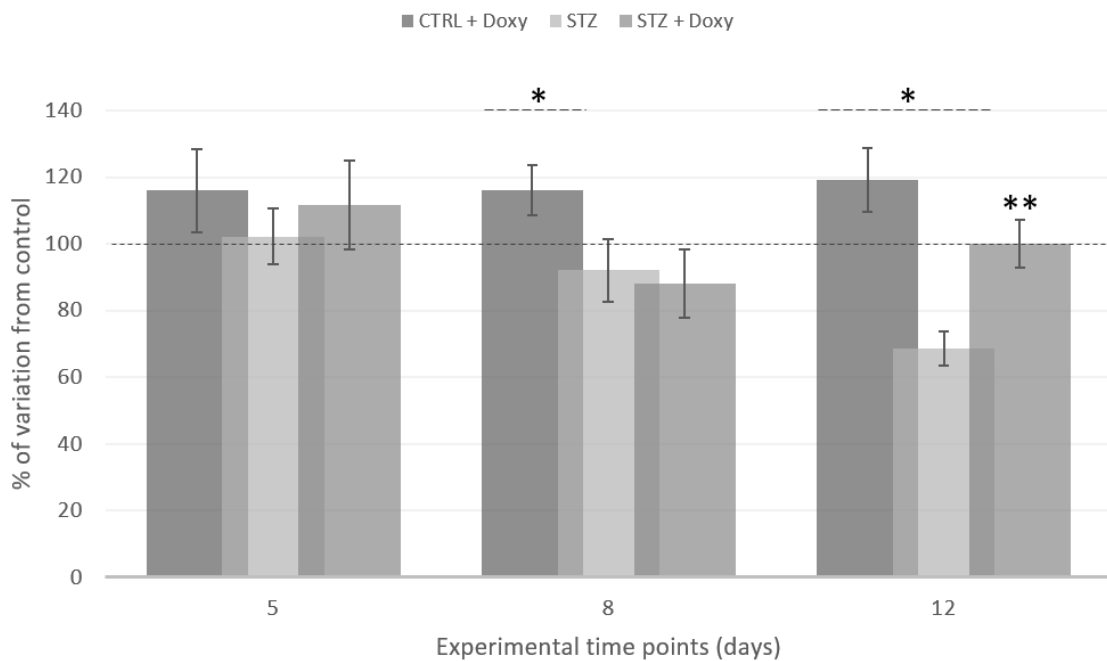


Figure 4.8 – Colorimetric determination of the total collagen stained product within the established MSCs cultures from both control and STZ-induced diabetic animals in presence and absence of doxycycline. Results were expressed as the

percentage variation from control corresponding to 100% at each time point. * - significantly different from control ($P \leq 0.05$). ** - significantly different from STZ ($P \leq 0.05$).

4.4.3.6 – GENE EXPRESSION

qPCR analysis showed the expression of significant osteogenic markers, from both control and STZ-derived cell cultures in the presence and absence of doxycycline. The results are shown in figure 4.9. Broadly, in STZ-derived cultures, a significantly reduced expression of the osteogenic genes BMP-2, COL1 α 1, OPN, LRP5, OC and OPG were verified, whether a higher ALP expression was attained, particularly at day 5. The addition of doxycycline broadly induced the expression of osteogenic markers, in both control and STZ-derived cultures.

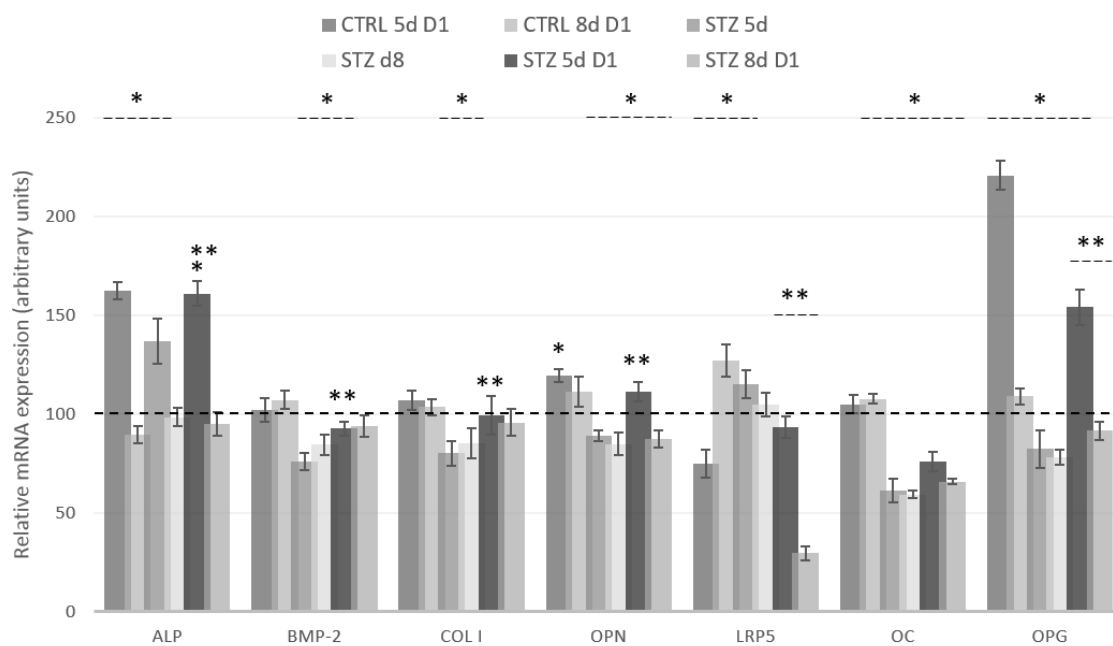


Figure 4.9 – qPCR gene expression analysis of ALP, BMP-2, Col 1, OPN, LRP5, OC, and OPG in MSCs cultures, established for days 5 and 8, from control ($n = 6$) and STZ-induced diabetic animals ($n = 6$). Cultures were grown in undifferentiating (STZ) and osteogenic-differentiating (Osteo STZ) conditions. Results were expressed as the percentage variation from control corresponding to 100% at each time point. * - significantly different from control ($P \leq 0.05$). ** - significantly different from STZ at the same time point ($P \leq 0.05$).

4.4.4 – CALVARIAL BONE DEFECT REGENERATION – EX VIVO MODEL

Organ cultures of new-born rat in physiologic and pathological diabetic-like conditions were maintained for 15 days. The method aimed to analyze the effects of

SDD in bone regeneration and remodeling in an *ex vivo* model which comprises other variables than a type-specific cell culture such as the organ structure and tissue properties while keeping the model under the complexity of a systemic interferences as in the case of *in vivo* bone defects regeneration protocols. The percentage of regenerated are was estimated by using the software ImageJ.

4.4.4.1 – PHASE CONTRAST MICROSCOPY EVALUATION

Calvaria bone defect regeneration was qualitatively addressed by phase contrast microscopy and the evolution throughout the organ culture span are shown in figure 4.10. Optical microscopy photodocumented images showed progressive and concentric bone defect regeneration with cognizable new bone tissue formation on defect borders, in the four experimental conditions, from day 0. At day 8, an apparent higher regeneration in both GLC and GLC Doxy groups was registered. However, at day 20, total bone regeneration was attained and new bone remodeling seemed to take place in all experimental groups with exception of GLC group which failed to achieve full regeneration of bone defect.

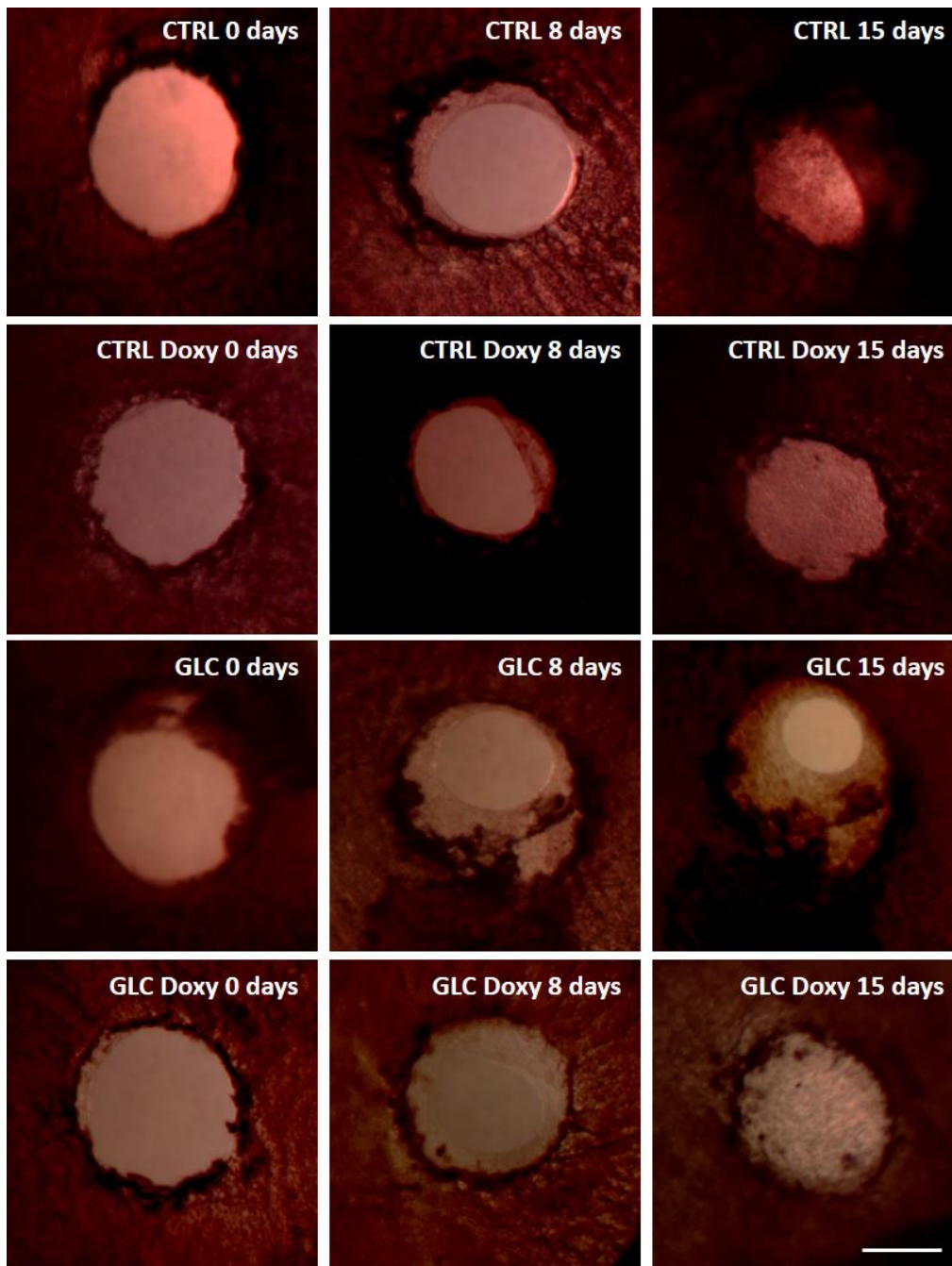


Figure 4.10 – Phase contrast optical microscopy images obtained at days 0, 10 and 20 for the established experimental conditions of new-born rat calvarial organ culture, following the establishment of the defect. Scale bar corresponds to 400 μm .

4.4.4.2 – CALVARIAL BONE DEFECT REGENERATION – SCANNING ELECTRON MICROSCOPY EVALUATION

Samples surface morphology and bone defect regeneration were analyzed by SEM and the results are shown at figure 4.11 below. The images obtained by SEM evaluation showed accordance with phase contrast microscopy in that bone regeneration occurred from day 0 with visible layers of newly formed bone along the defect borders. Accordingly, full bone regeneration was attained for all experimental conditions but the GLC condition.

The circular defects in CTRL, CTRL Doxy and GLC Doxy groups were closed however the phase of regeneration was different between conditions. SEM revealed a significantly thicker new bone membrane in the CTRL Doxy group and comparison with the other conditions. In contrast, in GLC group, newly formed tissue was considerably thinner in comparison with CTRL and GLC Doxy groups.

Through EDS analysis, it was possible to identify the deposition of Ca/P rich nodular structures, a process substantiating the development of a mineralized matrix within the regenerated area (figure 4.12). The addition of doxycycline seems to increase the mineral deposition within the mineralized tissues.

The percentages of regenerated area were calculated for each experimental condition. The results were expressed in a percentage of regenerated area in relation with the size of the original defect and are shown in figure 4.13. A reduced defect healing was verified for diabetic simulated conditions. However, the addition of doxycycline was found to enhance the healing process in diabetic conditions, being achieved results similar to control.

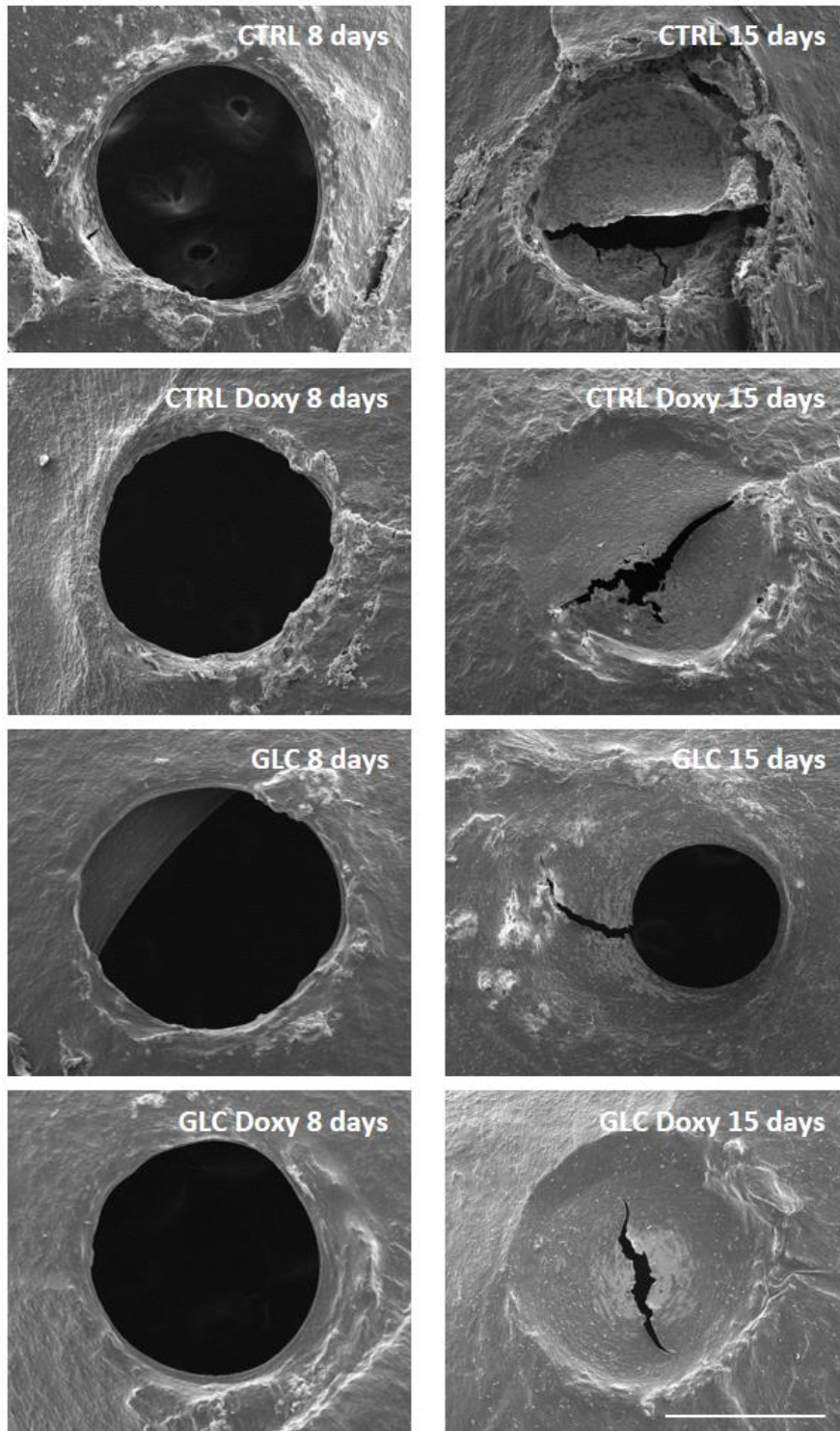


Figure 4.11 – SEM images of new-born rat parietal bone at days 8 and 15, following the establishment of the defect. Scale bar corresponds to 500 μm .

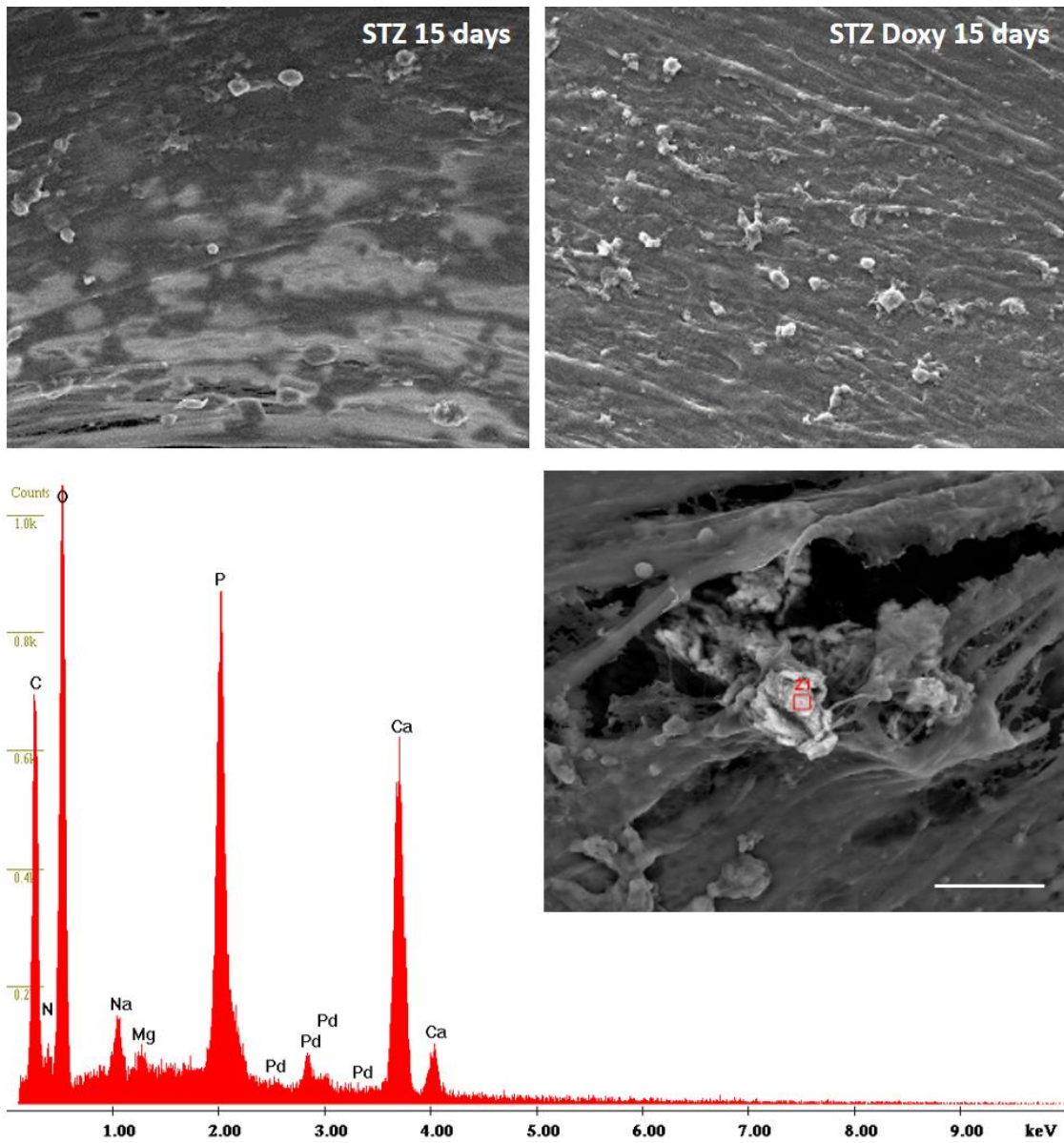


Figure 4.12 – SEM images of mineralization deposits after 15 days of culture of new-born rat parietal bones, following the establishment of the bone defect. Assessed area is within the newly formed tissue. Scale bar corresponds to 20 μm .

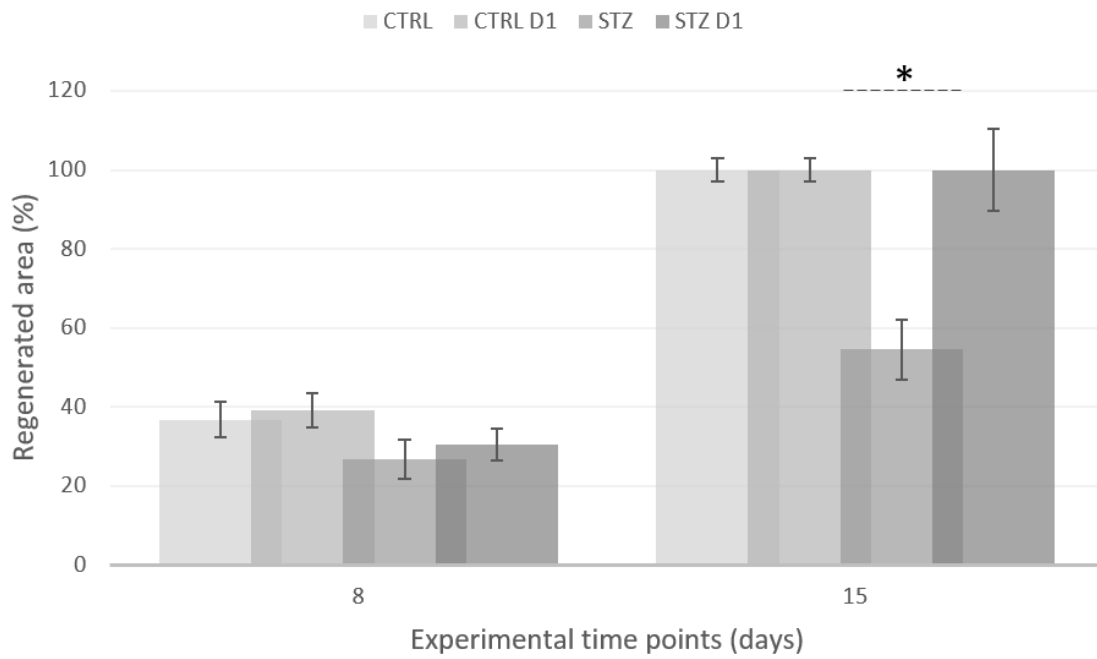


Figure 4.13 – Percentage of regenerated area along the 15 days of new-born rat parietal bones' culture, following the establishment of the defect. * - significantly different from control ($P \leq 0.05$).

4.5 – DISCUSSION

Diabetes has been previously shown to affect bone tissue remodeling and formation. Data from animal models and clinical trials sustain that osteopenia and osteoporosis may be frequent complications of T1D, both in children and adults, being associated with a decreased bone density and increased bone fracture risk (80, 221, 230). In contrast, whether T2D has not been typically associated with decreased mineral mass and, in fact, has been more often associated with increased BMD, new data show that bone quality and bone microarchitecture may be compromised in both conditions (5, 182), converging to a sustained increase in the risk to fracture, that may be contributory from both forms of diabetes.

Additionally, *in vitro* cell culture studies support a deficient function from osteoblastic and osteoprecursor populations (75, 93). We have previously shown that diabetic-derived MSCs grown on undifferentiating conditions, report an impaired cell functionality, with diminished cell proliferation, increased apoptosis and altered gene expression profile – i.e., decreased expression of Runx2 and several of its downstream targets and an increased adipogenic gene priming (224). These alterations may withstand a deficiency in the conversion of diabetic immature mesenchymal cells to the osteoblastic phenotype; a process that may be mediated by the decreased activity of ERK and WNT, and an increased signaling through p38 signaling pathway (217, 219).

In this work, we have shown that doxycycline, in a low dosage regimen, was found to enhance the osteogenic capability of MSCs derived from STZ-induced diabetic rats. Briefly, this antibacterial agent was found to enhance cell proliferation and metabolic

activity, without interfering with cell apoptosis. In addition, a higher total collagen production was verified in doxycycline-treated cultures, which, at later culture time points, was found to exceed the production of control. The expression of osteogenic genes was also found to be upregulated, particularly, at early culture time points. Within the *ex vivo* model, the addition of doxycycline was further found to improve defect healing in diabetic-simulated conditions and enhance mineral deposition.

Tetracyclines, due to their capability to inhibit collagenases and other host-derived matrix metalloproteinases (MMPs), in a process independent of their antibacterial activity, have been widely used in the modulation of local and systemic conditions in which the excessive activation of these enzymes is the hallmark feature of the disease pathogenesis (145, 231). More recently, the use of TCs within the modulation of conditions leading to reduced bone mass, either locally (e.g., periodontitis-mediated alveolar bone loss) or systemically (e.g., osteopenia/osteoporosis), has brought new attention into the clinical use of these drugs (232-234).

Low dosage regimens of tetracyclines were previously found to induce an anabolic action on the differentiation of osteoprecursor populations. Low levels of doxycycline (ranging from 0.1 to 1 μ M) were found to increase cell proliferation and to stimulate the osteogenic differentiation of precursor cells (235, 236). Our group has previously shown that low concentrations of both doxycycline and minocycline, added to growing human osteoblastic populations, were found to increase the metabolic activity and the osteogenic potential, with increased levels of alkaline phosphatase activity and culture mineralization (236). In accordance, treatment of osteoprogenitor cell cultures with low dosage doxycycline was found to report osteoinductive effects over growing cells, in a

similar way to the addition of bone morphogenic protein 2 (BMP-2) – a known osteogenic inducer (237). Osteoblastic cultures established on biomaterials' surfaces adsorbed with low levels of tetracyclines, were also found to reveal low cytotoxicity and an improved osteogenic activation (238, 239). Some reports sustained dissimilar results of tetracyclines activity over osteoblastic-related populations, supporting a cytotoxic effect of these drugs. These studies broadly addressed higher levels of tetracyclines and described an impaired osteoblastic proliferation and differentiation (240-242). Attained deleterious effects may be essentially dose-dependent, as in a previous report, addressing the effect of doxycycline and minocycline (1 to 50 $\mu\text{g}\cdot\text{ml}^{-1}$) in human osteoblastic populations, cytotoxic effects were significantly noticed when concentrations over 10 $\mu\text{g}\cdot\text{ml}^{-1}$ were used (236).

Anabolic effects of tetracyclines were also demonstrated in clinical studies. In a 2-year long placebo-controlled clinical trial, the subantimicrobial dosage doxycycline (SDD) regimen was found to significantly reduce the alveolar bone loss in pathologically-elevated periodontal pocket sites, exhibiting moderate to advanced periodontitis (232). Locally, SDD was found to significantly reduce collagenases and MMPs activity, at the same time that IL-1 β , a pro-inflammatory cytokine and a biomarker associated with bone resorption, was decreased (243). These data were highly correlated with the attained reduction of the levels of C-telopeptide to helix (ICTP), a pyridinoline-crosslink-containing degradation fragment of the C-terminal telopeptide region of type I collagen, a known biomarker of bone resorption. Most interestingly, SDD was also found to significantly reduced the serum ICTP levels, and to slightly reduced C-telopeptide cross-link of type I collagen (CTX), a deoxypyridinoline-containing degradation fragment of the C-terminal telopeptide region of type I collagen (234). SDD regimen was proven to

reduce serum biomarkers of systemic inflammation, including C-reactive protein (CRP) (233, 244), which has been found to reflect susceptibility to skeletal bone-deficiency disease (174). Overall, a reduced bone loss was verified, with clinical improvement, and evidence of a reduced collagen catabolism.

In accordance with the verified clinical improvement in bone's collagen metabolism, in the present experiment, doxycycline administration in STZ-derived cultures was found to enhance collagen synthesis to levels higher than those attained in control, as an increased expression of collagen type I gene and total collagen production were verified. Further, the expression of osteogenic genes and bone healing were verified.

Tetracyclines were previously found to have an anabolic effect on collagen synthesis in several tissues of the STZ-induced diabetic rat (245, 246). In addition to the ability to inhibit MMP-mediated extracellular collagen degradation (228), tetracyclines were found to increase both steady-state levels of type I procollagen mRNA and collagen synthesis (247, 248). Autoradiographic studies revealed that in the diabetic bone of STZ-induced rats, the synthesis of collagen and its precursors was restored to near-normal levels, following treatment with tetracyclines (249). Doxycycline was also found improve periodontal wound healing in experimental animal model of diabetes (250) and in the clinical forms of type I diabetes mellitus (251, 252) and type II diabetes mellitus (253), thus sustaining an enhanced collagen deposition within the regenerated tissues. Of additional relevance, tetracyclines may further prevent collagen degradation, as tetracycline impregnation was found to lessen degradation of collagen constructs in both diabetic and normoglycemic conditions (254).

While no data on the effect of tetracyclines on diabetes-derived osteoblastic populations has been reported, *in vivo* data supports an anabolic effect of these drugs on experimental models of diabetes, as further verified within the developed *ex vivo* assay. Low dose administration of minocycline to STZ-induced diabetic rats was found to preserve growth plate thickness, and to increase bone formation rates and cancellous bone areas to levels equivalent to those observed in control (255). Further, tetracyclines administration was found to prevent the development of the STZ-induced osteopenia in the rat, in a process associated with the restoration of the defective osteoblast morphology and metabolic activity (246). In fact, following treatment with tetracyclines, the osteoblastic synthesis of protein towards the osteoid matrix and alkaline phosphatase activity were broadly normalized in the humeri of diabetic rats (256).

4.6 CONCLUSION

Apart from the enhancement of the osteoblastic function in diabetic conditions, tetracyclines administration, in the particular case regarding a low dosage regimen of doxycycline, may further normalize the impaired osteogenic commitment of precursor populations, as detailed in the present study. Bone marrow derived mesenchymal stem cells, developed within a diabetic microenvironment were found to develop an increased commitment within the osteogenic lineage upon treatment with a low dosage regimen of doxycycline. Increased osteogenic gene expression was verified and a higher expression and synthesis of collagen were attained, and even found to overcome control levels. Further, within a bone defect healing model in diabetic-simulated conditions, doxycycline further enhanced tissue healing and mineralization.

This may further sustain that, apart from the modulatory effect over MMPs, with a positive effect on the diabetic bone, tetracyclines' release may further directly enhance the commitment of osteoblastic precursor populations, further enhancing the metabolic equilibrium within the diabetic bone.

**CHAPTER 5 – MINOCYCLINE-LOADED PMMA
BONE CEMENT AS A DELIVERY SYSTEM TO
ENHANCE BONE HEALING –
BIOCOMPATIBILITY EVALUATION IN A
DIABETIC MODEL**

5.1 – INTRODUCTION

Diabetes mellitus (DM) is becoming increasingly common and a major concern worldwide. It ensembles a group of metabolic disorders related with hindered insulin production and action, and consequent abnormal glucose metabolism. DM-associated long-term hyperglycaemia is known to cause severe damage and ultimately failure of a variety of tissues and organs (48, 53). Although the systemic causes are still unclear, it is accepted that type 1 diabetes affects the bone tissue more sharply than other diabetes forms (230). Accordingly, T1D is associated with numerous tissue alterations such as impaired cellular proliferation, differentiation and functionality, abnormal calcium metabolism and extracellular matrix organization (11, 224, 257, 258). These alterations together, lead to an unbalanced bone remodelling and bone mineral density reduction, which are consistent with reported bone weakening and increased occurrence of fractures (182).

With the increasing number of bone fractures, especially in long bones, the need for orthopaedic implants among diabetic patients is also increasing (11). Although the commonly used implantable medical devices have their cytocompatibility and biocompatible demonstrated prior to its clinical application, the biological response to foreign objects is still a major cause of implant failure and need for removal (259). Furthermore, DM is known to be associated with impaired inflammatory response and subsequent altered tissue healing, higher susceptibility to infections and greater rate of implant rejection (115, 116). Notwithstanding, the assessment of the biological

response to implanted biomaterials in diabetic conditions is rarely conducted and is fundamental for the safety biomaterials' application in compromised conditions.

Poly(methyl methacrylate) (PMMA) bone cements, represent a well-known and broadly used biomaterial group in orthopaedic surgeries, namely as fixatives of prosthetic devices and wound fillers. In addition to its biocompatibility, PMMA reveals other attractive properties such as toughness, high morphological adaptability and excellent resistance to biomechanical loading within the biological milieu (260). PMMA cements have been widely used as bone space-fillers, maintaining the targeted area cleaned of soft tissues and preventing wound contracture, while delaying bone regeneration until suitable conditions for bone healing and remodelling are attained (261). Nevertheless, the success of a device implantation may be compromised due to several factors including the injury extension, difficult access to the anatomical site, patient lifestyle (e.g. smoking, alcohol), medication, infections and chronic systemic metabolic diseases, such as diabetes (259).

Acute and chronic infections represent a major concern regarding bone implant surgeries as its development may lead to implant removal and infection management through a second surgery and a long lasting antibiotic treatment (259). A bright spot for bone cements implantation, aiming to minimize the risk of infection, is the successful development of antibiotic-loaded PMMA formulations. This local therapeutic approach was first developed with gentamicin-loaded PMMA and it presented advantages when compared to a systemic antibiotic therapy for bone infection management, including local targeted anatomic delivery of the drug to the wound site, lower overall dosage, minimization of potential systemic side effects of drug administration, among others

(259). Further, it was established that the desirable antibiotic to include in bone cements should presents specific properties beyond a broad-spectrum of activity. Since PMMA preparation occurs during the surgical procedure, antibiotics must also be thermally stables, water-soluble and must be available in powder phase, to improve mix with cement powder (262). Minocycline holds all these properties of a suitable antibiotic for PMMA-inclusion and it represents an attractive option due to its pharmacological characteristics. In addition to its chemical and thermal stability, minocycline possess a long half-life, combined with excellent absorption by the tissues (167).

Additionally, minocycline was broadly reported to exert beneficial effects in systemic conditions such as diabetes mellitus. The compound anti-inflammatory properties were previously described in a variety of experimental and clinical settings including cerebral (170) and renal ischemia (263), periodontal disease (7), and cutaneous inflammation (264), among other. Accordingly, these inflammation modulatory properties may contribute to an enhanced implant acceptance and integration, while the antibiotic action is ordinarily ensured by minocycline. Additionally, in which regards bone tissue, minocycline may represent an optimal compound as it was demonstrated to improve collagen matrix quality and organization and prevent tissue breakdown, by inhibiting collagenase activity (159). In other hand, minocycline was reported to impair significantly the structural disorganization of both osteoid and the layer of osteoblasts further enabling new bone formation and reducing trabecular bone loss (10).

5.2 – RESEARCH HYPOTHESIS AND OBJECTIVES

In this work, it is aimed the biological evaluation of minocycline-loaded PMMA bone cement, following the subcutaneous implantation within a relevant experimental animal model. Additionally, in order to characterize the biological response in simulated diabetic conditions, developed minocycline-releasing constructs will be further implanted in STZ-induced diabetic rats, a commonly used experimental animal model representative of the human type 1 diabetic condition.

5.3 – MATERIALS AND METHODS

5.3.1 – PMMA AND MINOCYCLINE-LOADED PMMA SAMPLES PREPARATION

The different bone cements were prepared following the previously described methods (265, 266). Commercial acrylic BC, CMW1® Radiopaque, and stabilized minocycline hydrochloride were provided by DePuy Iberia (Spain & Portugal) and Atral Cipan (Castanheira do Ribatejo, Portugal), respectively. Briefly, both CMW1® and minocycline powders and the liquid monomer were carefully mixed in a glass mortar till total homogenization into a homogeneous yellowish-toned mixture. When the desired consistency was obtained, BC mass was manually casted into aluminium molds and shaped in the form of square plates (*7 mm, per 7 mm, per 2 mm*).

Three different BC specimens were obtained: PMMA (PMMA without minocycline), LOW (PMMA loaded with $1 \mu\text{g} \cdot \text{ml}^{-1}$ minocycline), and HIGH (PMMA loaded with $2.5 \mu\text{g} \cdot \text{ml}^{-1}$ minocycline).

5.3.2 – PMMA AND MINOCYCLINE-LOADED PMMA SAMPLES CHARACTERIZATION

Bone cement samples and minocycline powder were characterized regarding their infrared spectrum absorption/emission, by the Fourier Transform Infrared (FTIR) spectroscopy; surface topography, by scanning electron microscopy (SEM); and *in vitro* drug release.

5.3.2.1 – FOURIER TRANSFORM INFRARED (FTIR) SPECTROSCOPY

FTIR spectra were obtained with IRAffinity-1 spectrophotometer (Shimadzu, Kyoto, Japan) at 400-4000 cm⁻¹ scanning range. Powder samples of minocycline, and powdered samples of the BC matrices control and loaded with 2.5% of minocycline, were incorporated with potassium bromide in an agate mortar. A pellet was obtained by compressing the powder mixture into disks in hydraulic press, under 10 ton pressure, for 3 minutes. The pellet was placed in the light path and spectra obtained were the results of averaging 30 scans.

5.3.2.2 – SURFACE CHARACTERIZATION

The surface of prepared BC materials was visualized by scanning electron microscopy (SEM), in quintuplicates (n=5). Material samples were rinsed with deionized water, cleaned with alcohol, sputter-coated with gold and observed in a JEOL JSM 6301F scanning electron microscope.

5.3.2.3 – DRUG RELEASE STUDIES

An *in vitro* release study was carried out in triplicate (n=3), with developed specimens, immersed at 37 °C, in saline solution, consisting of NaCl 0.9% (w/V)

(AppliChem GmbH) and 0.05% (V/V) of Tween20 (Sigma-Aldrich). At predetermined time points (0, 30 min, 1, 2, 4, 6, 24, 48 h, 1 and 2 weeks), aliquots of the supernatant were collected and then replaced with equal volume of fresh saline medium, thus ensuring the sink conditions during the whole study.

Minocycline content in the aliquots was determined with a UV-HPLC system (Shimadzu system LC-6A, Shimadzu Corporation). Chromatographic analysis was performed employing a 5 μm analytical column (LiChrospher[®] 100 RP-18 LiChroCART[®] 125-4 HPLC cartridge, Merck, Darmstadt, Germany), into a thermostatic column compartment at 25 °C. The mobile phase was set at a flow rate of 1.2 ml. min^{-1} and consisted in a mixture of acetonitrile (Sigma-Aldrich) and water, with a volume ratio of 15:85 (V/V), respectively, and 0.6% (V/V) of triethylamine (Panreac), adjusted to pH 3, using orthophosphoric acid (Panreac). The detection wavelength was set at 273 nm. All samples were spiked with 1% (V/V) of internal standard (Levofloxacin-water solution at 75 $\mu\text{g. ml}^{-1}$) before analysis. The unknown concentrations of minocycline were calculated using the internal standard method. The cumulative release ($\mu\text{g. ml}^{-1}$) was expressed as the total minocycline released over time.

5.3.3 – ANIMALS

This *in vivo* study was conducted according to the accepted standards of humane animal care, as outline in the Ethical Guidelines. All the procedures were authorized by *Direção Geral de Alimentação e Veterinária* (DGAV) and comprised the standards for the protection of experimental in accordance with Portuguese (Decree No. 113/2013) and European (Directive 2010/63) legislations.

In this study, 72 male Wistar rats (Charles River, Wilmington, MA), 7 to 8 weeks old, with a body weight of 250 to 300 g, were used. Following the arrival to the animal facility, animals were allowed to acclimatize for 1 week before the beginning of the study. Animals were then housed in groups, in conventional type II cages, on a controlled environment of temperature and humidity, in a 12 hours light/dark cycle. The identification was carried out with indelible ink and dry food and water were supplied *ad libitum*.

Experimental diabetes was chemically induced in healthy Wistar rats by a single intraperitoneal injection of STZ (60 mg. kg^{-1} , Sigma®), freshly prepared in ice cold 10 mM citrate buffer, $pH = 4.5$ – STZ group ($n = 36$). Control rats were injected with citrate buffer alone – control group ($n = 36$). Diabetic state and subsequent hyperglycaemia was confirmed by measuring tail vein blood glucose levels with a glucometer (Accu Check, Roche Diagnostics, Portugal), 72 hours after streptozotocin or vehicle administration. Animals with blood glucose levels $\geq 300 \text{ mg. dl}^{-1}$, were considered to be diabetic. Fifteen days following diabetes induction, the surgical procedures aiming for the subcutaneous implantation of the materials were conducted.

5.3.4 – SUBCUTANEOUS IMPLANTATION OF MINOCYCLINE-LOADED PMMA

The surgical procedure was fully photodocumented and the surgical main steps are shown in figure 5.1. Briefly, animals were anesthetized by an intraperitoneal (IP) injection of a solution containing 90 mg. kg^{-1} ketamine (Imalgène 1000, Merial®) and 10 mg. kg^{-1} xylazine (Rompun® 2%, Bayer Health Care). Once unconscious, the back was trichotomized (figure 5.1a) and the area was cleaned of remnant fur and disinfected with a povidone-iodine solution (Betadine®).

A superficial 2 cm incision was made in the skin (figure 5.1b) and surrounding skin tissue was internally debrided in order to get access to the posterior limbs and right anterior limb (figure 5.1c). Following, a sample of each biomaterial (figure 5.1d) – PMMA, LOW, and HIGH – was randomly implanted in the created subcutaneous pockets, around the left posterior limb, right posterior limb and right anterior limb (figure 5.1e).

The skin was then closed with a 3/0 suture (Silkem®, silk, B Braun) and the wound was disinfected with povidone-iodine solution (figure 5.1f) and subcutaneous injection (SC) of 10 mg. kg^{-1} tramadol was given to the animal, for postoperative analgesia. The animal was kept warm until gaining conscience, and was given food and water ad libitum. Also, it was monitored daily, in the postoperative period until euthanasia.

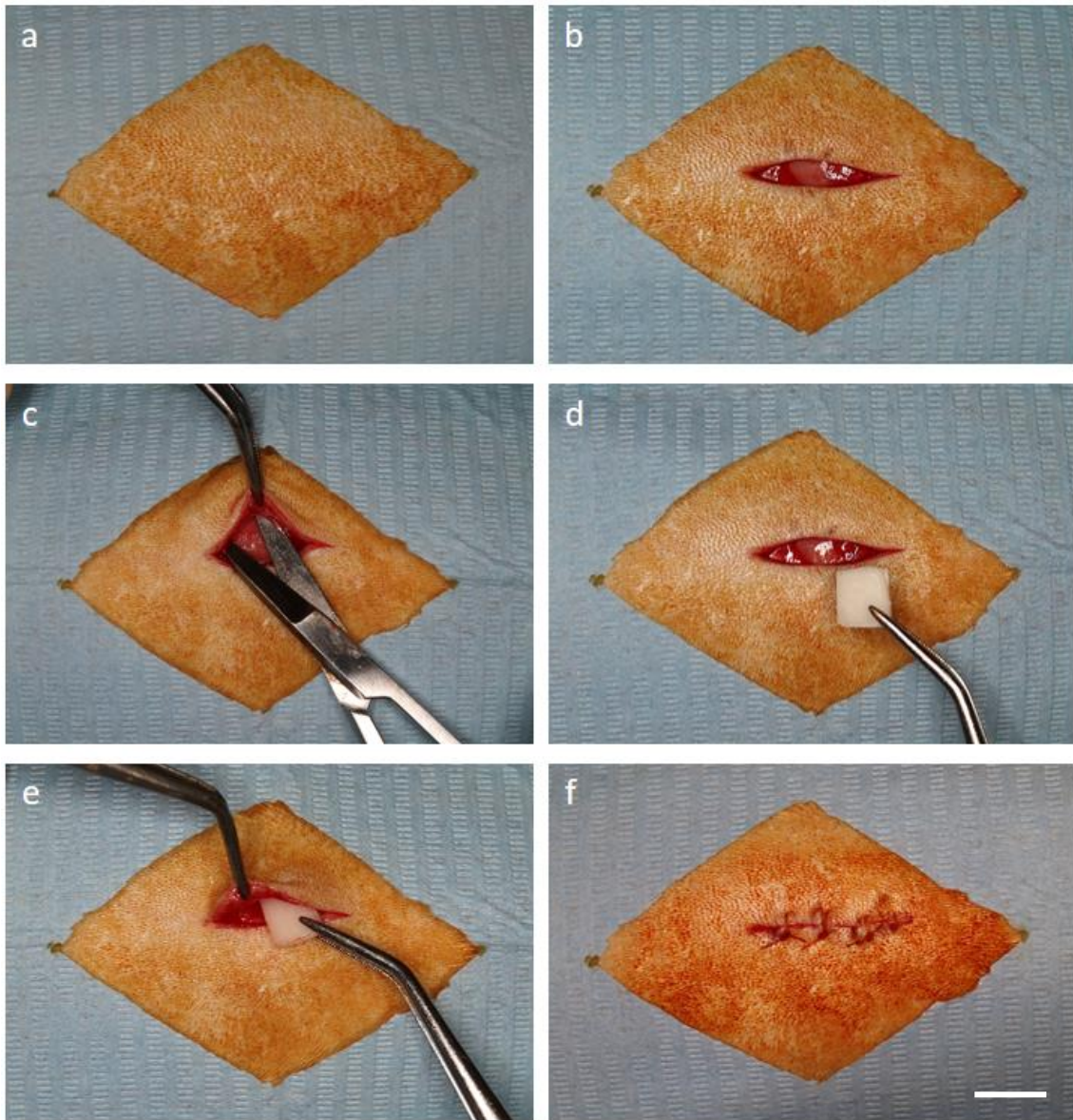


Figure 5.1 – Subcutaneous mPMMA implantation. Preparation of the surgical area by trichotomy and iodo-povidone disinfection (a); skin incision of around 2 cm (b) and subcutaneous tissue debridement (c); subcutaneous implantation of PMMA and mPMMA samples (d and e); Wound suture and disinfection (f). Scale bar corresponds to 1 cm.

5.3.5 – SAMPLE GATHERING AND FIXATION

At days 3, 14 and 28 after the implantation surgery, 6 rats of each group (control and STZ-induced) were euthanized by exsanguination under general anaesthesia (intraperitoneal injection of pentobarbital sodium 35 mg.kg^{-1}). Following, the implanted PMMA and mPMMA samples, including the surrounding tissue, were carefully excised and collected. For each animal, three explants (corresponding to PMMA, LOW and HIGH experimental groups), were fixed in 10% phosphate-buffered formalin.

5.3.6 – HISTOLOGICAL ANALYSIS OF INFLAMMATORY RESPONSE

Samples were processed 24 hours following their fixation. Accordingly, each sample embedded in paraffin and were sectioned longitudinally with a microtome Leica® 20035 (3 μm thickness). Then, sections were stained with haematoxylin and eosin solution (HE) and examined and semi-qualitatively evaluated using light microscopy (Nikon Eclipse 50i Microscope).

5.4 – RESULTS

5.4.1 – FTIR EVALUATION OF PMMA AND MINOCYCLINE-LOADED PMMA SAMPLES

The results concerning FT-IR spectroscopy characterization are shown at figure 5.2. FTIR evaluation indicated that minocycline loading, with either concentrations, resulted in none significant change, in the inner or outer structure of the BC. In fact, FT-IR results showed that no new bands were identified on HIGH samples, during evaluation.

5.4.2 – SURFACE ANALYSIS OF PMMA AND MINOCYCLINE-LOADED PMMA SAMPLES

Representative micrographs of SEM analysis of each distinct prepared bone cement samples are represented at figure 5.3. No significant differences between control and minocycline-loaded BC were attained. In general, a homogenous surface with minor topographic irregularities, was verified on all the assayed compositions.

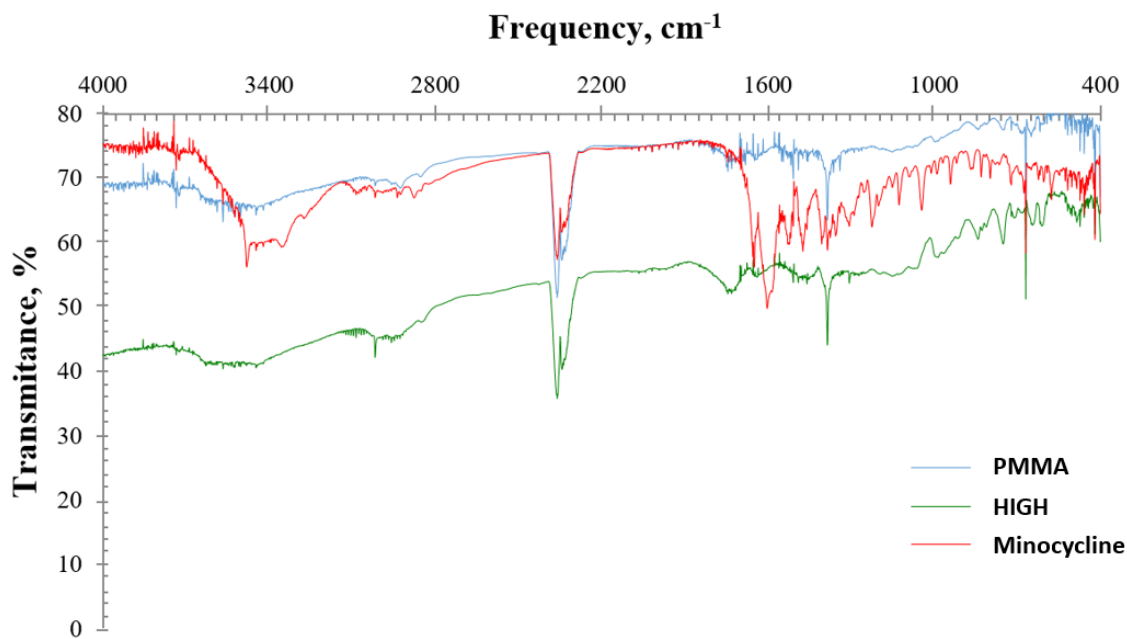


Figure 5.2 – FTIR spectra of PMMA, $2.5 \mu\text{g} \cdot \text{ml}^{-1}$ minocycline-loaded PMMA and free minocycline.

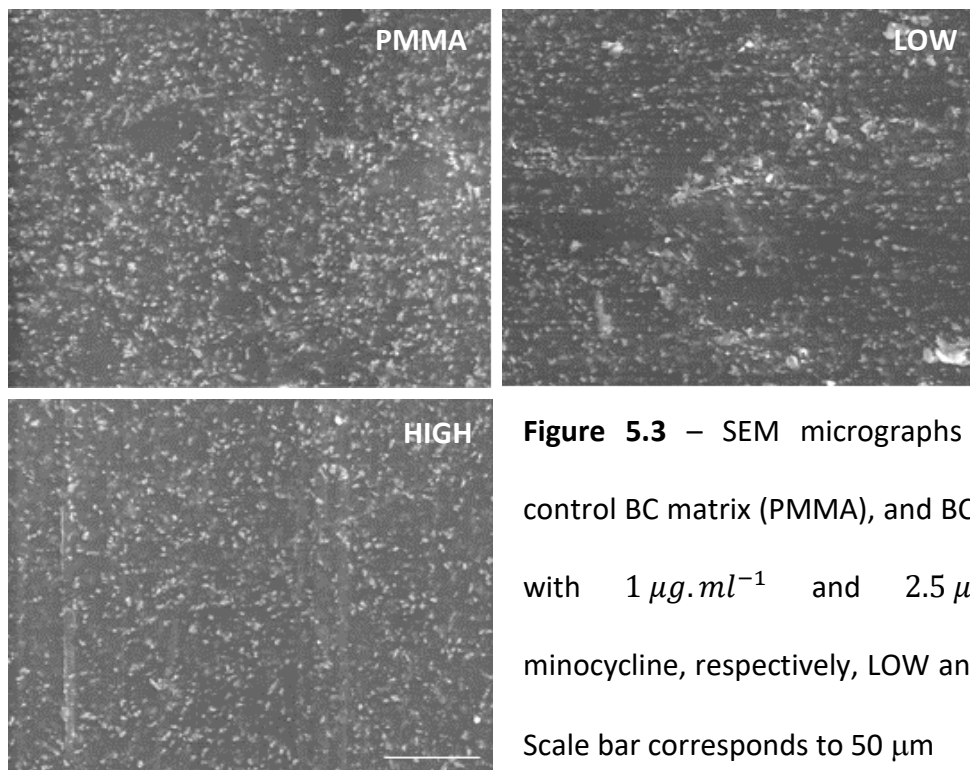


Figure 5.3 – SEM micrographs of the control BC matrix (PMMA), and BC loaded with $1 \mu\text{g} \cdot \text{ml}^{-1}$ and $2.5 \mu\text{g} \cdot \text{ml}^{-1}$ minocycline, respectively, LOW and HIGH. Scale bar corresponds to $50 \mu\text{m}$

5.4.3 – MINOCYCLINE RELEASE EVALUATION

Minocycline release studies were performed in a saline media, over a period of two weeks. Both profiles of LOW and HIGH are presented in figure 5.4, showing the cumulative minocycline release over time. Release profiles evidenced a two-phase stage, with an initial burst, followed by a sustained release - a profile more evident within the HIGH formulation. Additionally, the variation of minocycline release was found to be higher for the HIGH formulation, as comparing to LOW, throughout the assayed period.

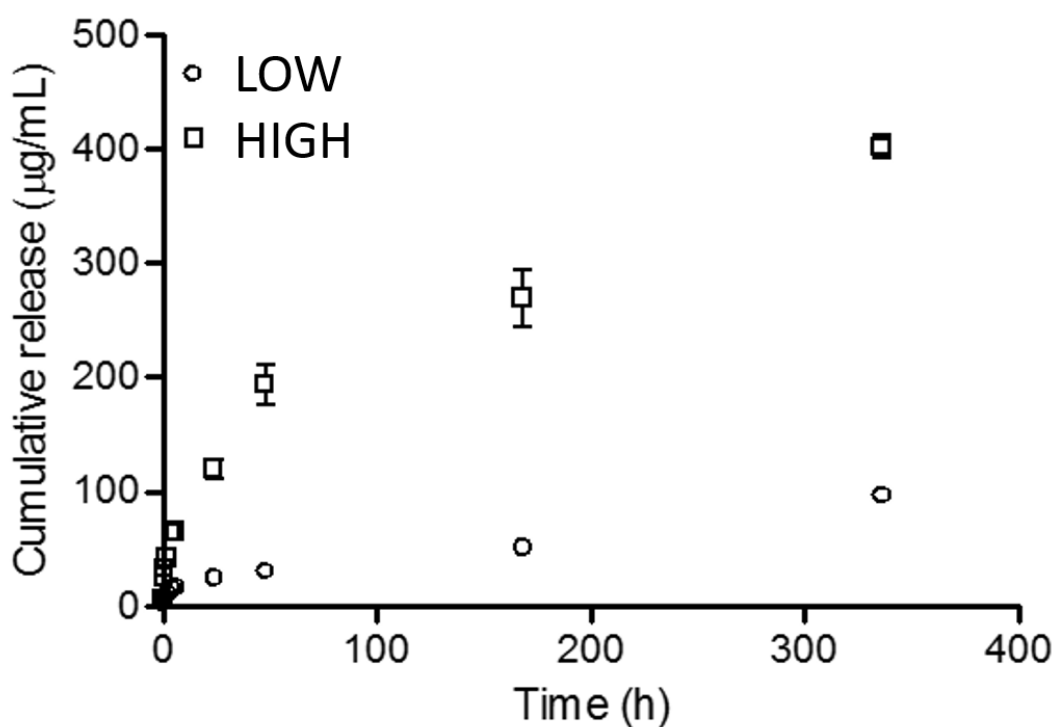


Figure 5.4 – *In vitro* release profiles of minocycline, in both LOW and HIGH concentrations, for up 2 weeks.

5.4.4 – DIABETIC EXPERIMENTAL MODEL

Diabetes mellitus was chemically induced by a single IP injection of streptozotocin. Hyperglycaemia was confirmed 72 hours following STZ administration. After 15 days, animals lost weight ($37.57\% \pm 8.65$) and this weight variation pattern prevailed during the experimental period. At euthanasia, STZ-induced animals had a significantly higher glycaemia ($> 300 \text{ mg. dl}^{-1}$) in comparison to basal glycaemic values ($\leq 125 \text{ mg. dl}^{-1}$).

5.4.5 – INFLAMMATORY RESPONSE TO PMMA AND MINOCYCLINE-IMPREGNATED PMMA

Images corresponding to the histological analysis of the tissues surrounding to the implanted PMMA constructs, in both control and STZ animals, at distinct time points, are shown at figures 5.5, 5.6 and 5.7. In figure 5.5, representative samples, of the PMMA-alone samples, in both control and diabetic conditions, are shown; In figure 5.6, representative samples of the assayed PMMA constructs with and without minocycline loading, in control conditions, are shown. In figure 5.7 representative samples of the assayed PMMA constructs with and without minocycline loading, in diabetic conditions, are shown. The tissue response to the implanted constructs was qualitatively evaluated by light microscopy following HE staining and the results were expressed in a scale of intensities ranging from “0” (absence of intensity or prevalence) to “+++” (high intensity or prevalence) for all the assayed parameters with the exception of macrophages and giant cells, which analysis consisted of counting the total amount of these cells and the

numbers were then converted in the intensity scale between “0” (no cell found) and “+++” (high number of cells). This qualitative evaluation is represented at table 5.1. The qualitatively addressed parameters included: inflammatory reaction (IR), fibrotic capsule formation (CAP), neutrophils infiltration (PMN), presence of lymphocytes (LYM), fibroblasts (FB), macrophages (MAC) and giant cells (GC), and neovascularization (NEO).

5.4.5.1 - INFLAMMATORY REACTION

The overall inflammatory reaction was qualitatively evaluated according to its intensity, for each sample, in both control and diabetic conditions. The evaluation was conducted by observing tissues appearance, presence of cell infiltrate, new vessels, fibrotic formation. The resulting evaluation is represented at table 5.1. The analysis revealed a more exuberant inflammatory reaction in samples collected at early time points (i.e. day 3) in control animals. The overall inflammatory response seemed to diminish with time, particularly in control conditions. In STZ animals it was broadly low, throughout the assayed time points. PMMA loaded with high and low doses of minocycline seemed to exert a significantly reduced IR as compared with PMMA alone, in both control and diabetic animals (figure 5.5 and table 5.1).

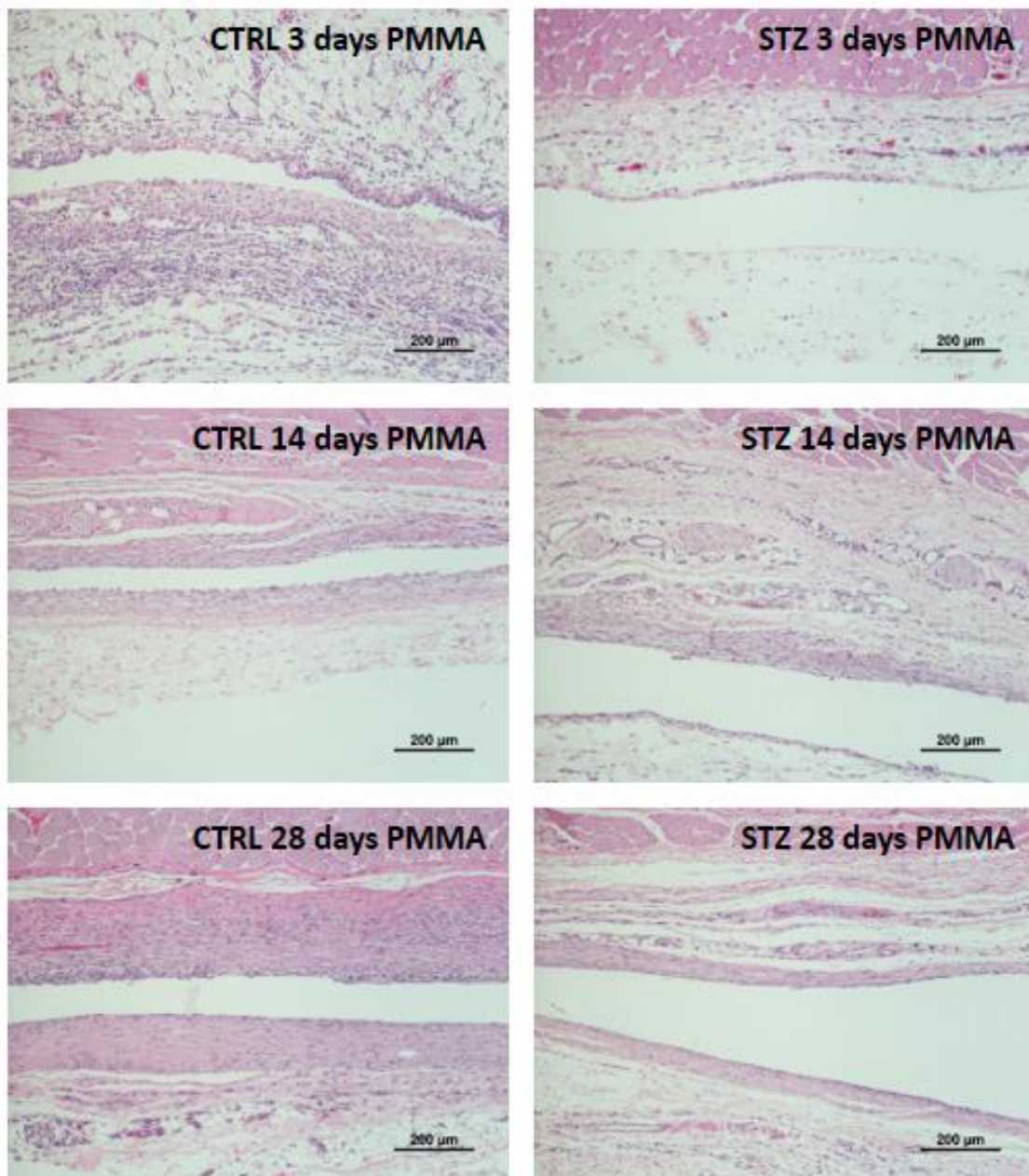


Figure 5.5 – Histological analysis of the tissues surrounding PMMA constructs, after 3, 14 and 28 days of *in vivo* subcutaneous implantation, in control and diabetic animals. HE staining. Scale bar corresponds to 200 μm.

5.4.5.2 – POLYMORPHONUCLEAR NEUTROPHILS

Neutrophils play a central role in the modulation of early events within the acute inflammatory response. Their infiltration within tissues neighbouring the implanted PMMA constructs was addressed according to its intensity (table 5.1). PMN infiltration was highly intense at day 3 in PMMA samples of control animals. Comparatively, minocycline-loaded PMMA seemed to reduce neutrophil recruitment, as their presence in LOW and HIGH groups was found to be significantly lower when compared with PMMA alone. In diabetic animals the presence of PMNs was meaningfully reduced as compared with samples obtained from control animals, however minocycline groups seemed to slightly reduce neutrophils recruitment. Subsequently, neutrophils infiltration was found to be progressively reduced with implantation time, sustaining the prime role of these cells within the early events of the inflammatory response (figures 5.5, 5.4 and 5.6 and table 5.1).

5.4.5.3 – MACROPHAGES AND GIANT CELLS

Macrophages and Giant cells count was determined in the sections of implanted PMMA constructs. Macrophages were firstly noticed at day 14 in mild numbers, and their presence intensity remained constant, till day 28. These results were similar between both control and diabetic conditions, in the tissues surrounding the implanted samples with and without minocycline (table 5.1). The same emerging pattern was observed regarding GCs, however their presence was more intense from day 14 with

increasing prevalence till day 28. No significant differences were achieved when comparing PMMA with low and high doses mPMMA samples (table 5.1).

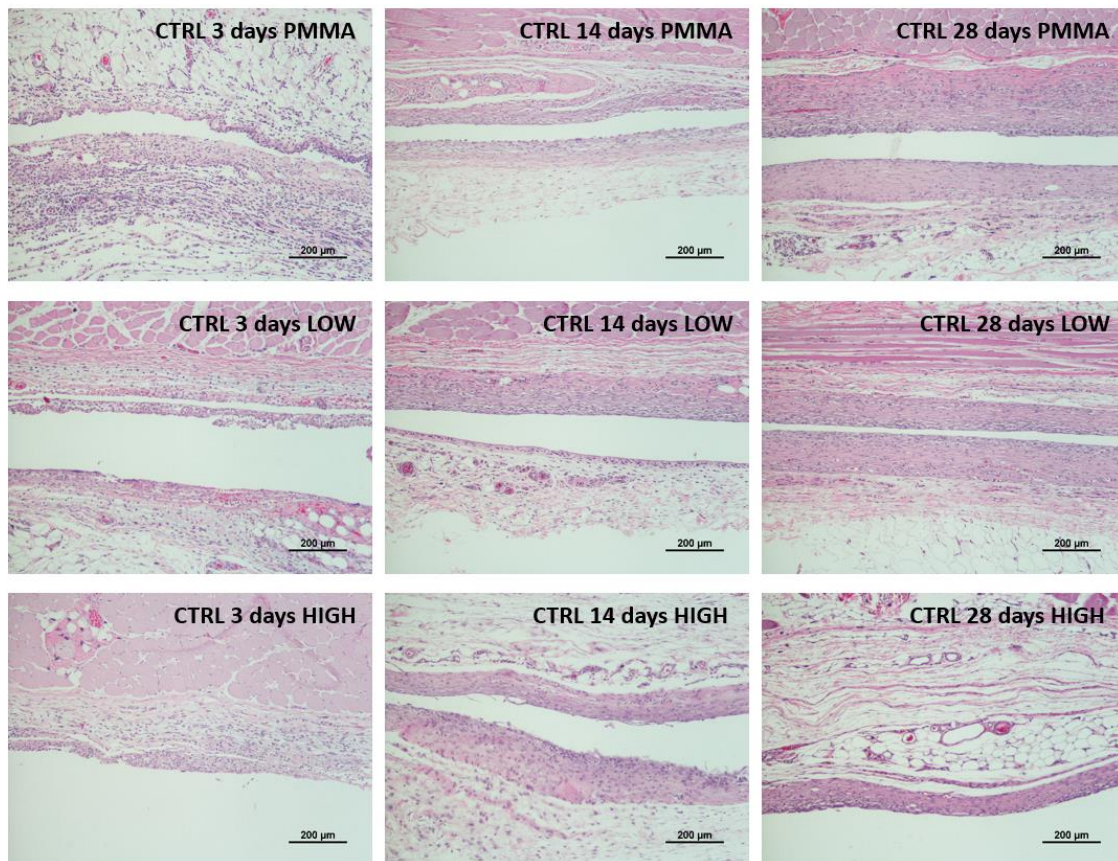


Figure 5.6 – Histological analysis of tissues surrounding PMMA and mPMMA constructs, after 3, 14 and 28 days of *in vivo* subcutaneous implantation, in control animals. HE staining. Scale bar corresponds to 200 µm.

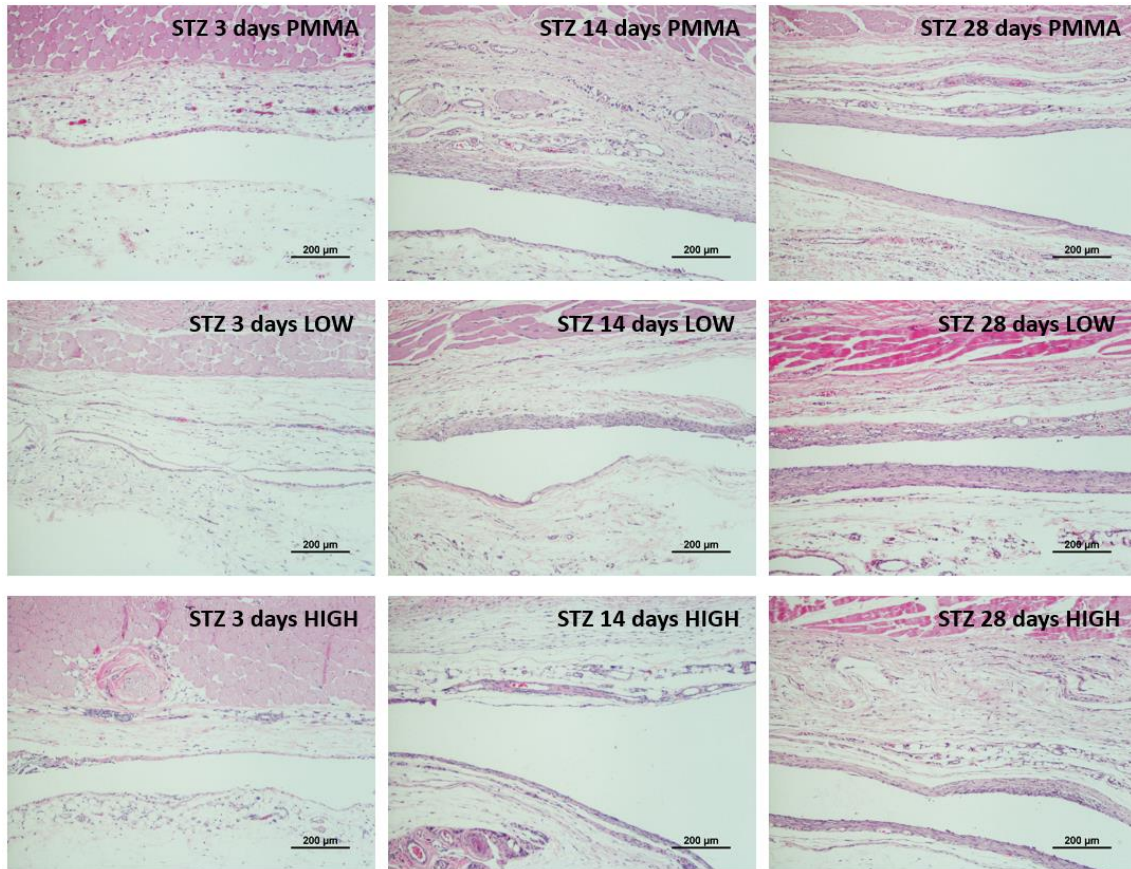


Figure 5.7 – Histological analysis of tissues surrounding PMMA and mPMMA constructs, after 3, 14 and 28 days of *in vivo* subcutaneous implantation, in diabetic animals. HE staining. Scale bar corresponds to 200 µm.

5.4.5.4 – FIBROBLASTS

The assessment of fibroblasts migration/proliferation in the wounded area was also evaluated (table 5.1). Histological analysis showed a considerable high presence of fibroblastic-like cells at the earlier days after subcutaneous implantation in control animals with a trend for a diminished intensity in both LOW and HIGH groups, at day 3. This difference between samples has not been noticed at later experimental time points; moreover, at day 28, fibroblast presence was significantly diminished. Concerning diabetic animals, fibroblastic cells presence was significantly lower as compared with control animals and no differences were attained comparing PMMA with LOW and HIGH groups (figures 5.6 and 5.7).

5.4.5.5 – FIBROTIC ENCAPSULATION

The results regarding the semi-qualitative analysis of PMMA and mPMMA samples fibrotic encapsulation are shown at table 5.1. The analysis was performed by taking in account the capsule thickness. Encapsulation by fibroblasts was observed from day 14 in both control and diabetic animals. In PMMA samples, an increasing capsule thickness was evident from day 14 to day 28 in both control and STZ experimental groups. High concentration of minocycline-loaded PMMA was able to interfere with capsule formation as a reduced CAP thickness was observed involving these samples at the later experimental time point. Despite the progressive development in both conditions, CAP

showed to be thicker in those samples implanted in healthy animals presenting a stronger net of fibroblasts and collagen around each of materials.

Table 5.1 – Semi-qualitative analysis of overall inflammatory reaction and inflammatory response parameters around PMMA and mPMMA samples, after 3, 14 and 28 day of *in vivo* subcutaneous implantation, in both control and diabetic conditions. “0” represents the lowest intensity or presence and “+++” represents the highest intensity or presence within the tissues around the samples. “PMMA” refers to PMMA-alone samples; “LOW”, PMMA loaded with $1 \mu\text{g.ml}^{-1}$ minocycline; and “HIGH”, PMMA loaded with $2.5 \mu\text{g.ml}^{-1}$ minocycline. “IR” refers to inflammatory reaction; “PMN”, polymorphonuclear neutrophils; “MAC”, macrophages; “GC”, giant cells; “FB”, fibroblasts; “CAP”, fibrotic capsule; “LYM”, lymphocytes; and “NEO” stands for neovascularization.

Condition		IR	Inflammatory Response Parameters						
			PMN	MAC	GC	FB	CAP	LYM	NEO
CTRL 3 days	PMMA	+++	+++	0	0	++/+++	0	++	++
	LOW	++	+ / ++	0	0	++	0	+ / ++	+ / ++
	HIGH	++	++	0	0	++	0	+	++
STZ 3 days	PMMA	+ / ++	+ / ++	0	0	+	0	+	++
	LOW	+	+	0	0	+	0	0 / +	+
	HIGH	+	+	0	0	+	0	+	++
CTRL 14 days	PMMA	++	+	+	+	+ / ++	+	+	+
	LOW	++	+	+	++	++	+	+	+
	HIGH	+ / ++	+	+	++	++	+	+	+ / ++
STZ 14 days	PMMA	+ / ++	+	+	++	++	+	+ / ++	+
	LOW	+	+	+	++	+	+	+	+
	HIGH	+	+	+	+ / ++	+	+	+	+
CTRL 28 days	PMMA	+ / ++	0 / +	+	++ / +++	+	++ / +++	++	+ / ++
	LOW	+	0 / +	+	+ / ++	+	++ / +++	+	++
	HIGH	+ / ++	0 / +	+	+ / ++	+ / ++	++	+	+ / ++
STZ 28 days	PMMA	+ / ++	+	+	++ / +++	+	+ / ++	++	++
	LOW	++	+	+	++	+	++	+	++
	HIGH	+ / ++	+	+	++ / +++	+	+	+ / ++	++

5.4.5.6 – LYMPHOCYTES

Presence of lymphocytes was addressed as an evidence of immune system activation against developed PMMA systems. At day 3, a moderate presence of lymphocytes was registered with significantly diminished presence around PMMA loaded with high doses of minocycline, in control animals. At day 14, lymphocyte presence was less intense and no differences were achieved between PMMA and minocycline-loaded samples. 28 days after the implantation, an increased presence, similar to that obtained at day 3, was observed in PMMA group. In diabetic animals a significantly lower number of lymphocytes was found at day 3 when compared with control groups. Also, no differences between samples were found at this time point. Over the experimental course, lymphocytes number seemed to slightly increase in PMMA samples with significant differences between PMMA and the other two conditions, at day 28.

5.4.5.7 – NEOVASCULARIZATION

In which regards the formation of new blood vessels, the addressment of this parameter was conducted by counting the blood vessels present in the tissues around the implants. No clear difference was found between experimental time points, nor between control and diabetic groups. Also, minocycline-loaded samples seemed to have no significant effect in neovascularization (table 5.1).

5.5 – DISCUSSION

Diabetes mellitus, one of the most established systemic conditions, nowadays, representing a major cause of death and disability worldwide (267). Chronic hyperglycaemia is known to severely affect bone tissue in a variety of ways leading to a substantial increase of fractures occurrence (76, 78) combined with impaired healing and abnormal inflammatory response (115), resulting in diabetic patients' increased morbidity or even death (6). In which regards the cellular affection, DM was broadly described to cause bone remodelling unbalances, by disrupting osteoblastic precursor cells differentiation and further hindering their specialized function to renew bone (83, 91). This unbalance leads to a cycle of higher bone resorption over new bone formation contributing to a continuous decrease of mineral density and increased trabeculae gaps, ultimately establishing an osteopenic state and subsequent osteoporosis development (6).

Conformably, diabetic patients are more likely to experience longer periods of therapy to regenerate bone wounds, as longer periods for osseointegration are required, when biomaterials are implanted (11, 121). Furthermore, hindered healing process in DM is intimately associated with abnormal inflammatory response and higher risk of surgical and post-surgical infections (113, 116), both contributing as major causes of implant failure and rejection, in diabetes mellitus patients.

In order to avoid infections due to biocompatible devices implantation, new formulations of antibiotic-impregnated bone cements emerged as favourable alternative to systemic administration of antibiotics. PMMA represents a suitable

biomaterial to support bone regeneration not only as an implant fixative but also a bony defect filler preventing structural collapse while keeping the defect clean of invasive soft and scar tissues (262). Due to its chemical properties, PMMA bone cements may be easily loaded with a proper antibiotic and applied locally during the surgery, being widely adaptable to the wound morphology. Antibiotic-loaded PMMA cements have been broadly used in the treatment of bone fractures and osteomyelitis (268), aiming to attain a local antibiotic therapy with suitable antibiotic concentrations, without the need of antibiotic systemic administration, which may not specifically target the compromised tissues or organs (260, 262).

Minocycline, a second generation, semi-synthetic tetracycline has been intensively for more than three decades due to its broad spectrum of activity against both gram-positive and -negative bacteria. More recently, it was described to exert beneficial non-antibacterial properties including anti-inflammatory and anti-apoptotic activity (10, 170, 263). Those properties were thought to be useful as combined with biocompatible of PMMA systems.

In this study, we aimed to evaluate the biological response of PMMA impregnated with two different concentrations of minocycline, upon subcutaneous implantation in both control and diabetic-induced animals. The subcutaneous implantation was widely used to assess tissue biocompatibility and potential inflammatory response to biomedical materials, as it allows to conduct site specific studies with minimal invasiveness and long-term trauma to the animals (269-271). Our intent was to address not only the inflammatory response, but also the evidences of enhanced surrounding tissue healing, neovascularization and implant acceptance or rejection.

The selected model of diabetic pathology was the streptozotocin-diabetic-induced rat. STZ, a broad-spectrum antibiotic, is able to damage selectively pancreatic β -cells leading to a hyperglycaemic state similar to the one of human pathology (92, 105). A single dose of 60 mg. kg^{-1} , was reported to be enough to induce diabetes in rodents (106) with minimal mortality. Following STZ intraperitoneal administration, hyperglycaemia is established in the first 48 hours. At day 15 after induction, diabetic animals demonstrated the characteristic symptoms of the diabetic state, including weight loss, increased water consumption and consequent increased urine volume (109). Also, in comparison with controls, STZ-injected animals presented higher glycaemia, ranging from $300 \text{ to } 400 \text{ mg. dl}^{-1}$, thus confirming the hyperglycemic state.

Tissue response following biomaterial implantation was found to be significantly different between control and diabetic conditions. In the present study, specially at earlier days after subcutaneous biomaterials implantation, inflammatory reaction seemed to be delayed in diabetes as its intensity, around all PMMA and minocycline-loaded PMMA samples was diminished, as compared with the reaction obtained around materials subcutaneously implanted in control animals. This phenomenon was reviewed intensively in literature, in which numerous reports support that diabetes alters the host response to implants, initially due to the impairment of inflammatory cells recruitment and activation (272-274). Accordingly, in diabetic wounds, an impaired expression of chemokines was found to cause substantial reduction of growth factors secretion, which results in delayed inflammatory cells infiltration (272). Additionally to efficient inflammatory cell recruitment, wound healing requires a functional and well-structured provisional matrix, in diabetes these conditions do not seem to occur (272). Further, our data suggests that minocycline, in both experimental doses, exerted an acute and

substantial reduction of inflammatory reaction triggering, in both control and diabetic conditions.

In physiological conditions, neutrophils predominate in the early inflammatory infiltrate and are later replaced by macrophages. Following vasodilation and microvasculature permeability, PMN neutrophils begin to accumulate along the vascular endothelial surface (margination process) in order to migrate to inflammation focus (275). Commonly, these processes take place during the first three days after inflammation triggering. This was observed in our histological evaluation, in which PMNs presence was intense at day 3 after subcutaneous PMMA samples implantation in control animals group. In contrast, in diabetic samples, the presence of recruited PMNs was significantly reduced. Conformably, many studies have found severe changes in neutrophils' abilities and abnormal functionality, including impaired adhesion to endothelium and recruitment to inflammation site (276), bacterial and phagocytic activity (277, 278), and chemotaxis (279-281). Neutrophils play a major importance role as they are able to synthesize pro- and anti-inflammatory cytokines and growth factors that modulate inflammatory response. Further, factors such as IL-8 (11, 282), tumor necrosis factor- α (TNF- α) and IL-1 β are pro-inflammatory cytokines with critical role in the inflammation processes (283). IL-8 was reported to exert chemotactic stimuli, providing the recruitment of greater number of PMN leukocytes and support neovascularization processes (284). Its expression was reported to be lowered in diabetic conditions (11). TNF- α is known to mediate the systemic effects of inflammation (i.e. fever, haematopoiesis) but is also a strong modulator of neutrophils metabolic functions. Its expression was described to be greatly higher in diabetic patients which combined with hyperglycaemia, lead to abnormal augmentation of intracellular Ca²⁺ of

neutrophils and consequent over production of cytokines (285). The uncontrolled release of factors contributes to chronic activation of phagocytes, despite also triggering neutrophils apoptosis (286). Concerning IL-1 β , its overexpression combined with altered expression of IL-8 and TNF- α , was described to lead to tissue injury and wound healing impairment (285).

With respect to PMMA samples with minocycline controlled release, the added drug was able to reduce neutrophil recruitment in both concentrations, as their presence was notably reduced when compared to PMMA group. This decreased neutrophil recruitment was previously reported by Shine and co-workers (287). As expected, in control animals PMNs presence diminished continually till day 28, however in diabetic animals, neutrophils presence had the same intensity thus suggesting a hindered migration of neutrophils, a chronic presence of a reduced number of these cells, and subsequent chronic expression of inflammation cytokines.

Macrophages recruitment represent the dominant feature in chronic inflammation. Following monocyte migration to the inflammatory site, macrophages are differentiated and activated by a variety of factors including microbes, dead cells or cellular debris, cytokines (i.e. interferon- γ , IFN- γ), and other (275). In the present study, data shows that macrophages emerged following 14 days of PMMA constructs implantation. Their number was constant till day 28 and no relevant differences were achieved between control and diabetic animals. The same behaviour was observed for the assessment of giant cells, nevertheless these were in higher number than macrophages suggesting an advanced stage of macrophage fusion, at least from day 14 onwards, in both control and diabetic conditions. Despite the lack of verified differences

between control and diabetic animals, diabetes is known to affect macrophage function (11, 288, 289). At the molecular level, diabetic macrophages were reported to produce higher levels of pro-inflammatory cytokines thus increasing the number of PMN cells merging to inflammation area (290). Contrariwise, in diabetes, macrophages and giant cell phagocytic ability was described to be hindered leading to an inappropriate clearance of dead cells and other cellular debris (291, 292). Overall, these effects may mutually compensate – i.e., in diabetes, whether activated macrophages were found to produce higher levels of inflammatory mediators, the functional activity of macrophages and giant cells was found to be hindered. Counterbalanced effects may converge to the absence of differences verified between control and diabetic animals in the present study. Additionally, macrophage chemotaxis is also associated with IL-8 which was previously mentioned to be diminished in diabetic wound healing (11). Moreover IL-8 was demonstrated to be responsible for the majority of the monocyte-macrophage-associated angiogenic activity (293). In this way, IL-8 unbalances may also affect macrophage function during diabetic wound healing or biomaterial implantation and, in the second case, contribute to the altered tissue implant interaction (273). In which regards minocycline-impregnated cements, PMMA-loaded samples did not seem to exert any modulator effect on macrophages/giant cells migration or fusion since no significant differences were detected between PMMA alone samples and LOW and HIGH groups within each condition.

Fibroblasts are known to play a critical role in healing processes. Posteriorly to wound clearance and secretion of determinant growth factors, fibroblasts and other epithelial cells migrate to inflammation site to initiate the re-epithelialization and healing of damaged tissues (11, 275). Our results showed a decreased presence of

fibroblasts in diabetic animals, in comparison with control animals. In diabetes, the distinct stages of wound healing seem to be impaired and a substantial depletion of growth factors have been reported (11). Numerous studies demonstrated that diabetes disrupt the normal fibroblast proliferation and migration behaviour during healing processes. Furthermore, the abnormal inflammatory response in diabetes is characterized by decreased expression of IGF-1, transforming growth factor- β 1 (TGF- β 1), TNF- α and platelet-derived growth factor (PDGF), which are known to promote fibroblasts activation, proliferation and migration (11, 275, 294). Moreover, macrophages activation in physiological conditions affects directly fibroblasts proliferation, collagen synthesis, and other factors expression (275). Since macrophages activity is impaired in diabetes, these cells may also be associated with hindered fibroblasts recruitment and function in diabetic conditions. Minocycline appeared to not modulate fibroblastic behaviour in either control or diabetic experimental conditions.

Another important remark of inflammatory reaction upon biomaterial implantations regards the formation of a fibrotic capsule, which intends to isolate the implant or other intruder, being recognized as a foreign body. It is broadly known that the inclusion of foreign bodies, including biomaterials, leads the formation of a dense, hypocellular, collagen-rich capsule (295). Our analysis showed that fibrotic encapsulation takes place in all experimental conditions, posteriorly to day 3 and sometime before day 14. At day 14, a well-formed CAP was present in both control and diabetic animals. The evaluation of CAP thickness, showed similarities in both experimental groups at day 14, however, significant differences were observed at day 28 after PMMA implantation. In control groups, a significant thicker CAP was found in comparison with the one attained in diabetic animals. Only few studies provided a

deeper insight in the relation between insulin-dependent diabetes and foreign-body capsule formation. Despite the lack of information, the development of this dense layer of fibrotic connective tissue was already considered a major cause of implant failure, safety and biocompatibility, in both physiological and diabetic conditions (295-297). Recent data reported that attenuated fibrous encapsulation in hyperglycaemic environment (270) may be correlated with the high levels of TNF- α expression and consequent higher apoptotic index of fibroblastic cells in diabetic conditions (270, 298). Accordingly, we found a reduced fibroblastic development in diabetic conditions. These findings support our analysis, as CAP were able to grow thicker in control animals at later experimental time points. Additionally, the present study revealed that minocycline was able to reduce foreign-body encapsulation thickness, slightly in control group and significantly in diabetic conditions.

Lymphocytes are commonly the last type of immuno-inflammatory cells emerging to the inflammation area. They are mobilized to the setting of any specific immune stimulus, as infections, or other non-immune-mediated processes, as tissue trauma. Both T and B lymphocytes are recruited to the inflamed area by the same chemokines that mobilizes other inflammatory cells (275). Our findings suggest that lymphocyte presence was significantly diminished in diabetic animals, as compared with controls, at day 3. Over experimental time points, lymphocytes presence diminished in both conditions, nevertheless, at later time points, their presence was still noticed, endorsing the existence of a persistent inflammation state, immune activation, and leukocyte dysfunction. This comes in line with the delayed migration, verified at earlier inflammation time points in diabetic conditions, and found to be associated with several dysregulated cellular functions. Accordingly, apart from the previously mentioned

defects in leukocyte chemotaxis, phagocytosis and abnormal functional activity of fibroblasts and epidermal cells, diabetes is known to yield defective T-cell immunity (47, 118). A study demonstrated that, in diabetic wounds, CD4/CD8 ratio was reported to be significantly lower as compared with normal wounds, due to relatively lowered number of CD4⁺ T cells (299). Moreover, the predominance of CD8⁺ T cells was previously reported to be associated with impairment of certain stages of healing processes (299-301).

In which regards the minocycline-impregnated implants results were convergent to a reduction in the number of recruited lymphocytes. The first significant difference was observed in control group, at day 3, in which both doses of minocycline were able to reduce the number of these cell in the inflammation site. At day 28, these differences were noticed but, this time, in both control and diabetic groups. This may support that minocycline local administration at earlier time points of an inflammation process may play a decisive role preventing a sharp chronic invasion of lymphocytes and consequent immune-derived healing impairment in diabetic wounds or biomaterial subcutaneous implantation.

Shortly after injury and inflammatory response triggering, hypoxia is induced in damaged tissue. As the new extracellular matrix produced and epithelial cells renew the damaged area, macrophages and fibroblast tend to compensate the hypoxia secreting specific pro-angiogenic factors such as vascular endothelial growth factor (VEGF) and fibroblast growth factor (FGF) to promote neovascularization. Despite our analysis does not indicate substantial differences between physiological and diabetic conditions, diabetes is widely known to hinder new vessel formation and quality, further leading to

vascular dysfunctions, such as structural abnormalities, increased permeability and vasodilatation (270, 271, 302). In diabetic wounds, the nitric oxide (NO) reduction has been reported to exert negative effects in both tissue healing and response to infection (303). Moreover, increasing NO levels were demonstrated to play a key role in angiogenesis by initiating the recruitment of endothelial progenitor cells from bone marrow (121) and by activating VEGF expression by fibroblasts and macrophages (304). Thus, diminished levels of NO in diabetic conditions were correlated with insufficient chemokine signalling to recruit endothelial cells resulting in decreased neovascularization (121). Some approaches have been developed with the aim to improve vascularization in diabetic wounds, as well as around implants (273). Accordingly, insulin administration and hyperglycaemic control was reported to restore the inflammatory response and neovascularization, to a process similar to the one verified in physiologic conditions (305). On the other hand, crucial differences may be attained in time points different from those assessed, as between day 3 and day 14.

In our histological analysis minocycline seemed not to influence neovascularization, however, it was a semi-quantitative analysis which should posteriorly be endorsed with molecular assays in order to address more accurately the cellular component of the observed vessels, as well as the dimensional and structural organization around the biomaterial. In fact, tetracycline and derivatives such as minocycline and doxycycline were broadly associated with anti-angiogenic properties, which were widely reported to be useful in pathological conditions associated with increased vessel formation and altered vasculature structure such as tumour and metastasis (9, 10, 144).

5.6 – CONCLUSIONS

In the present study, a successful animal model of chemically-induced hyperglycaemia was developed and allowed to mimic the human diabetic condition. Subsequently, developed PMMA system for the controlled release of minocycline, aiming the application in bone trauma, was characterized for its biocompatibility following subcutaneous implantation in both control and diabetic animals.

Our data endorses an impaired inflammatory response in diabetic conditions, as several important inflammation parameters showed to be down-regulated or functionally hindered, including neutrophils infiltration at earlier time points of inflammatory reaction, chronic presence of macrophages and giant cells, and delayed infiltration of lymphocytes corroborating the chronic inflammatory and immune activation at later time points. Also, fibrotic encapsulation was found to be reduced in diabetic conditions which may represent a positive point regarding biomaterials implantation and acceptance.

Minocycline was observed to modulate inflammatory response by affecting some of the studied parameters. Accordingly, the antibiotic in both $1 \mu\text{g}.\text{ml}^{-1}$ (low) and $2.5 \mu\text{g}.\text{ml}^{-1}$ (high) concentrations, demonstrated to attenuate the overall inflammatory reaction over time, in control animals, as well as in later time points, in diabetic animals. Present data seems to suggest that the developed minocycline-delivery system, based on a PMMA cement, may be of clinical relevance, not only for the eventual antibacterial properties ensured by minocycline release, but also regarding

the possible anti-inflammatory effect, that may modulate tissue healing in the post-operative period.

CHAPTER 6 – CONCLUSIONS AND FUTURE PERSPECTIVES

6.1 – GENERAL CONCLUSIONS

Diabetes mellitus is well known to impair bone metabolism and consequently increase the risk of fractures and delay healing processes. Despite numerous studies focused the understanding of diabetic osteopenia, the mechanisms behind diabetes-derived bone complications are still unknown, or not fully understood.

Our work showed that DM is likely to affect MSCs signalling and functionality in a deep and long-lasting way, promoting bone weakening. The long-term hyperglycaemia was demonstrated to interfere in the behaviour of Wistar rat MSCs, hindering the osteogenic differentiation, even in the presence of osteogenic-inducers. These results support that local or systemic strategies, such as modulatory-drug delivery systems, targeted to specific tissue or hindrances, may enhance the MSCs functionality and maturation in diabetes, and subsequently enhance bone metabolism and regeneration in this pathological condition.

Tetracyclines have been described to possess exceptional properties beyond their natural antibiotic activity. Our *in vivo* and *ex vivo* experiments demonstrated that, in addition to the enhancement of osteoblastic function in diabetic conditions, doxycycline administration, in low dosage regimens, is able to normalize the impaired osteogenic commitment of precursor populations. Upon doxycycline treatment, MSCs cultures from diabetic models, showed increased commitment within the osteogenic lineage, as well as increased osteogenic priming and collagen synthesis, suggesting that doxycycline improves matrix quality for bone formation to occur. In later time points, the compound revealed to enhance tissue healing and promote mineralization in the newborn rat

calvarial bone defect model. These data converged to the idea that minocycline and doxycycline represent optimal candidates to be applied in clinical local therapies for bone regeneration enhancement, particularly in compromised conditions induced by diabetes.

In an attempt to create a reliable tetracycline delivery system for bone regeneration local therapies, we developed a new formulation of PMMA bone cement, loaded with different concentrations of minocycline. Minocycline-impregnated PMMA subcutaneously implanted in Wistar rats showed to be biocompatible and able to modulate the immune-inflammatory response, enabling a more favourable biomaterial acceptance and long-term functionality, in both control and diabetic animals.

6.2 – FUTURE PERSPECTIVES

Minocycline and doxycycline have proven to be strong osteogenic-inducers, promoting osteogenic priming and enhancing new bone formation. Its association with a biocompatible material such as PMMA presents valuable advantages for clinical application in situations in which local therapies are required, rather than systemic administrations, which reduces significantly the eventual undesirable effects of tetracyclines or other antibiotics, over the tissues.

Despite the positive effects attained in our study, future work is greatly envisaged. Accordingly, experimental local application of minocycline or doxycycline-loaded PMMA at bone defects or fractures models is essential to address the osteogenic potential of these tetracycline-derivatives. Further, the carrier material represents another major concern depending on its properties and application. For example, implant osseointegration is known to be impaired in diabetes as well, thereby it is important to evaluate osseointegration of PMMA bone cements in diabetic conditions, in both situations with and without impregnated-tetracyclines. As a bone cement used as filler, bone-material interface represents a critical point to be addressed. Moreover, porous PMMA is also available, which may constitute a new hypothesis in which minocycline or doxycycline are loaded in a bone cement, with beneficial structural properties as it mimic the porous component of bone.

REFERENCES

1. American Diabetes Association. Standards of medical care in diabetes - 2015. *Diabetes care*. 2015;38(Supplement 1):S1-S94.
2. Heydari I, Radi V, Razmjou S, Amiri A. Chronic complications of diabetes mellitus in newly diagnosed patients. *International Journal of Diabetes Mellitus*. 2010;2(1):61-3.
3. Schwartz A. Diabetes mellitus: does it affect bone? *Calcified tissue international*. 2003;73(6):515-9.
4. Bouillon R. Diabetic bone disease. *Calcified tissue international*. 1991;49(3):155-60.
5. De Liefde I, Van der Klift M, De Laet C, Van Daele P, Hofman A, Pols H. Bone mineral density and fracture risk in type-2 diabetes mellitus: the Rotterdam Study. *Osteoporosis International*. 2005;16(12):1713-20.
6. Isidro ML, Belen R. Bone Disease in Diabetes. *Current Diabetes Reviews*. 2010;6(3):144-55.
7. Gomes PS, Fernandes MH. Effect of therapeutic levels of doxycycline and minocycline in the proliferation and differentiation of human bone marrow osteoblastic cells. *archives of oral biology*. 2007;52(3):251-9.
8. Golub LM, Lee H-M, Stoner JA, Reinhardt RA, Sorsa T, Goren AD, et al. Doxycycline effects on serum bone biomarkers in post-menopausal women. *Journal of dental research*. 2010;89(6):644-9.
9. Sapadin AN, Fleischmajer R. Tetracyclines: nonantibiotic properties and their clinical implications. *Journal of the American Academy of Dermatology*. 2006;54(2):258-65.
10. Garrido-Mesa N, Zarzuelo A, Galvez J. Minocycline: far beyond an antibiotic. *British journal of pharmacology*. 2013;169(2):337-52.
11. Le NN, Rose MB, Levinson H, Klitzman B. Implant Healing in Experimental Animal Models of Diabetes. *Journal of Diabetes Science and Technology*. 2011;5(3):605-18.
12. Weiner S, Wagner HD. The material bone: structure-mechanical function relations. *Annual Review of Materials Science*. 1998;28(1):271-98.
13. College O. Bone Classification. *Anatomy & Physiology Connexions Web Site*; 2013.
14. Weiner S, Traub W, Wagner HD. Lamellar bone: structure–function relations. *Journal of structural biology*. 1999;126(3):241-55.
15. Bronner F, Worrell RV. *Orthopaedics: principles of basic and clinical science*: CRC Press; 1999.
16. Bilezikian JP, Raisz LG, Martin TJ. *Principles of Bone Biology: Vol. 1*: Boca Raton: Academic Press; 2008.
17. Guyton AC, Hall JE. *Parathyroid Hormone, Calcitonin, Calcium and Phosphate Metabolism, Vitamin D, Bone, and Teeth*. *Textbook of Medical Physiology*. 11th ed. Philadelphia, Pennsylvania: Elsevier Saunders; 2006. p. 978-95.
18. Florencio-Silva R, Sasso GRdS, Sasso-Cerri E, Simões MJ, Cerri PS. *Biology of Bone Tissue: Structure, Function, and Factors That Influence Bone Cells*. *BioMed Research International*. 2015;2015:421746.
19. Sims NA, Gooi JH, editors. *Bone remodeling: Multiple cellular interactions required for coupling of bone formation and resorption*. *Seminars in cell & developmental biology*; 2008: Elsevier.
20. Standring S, Wigley C, Healy JC. *Cells, Tissues and Systems*. *Gray's Anatomy*. 40th ed: Churchill Livingstone Elsevier; 2008. p. 81-125.
21. Gorski JP. Is all bone the same? Distinctive distributions and properties of non-collagenous matrix proteins in lamellar vs. woven bone imply the existence of different

- underlying osteogenic mechanisms. *Critical Reviews in Oral Biology & Medicine*. 1998;9(2):201-23.
22. Crockett J, Mellis D, Scott D, Helfrich M. New knowledge on critical osteoclast formation and activation pathways from study of rare genetic diseases of osteoclasts: focus on the RANK/RANKL axis. *Osteoporosis international*. 2011;22(1):1-20.
 23. Yavropoulou M, Yovos J. Osteoclastogenesis--current knowledge and future perspectives. *J Musculoskelet Neuronal Interact*. 2008;8(3):204-16.
 24. Boyce BF, Xing L. Functions of RANKL/RANK/OPG in bone modeling and remodeling. *Archives of biochemistry and biophysics*. 2008;473(2):139-46.
 25. Clarke B. Normal bone anatomy and physiology. *Clinical journal of the American Society of Nephrology*. 2008;3(Supplement 3):S131-S9.
 26. Teitelbaum SL. Bone resorption by osteoclasts. *Science*. 2000;289(5484):1504-8.
 27. Capulli M, Paone R, Rucci N. Osteoblast and osteocyte: Games without frontiers. *Archives of biochemistry and biophysics*. 2014;561:3-12.
 28. Anderson HC. Matrix vesicles and calcification. *Current rheumatology reports*. 2003;5(3):222-6.
 29. Ali S, editor *Analysis of matrix vesicles and their role in the calcification of epiphyseal cartilage. Federation proceedings*; 1976.
 30. Boivin G, Meunier P. The degree of mineralization of bone tissue measured by computerized quantitative contact microradiography. *Calcified Tissue International*. 2002;70(6):503-11.
 31. Coelho M, Fernandes M. Human bone cell cultures in biocompatibility testing. Part II: effect of ascorbic acid, β -glycerophosphate and dexamethasone on osteoblastic differentiation. *Biomaterials*. 2000;21(11):1095-102.
 32. Jilka RL, Weinstein RS, Bellido T, Parfitt AM, Manolagas SC. Osteoblast Programmed Cell Death (Apoptosis): Modulation by Growth Factors and Cytokines. *Journal of Bone and Mineral Research*. 1998;13(5):793-802.
 33. Franz-Odenaal TA, Hall BK, Witten PE. Buried alive: how osteoblasts become osteocytes. *Developmental Dynamics*. 2006;235(1):176-90.
 34. Schaffler MB, Cheung W-Y, Majeska R, Kennedy O. Osteocytes: master orchestrators of bone. *Calcified tissue international*. 2014;94(1):5-24.
 35. Bonewald LF. The amazing osteocyte. *Journal of Bone and Mineral Research*. 2011;26(2):229-38.
 36. Rochefort G, Pallu S, Benhamou C-L. Osteocyte: the unrecognized side of bone tissue. *Osteoporosis International*. 2010;21(9):1457-69.
 37. Han Y, Cowin SC, Schaffler MB, Weinbaum S. Mechanotransduction and strain amplification in osteocyte cell processes. *Proceedings of the National Academy of Sciences of the United States of America*. 2004;101(47):16689-94.
 38. Miller SC, de Saint-Georges L, Bowman B, Jee W. Bone lining cells: structure and function. *Scanning microscopy*. 1989;3(3):953-60; discussion 60-1.
 39. Parfitt A. The bone remodeling compartment: a circulatory function for bone lining cells. *Journal of Bone and Mineral Research*. 2001;16(9):1583-5.
 40. Lanyon L. Osteocytes, strain detection, bone modeling and remodeling. *Calcified tissue international*. 1993;53(1):S102-S7.
 41. Raisz LG. Pathogenesis of osteoporosis: concepts, conflicts, and prospects. *The Journal of clinical investigation*. 2005;115(12):3318-25.
 42. Mulari M, Vääräniemi J, Väänänen HK. Intracellular membrane trafficking in bone resorbing osteoclasts. *Microscopy research and technique*. 2003;61(6):496-503.
 43. Arana-Chavez VE, Bradaschia-Correa V. Clastic cells: mineralized tissue resorption in health and disease. *The international journal of biochemistry & cell biology*. 2009;41(3):446-50.
 44. Robling AG, Castillo AB, Turner CH. Biomechanical and molecular regulation of bone remodeling. *Annu Rev Biomed Eng*. 2006;8:455-98.

45. Carano RA, Filvaroff EH. Angiogenesis and bone repair. *Drug discovery today*. 2003;8(21):980-9.
46. Petite H, Viateau V, Bensaid W, Meunier A, de Pollak C, Bourguignon M, et al. Tissue-engineered bone regeneration. *Nature biotechnology*. 2000;18(9):959-63.
47. Guo Sa, DiPietro LA. Factors affecting wound healing. *Journal of dental research*. 2010;89(3):219-29.
48. Kuzuya T, Nakagawa S, Satoh J, Kanazawa Y, Iwamoto Y, Kobayashi M, et al. Report of the Committee on the classification and diagnostic criteria of diabetes mellitus. *Diabetes research and clinical practice*. 2002;55(1):65-85.
49. Guyton AC, Hall JE. *Insulin, Glucagon, and Diabetes Mellitus*. *Textbook of Medical Physiology*. 11th ed. Philadelphia, Pennsylvania: Elsevier Saunders; 2006. p. 961-77.
50. Diamond J. The double puzzle of diabetes. *Nature*. 2003;423(6940):599-602.
51. American Diabetes Association. Classification and Diagnosis of diabetes mellitus. *Diabetes care*. 2016;39(Supplement 1):S13-S22.
52. Bach J-F. Insulin-dependent diabetes mellitus as an autoimmune disease. *Endocrine reviews*. 1994;15(4):516-42.
53. Van Belle TL, Coppieters KT, Von Herrath MG. Type 1 diabetes: etiology, immunology, and therapeutic strategies. *Physiological reviews*. 2011;91(1):79-118.
54. Davies JL, Kawaguchi Y, Bennett ST, Copeman JB, Cordell HJ, Pritchard LE, et al. A genome-wide search for human type 1 diabetes susceptibility genes. *Nature*. 1994;371(6493):130-6.
55. Nejentsev S, Howson JM, Walker NM, Szeszeko J, Field SF, Stevens HE, et al. Localization of type 1 diabetes susceptibility to the MHC class I genes HLA-B and HLA-A. *Nature*. 2007;450(7171):887-92.
56. Jahromi MM, Eisenbarth GS. Cellular and molecular pathogenesis of type 1 diabetes. *Cellular and molecular life sciences*. 2007;64(7-8):865-72.
57. Yoon J-W, Austin M, Onodera T, Notkins AL. Virus-induced diabetes mellitus: isolation of a virus from the pancreas of a child with diabetic ketoacidosis. *New England Journal of Medicine*. 1979;300(21):1173-9.
58. Ylipaasto P, Klingel K, Lindberg AM, Otonkoski T, Kandolf R, Hovi T, et al. Enterovirus infection in human pancreatic islet cells, islet tropism in vivo and receptor involvement in cultured islet beta cells. *Diabetologia*. 2004;47(2):225-39.
59. Sechi LA, Paccagnini D, Salza S, Pacifico A, Ahmed N, Zanetti S. *Mycobacterium avium* subspecies paratuberculosis bacteremia in type 1 diabetes mellitus: an infectious trigger? *Clinical Infectious Diseases*. 2008;46(1):148-9.
60. Pankaj B, Shalini M. Immunology of Diabetes Mellitus. *Journal of Medical Science & Research*. 2012;3(1).
61. Kitabchi AE, Umpierrez GE, Murphy MB, Barrett EJ, Kreisberg RA, Malone JI, et al. Management of Hyperglycemic Crises in Patients With Diabetes. *Diabetes Care*. 2001;24(1):131-53.
62. Saltiel AR. New perspectives into the molecular pathogenesis and treatment of type 2 diabetes. *Cell*. 2001;104(4):517-29.
63. Weyer C, Funahashi T, Tanaka S, Hotta K, Matsuzawa Y, Pratley RE, et al. Hypoadiponectinemia in obesity and type 2 diabetes: close association with insulin resistance and hyperinsulinemia. *The Journal of Clinical Endocrinology & Metabolism*. 2001;86(5):1930-5.
64. Rother KI. Diabetes treatment—bridging the divide. *The New England Journal of Medicine*. 2007;356(15):1499.
65. Narayan KV, Boyle JP, Geiss LS, Saaddine JB, Thompson TJ. Impact of recent increase in incidence on future diabetes burden. *Diabetes care*. 2006;29(9):2114-6.
66. Dabelea D, Mayer-Davis EJ, Saydah S, Imperatore G, Linder B, Divers J, et al. Prevalence of type 1 and type 2 diabetes among children and adolescents from 2001 to 2009. *Jama*. 2014;311(17):1778-86.

67. Florez JC, Hirschhorn J, Altshuler D. The inherited basis of diabetes mellitus: implications for the genetic analysis of complex traits. *Annual review of genomics and human genetics*. 2003;4(1):257-91.
68. Go VLW. *The exocrine pancreas: biology, pathobiology, and diseases*: Raven Press; 1986.
69. American Diabetes Association. *Diagnosis and Classification of Diabetes Mellitus*. *Diabetes Care*. 2013;36(Supplement 1):S67-S74.
70. Jovanovic L, Pettitt DJ. Gestational diabetes mellitus. *Jama*. 2001;286(20):2516-8.
71. Catalano PM, McIntyre HD, Cruickshank JK, McCance DR, Dyer AR, Metzger BE, et al. The Hyperglycemia and Adverse Pregnancy Outcome Study Associations of GDM and obesity with pregnancy outcomes. *Diabetes care*. 2012;35(4):780-6.
72. Buchanan TA, Xiang AH. Gestational diabetes mellitus. *The Journal of clinical investigation*. 2005;115(3):485-91.
73. Sacks DB. A1C Versus Glucose Testing: A Comparison. *Diabetes Care*. 2011;34(2):518-23.
74. Sacks DB, Arnold M, Bakris GL, Bruns DE, Horvath AR, Kirkman MS, et al. Position statement executive summary: guidelines and recommendations for laboratory analysis in the diagnosis and management of diabetes mellitus. *Diabetes Care*. 2011;34(6):1419-23.
75. Krakauer JC, McKenna MJ, Buderer NF, Rao DS, Whitehouse FW, Parfitt AM. Bone loss and bone turnover in diabetes. *Diabetes*. 1995;44(7):775-82.
76. Ivers RQ, Cumming RG, Mitchell P, Peduto AJ. Diabetes and risk of fracture. *Diabetes care*. 2001;24(7):1198-203.
77. Blakytyn R, Spraul M, Jude EB. Review: the diabetic bone: a cellular and molecular perspective. *The international journal of lower extremity wounds*. 2011;10(1):16-32.
78. Janghorbani M, Van Dam RM, Willett WC, Hu FB. Systematic review of type 1 and type 2 diabetes mellitus and risk of fracture. *American journal of epidemiology*. 2007;166(5):495-505.
79. Hofbauer LC, Brueck CC, Singh SK, Dobnig H. Osteoporosis in patients with diabetes mellitus. *Journal of Bone and Mineral Research*. 2007;22(9):1317-28.
80. Massé PG, Pacifique MB, Tranchant CC, Arjmandi BH, Ericson KL, Donovan SM, et al. Bone metabolic abnormalities associated with well-controlled type 1 diabetes (IDDM) in young adult women: a disease complication often ignored or neglected. *Journal of the American College of Nutrition*. 2010;29(4):419-29.
81. Merlotti D, Gennari L, Dotta F, Lauro D, Nuti R. Mechanisms of impaired bone strength in type 1 and 2 diabetes. *Nutrition, Metabolism and Cardiovascular Diseases*. 2010;20(9):683-90.
82. Silva MJ, Brodt MD, Lynch MA, McKenzie JA, Tanouye KM, Nyman JS, et al. Type 1 diabetes in young rats leads to progressive trabecular bone loss, cessation of cortical bone growth, and diminished whole bone strength and fatigue life. *Journal of Bone and Mineral Research*. 2009;24(9):1618-27.
83. Lumachi F, Camozzi V, Tombolan V, Luisetto G. Bone Mineral Density, Osteocalcin, and Bone-specific Alkaline Phosphatase in Patients with Insulin-dependent Diabetes Mellitus. *Annals of the New York Academy of Sciences*. 2009;1173(s1):E64-E7.
84. Pastor MC, Lopez-Ibarra P, Escobar-Jimenez F, Pardo MS, Garcia-Cervigon A. Intensive insulin therapy and bone mineral density in type 1 diabetes mellitus: a prospective study. *Osteoporosis International*. 2000;11(5):455-9.
85. López-Ibarra P-J, Pastor MMC, Escobar-Jiménez F, Pardo MDS, González AG, Luna JDD, et al. Bone mineral density at time of clinical diagnosis of adult-onset type 1 diabetes mellitus. *Endocrine Practice*. 2001;7(5):346-51.
86. Shyng Y, Devlin H, Sloan P. The effect of streptozotocin-induced experimental diabetes mellitus on calvarial defect healing and bone turnover in the rat. *International journal of oral and maxillofacial surgery*. 2001;30(1):70-4.
87. He H, Liu R, Desta T, Leone C, Gerstenfeld LC, Graves DT. Diabetes causes decreased osteoclastogenesis, reduced bone formation, and enhanced apoptosis of osteoblastic cells in bacteria stimulated bone loss. *Endocrinology*. 2004;145(1):447-52.

88. Atkins RC, Zimmet P. Diabetic kidney disease: Act now or pay later. *Therapeutic Apheresis and Dialysis*. 2010;14(1):1-4.
89. Bouillon R, Bex M, Van Herck E, Laureys J, Dooms L, Lesaffre E, et al. Influence of age, sex, and insulin on osteoblast function: osteoblast dysfunction in diabetes mellitus. *The Journal of Clinical Endocrinology & Metabolism*. 1995;80(4):1194-202.
90. Fowlkes JL, Bunn RC, Liu L, Wahl EC, Coleman HN, Cockrell GE, et al. Runt-related transcription factor 2 (RUNX2) and RUNX2-related osteogenic genes are down-regulated throughout osteogenesis in type 1 diabetes mellitus. *Endocrinology*. 2008;149(4):1697-704.
91. Lu H, Kraut D, Gerstenfeld LC, Graves DT. Diabetes interferes with the bone formation by affecting the expression of transcription factors that regulate osteoblast differentiation. *Endocrinology*. 2003;144(1):346-52.
92. Ward DT, Yau SK, Mee AP, Mawer EB, Miller CA, Garland HO, et al. Functional, molecular, and biochemical characterization of streptozotocin-induced diabetes. *Journal of the American Society of Nephrology*. 2001;12(4):779-90.
93. Thrailkill KM, Liu L, Wahl EC, Bunn RC, Perrien DS, Cockrell GE, et al. Bone formation is impaired in a model of type 1 diabetes. *Diabetes*. 2005;54(10):2875-81.
94. Cummings SR, Nevitt MC, Browner WS, Stone K, Fox KM, Ensrud KE, et al. Risk factors for hip fracture in white women. *New England journal of medicine*. 1995;332(12):767-74.
95. Nicodemus KK, Folsom AR. Type 1 and type 2 diabetes and incident hip fractures in postmenopausal women. *Diabetes care*. 2001;24(7):1192-7.
96. Schwartz AV, Sellmeyer DE, Ensrud KE, Cauley JA, Tabor HK, Schreiner PJ, et al. Older women with diabetes have an increased risk of fracture: a prospective study. *The Journal of Clinical Endocrinology & Metabolism*. 2001;86(1):32-8.
97. Isaia G, Ardisson P, Di Stefano M, Ferrari D, Martina V, Porta M, et al. Bone metabolism in type 2 diabetes mellitus. *Acta diabetologica*. 1999;36(1-2):35-8.
98. Barrett-Connor E, Holbrook TL. Sex Differences in Osteoporosis in Older Adults With Non—Insulin-Dependent Diabetes Mellitus. *Jama*. 1992;268(23):3333-7.
99. Ding EL, Song Y, Manson JE, Hunter DJ, Lee CC, Rifai N, et al. Sex hormone-binding globulin and risk of type 2 diabetes in women and men. *New England Journal of Medicine*. 2009;361(12):1152-63.
100. Haffner SM, Valdez RA, Morales PA, Hazuda HP, Stern MP. Decreased sex hormone-binding globulin predicts noninsulin-dependent diabetes mellitus in women but not in men. *The Journal of Clinical Endocrinology & Metabolism*. 1993;77(1):56-60.
101. Schwartz AV, Hillier TA, Sellmeyer DE, Resnick HE, Gregg E, Ensrud KE, et al. Older women with diabetes have a higher risk of falls A prospective study. *Diabetes care*. 2002;25(10):1749-54.
102. Gregg EW, Mangione CM, Cauley JA, Thompson TJ, Schwartz AV, Ensrud KE, et al. Diabetes and incidence of functional disability in older women. *Diabetes care*. 2002;25(1):61-7.
103. McNeill JH. *Experimental models of diabetes*: CRC Press; 1999.
104. Rees D, Alcolado J. Animal models of diabetes mellitus. *Diabetic medicine*. 2005;22(4):359-70.
105. Lenzen S. The mechanisms of alloxan-and streptozotocin-induced diabetes. *Diabetologia*. 2008;51(2):216-26.
106. Szkudelski T. The mechanism of alloxan and streptozotocin action in B cells of the rat pancreas. *Physiological research*. 2001;50(6):537-46.
107. Wöhler F, Liebig J. Untersuchungen über die Natur der Harnsäure. [Investigations on the nature of uric acid]. *Ann Pharm*. 1838;26(3):241-336.
108. Dunn JS, McLetchie N. Experimental alloxan diabetes in the rat. *The Lancet*. 1943;242(6265):384-7.
109. Deeds M, Anderson J, Armstrong A, Gastineau D, Hiddinga H, Jahangir A, et al. Single dose streptozotocin-induced diabetes: considerations for study design in islet transplantation models. *Laboratory animals*. 2011;45(3):131-40.

110. Rakietyen N, Rakietyen M, Nadkarni M. Studies on the diabetogenic action of streptozotocin (NSC-37917). *Cancer chemotherapy reports Part 1*. 1963;29:91-8.
111. Boyle JP, Honeycutt AA, Narayan KV, Hoerger TJ, Geiss LS, Chen H, et al. Projection of diabetes burden through 2050 impact of changing demography and disease prevalence in the US. *Diabetes care*. 2001;24(11):1936-40.
112. Bauer TW, Schils J. The pathology of total joint arthroplasty. *Skeletal radiology*. 1999;28(9):483-97.
113. Darouiche RO. Treatment of infections associated with surgical implants. *New England Journal of Medicine*. 2004;350(14):1422-9.
114. Weinstein RA, Darouiche RO. Device-associated infections: a macroproblem that starts with microadherence. *Clinical Infectious Diseases*. 2001;33(9):1567-72.
115. Fahey TJ, Sadaty A, Jones WG, Barber A, Smoller B, Shires GT. Diabetes impairs the late inflammatory response to wound healing. *Journal of Surgical Research*. 1991;50(4):308-13.
116. Calvet HM, Yoshikawa TT. Infections in diabetes. *Infectious disease clinics of North America*. 2001;15(2):407-21.
117. Morris HF, Ochi S, Winkler S. Implant survival in patients with type 2 diabetes: placement to 36 months. *Annals of Periodontology*. 2000;5(1):157-65.
118. Sibbald R, Woo KY. The biology of chronic foot ulcers in persons with diabetes. *Diabetes/metabolism research and reviews*. 2008;24(S1):S25-S30.
119. Falanga V. Wound healing and its impairment in the diabetic foot. *The Lancet*. 2005;366(9498):1736-43.
120. Lipsky BA, Berendt AR, Deery HG, Embil JM, Joseph WS, Karchmer AW, et al. Diagnosis and treatment of diabetic foot infections. *Clinical Infectious Diseases*. 2004;39(7):885-910.
121. Brem H, Tomic-Canic M. Cellular and molecular basis of wound healing in diabetes. *The Journal of clinical investigation*. 2007;117(5):1219-22.
122. Oh BK, Robbins ME, Nablo BJ, Schoenfisch MH. Miniaturized glucose biosensor modified with a nitric oxide-releasing xerogel microarray. *Biosensors and Bioelectronics*. 2005;21(5):749-57.
123. Mellado Valero A, Ferrer García JC, Herrera Ballester A, Labaig Rueda C. Effects of diabetes on the osseointegration of dental implants. *Medicina Oral, Patología Oral y Cirugía Bucal (Internet)*. 2007;12(1):38-43.
124. McCracken M, Lemons JE, Rahemtulla F, Prince CW, Feldman D. Bone response to titanium alloy implants placed in diabetic rats. *International Journal of Oral & Maxillofacial Implants*. 2000;15(3).
125. Nevins ML, Karimbux NY, Weber HP, Giannobile WV, Fiorellini JP. Wound healing around endosseous implants in experimental diabetes. *International Journal of Oral & Maxillofacial Implants*. 1998;13(5).
126. Siqueira JT, Cavalher-Machado SC, Arana-Chavez VE, Sannomiya P. Bone formation around titanium implants in the rat tibia: role of insulin. *Implant dentistry*. 2003;12(3):242-51.
127. Kwon PT, Rahman SS, Kim DM, Kopman JA, Karimbux NY, Fiorellini JP. Maintenance of osseointegration utilizing insulin therapy in a diabetic rat model. *Journal of periodontology*. 2005;76(4):621-6.
128. Javed F, Romanos GE. Impact of diabetes mellitus and glycemic control on the osseointegration of dental implants: a systematic literature review. *Journal of Periodontology*. 2009;80(11):1719-30.
129. Fiorellini JP, Nevins ML, Norkin A, Weber HP, Karimbux NY. The effect of insulin therapy on osseointegration in a diabetic rat model. *Clinical oral implants research*. 1999;10(5):362-8.
130. Riond J, Riviere J. Pharmacology and toxicology of doxycycline. *Veterinary and human toxicology*. 1988;30(5):431-43.
131. Nelson ML, Levy SB. The history of the tetracyclines. *Annals of the New York Academy of Sciences*. 2011;1241(1):17-32.

132. Finlay A, Hobby G, P'an S, Regna P, Routien J, Seeley D, et al. Terramycin, a new antibiotic. American Association for the Advancement of Science Science. 1950:85-7.
133. Boothe J, Morton J, Petisi J, Wilkinson R, Williams J. Chemistry of tetracycline. *Antibiot Ann.* 1953:46-8.
134. Stephens C, Conover L, Pasternack R, Hochstein F, Moreland W, Regna P, et al. The structure of Aureomycin¹. *Journal of the American Chemical Society.* 1954;76(13):3568-75.
135. Golub L, Suomalainen K, Sorsa T. Host modulation with tetracyclines and their chemically modified analogues. *Current opinion in dentistry.* 1992;2:80-90.
136. Nguyen F, Starosta Agata L, Arenz S, Sohmen D, Dönhöfer A, Wilson Daniel N. Tetracycline antibiotics and resistance mechanisms. *Biological Chemistry* 2014. p. 559.
137. Nelson M. Chemical and biological dynamics of tetracyclines. *Advances in dental research.* 1998(12):5-11.
138. Goldman RA, Hasan T, Hall CC, Strycharz WA, Cooperman BS. Photoincorporation of tetracycline into *Escherichia coli* ribosomes. Identification of the major proteins photolabeled by native tetracycline and tetracycline photoproducts and implications for the inhibitory action of tetracycline on protein synthesis. *Biochemistry.* 1983;22(2):359-68.
139. Brodersen DE, Clemons WM, Carter AP, Morgan-Warren RJ, Wimberly BT, Ramakrishnan V. The structural basis for the action of the antibiotics tetracycline, pactamycin, and hygromycin B on the 30S ribosomal subunit. *Cell.* 2000;103(7):1143-54.
140. Counis R, Raulin J, Koumanov K, Infante R. Interprétation du rôle antipolypolique de la tétracycline. *European Journal of Biochemistry.* 1973;37(2):244-7.
141. Epe B, Woolley P, Hornig H. Competition between tetracycline and tRNA at both P and A sites of the ribosome of *Escherichia coli*. *FEBS letters.* 1987;213(2):443-7.
142. Oliva B, Gordon G, McNicholas P, Ellestad G, Chopra I. Evidence that tetracycline analogs whose primary target is not the bacterial ribosome cause lysis of *Escherichia coli*. *Antimicrobial agents and chemotherapy.* 1992;36(5):913-9.
143. Golub L, Lee H, Lehrer G, Nemiroff A, McNamara T, Kaplan R, et al. Minocycline reduces gingival collagenolytic activity during diabetes. *Journal of periodontal research.* 1983;18(5):516-26.
144. Tamargo RJ, Bok RA, Brem H. Angiogenesis inhibition by minocycline. *Cancer Research.* 1991;51(2):672-5.
145. Golub LM, Ramamurthy N, McNamara TF, Greenwald RA, Rifkin BR. Tetracyclines inhibit connective tissue breakdown: new therapeutic implications for an old family of drugs. *Critical Reviews in Oral Biology & Medicine.* 1991;2(3):297-321.
146. Sasaki T, Ramamurthy NS, Golub LM. Tetracycline administration increases collagen synthesis in osteoblasts of streptozotocin-induced diabetic rats: a quantitative autoradiographic study. *Calcified tissue international.* 1992;50(5):411-9.
147. Golub LM, Ramamurthy NS, Llawaneras A, Ryan ME, Lee HM, Liu Y, et al. A Chemically Modified Nonantimicrobial Tetracycline (CMT-8) Inhibits Gingival Matrix Metalloproteinases, Periodontal Breakdown, and Extra-Oral Bone Loss in Ovariectomized Rats. *Annals of the New York Academy of Sciences.* 1999;878(1):290-310.
148. Blackwood RK, Beereboom JJ, Rennhard HH, von Wittenau MS, Stephens CR. 6-Methylenetetraacyclines. 1 I. A new class of tetracycline antibiotics. *Journal of the American Chemical Society.* 1961;83(12):2773-5.
149. Stephens CR, Beereboom JJ, Rennhard HH, Gordon PN, Murai K, Blackwood RK, et al. 6-Deoxytetraacyclines. IV. 1, 2 Preparation, C-6 Stereochemistry, and Reactions. *Journal of the American Chemical Society.* 1963;85(17):2643-52.
150. Cunha B, Domenico P, Cunha C. Pharmacodynamics of doxycycline. *Clinical Microbiology and Infection.* 2000;6(5):270-3.
151. Hanemaaijer R, Sorsa T, Konttinen YT, Ding Y, Sutinen M, Visser H, et al. Matrix Metalloproteinase-8 Is Expressed in Rheumatoid Synovial Fibroblasts and Endothelial Cells:

Regulation by tumor necrosis factor- α and doxycycline. *Journal of Biological Chemistry*. 1997;272(50):31504-9.

152. O'Dell JR, Elliott JR, Mallek JA, Mikuls TR, Weaver CA, Glickstein S, et al. Treatment of early seropositive rheumatoid arthritis: doxycycline plus methotrexate versus methotrexate alone. *Arthritis & Rheumatism*. 2006;54(2):621-7.

153. Sanchez J, Somolinos AL, Almodóvar PI, Webster G, Bradshaw M, Powala C. A randomized, double-blind, placebo-controlled trial of the combined effect of doxycycline hyclate 20-mg tablets and metronidazole 0.75% topical lotion in the treatment of rosacea. *Journal of the American Academy of Dermatology*. 2005;53(5):791-7.

154. Valentín S, Morales A, Sánchez JL, Rivera A. Safety and efficacy of doxycycline in the treatment of rosacea. *Clin Cosmet Investig Dermatol*. 2009;2:129-40.

155. Duivenvoorden WC, Popović SV, Lhoták Š, Seidlitz E, Hirte HW, Tozer RG, et al. Doxycycline decreases tumor burden in a bone metastasis model of human breast cancer. *Cancer research*. 2002;62(6):1588-91.

156. Hanemaaijer R, Visser H, Koolwijk P, Sorsa T, Salo T, Golub LM, et al. Inhibition of MMP synthesis by doxycycline and chemically modified tetracyclines (CMTs) in human endothelial cells. *Advances in dental research*. 1998;12(1):114-8.

157. Caton JG, Ciancio SG, Blieden TM, Bradshaw M, Crout RJ, Hefti AF, et al. Treatment with subantimicrobial dose doxycycline improves the efficacy of scaling and root planing in patients with adult periodontitis. *Journal of periodontology*. 2000;71(4):521-32.

158. Payne JB, Stoner JA, Nummikoski PV, Reinhardt RA, Goren AD, Wolff MS, et al. Subantimicrobial dose doxycycline effects on alveolar bone loss in post-menopausal women. *Journal of clinical periodontology*. 2007;34(9):776-87.

159. Golub L, Lee H-M, Greenwald R, Ryan M, Sorsa T, Salo T, et al. A matrix metalloproteinase inhibitor reduces bone-type collagen degradation fragments and specific collagenases in gingival crevicular fluid during adult periodontitis. *Inflammation Research*. 1997;46(8):310-9.

160. Walter M, Frank M, Satué M, Monjo M, Rønold H, Lyngstadaas S, et al. Bioactive implant surface with electrochemically bound doxycycline promotes bone formation markers in vitro and in vivo. *Dental Materials*. 2014;30(2):200-14.

161. Eglence A, Colterjohn N, Duivenvoorden WC, Ghert M, Singh G. Effect of bone morphogenetic protein-2 and doxycycline on the differentiation of osteoprogenitors from human femoral bone. *Open Bone J*. 2009;1:1-7.

162. Carbone EJ, Rajpura K, Jiang T, Laurencin CT, Lo KW-H. Regulation of bone regeneration with approved small molecule compounds. *Advances in Regenerative Biology*. 2014;1.

163. Kaur K, Sikri P. Evaluation of the effect of allograft with doxycycline versus the allograft alone in the treatment of infrabony defects: a controlled clinical and radiographical study. *Dental research journal*. 2013;10(2):238.

164. Vernillo A, Ramamurthy N, Golub L, Rifkin B. The nonantimicrobial properties of tetracycline for the treatment of periodontal disease. *Current opinion in periodontology*. 1993;111-8.

165. Payne JB, Golub LM. Using tetracyclines to treat osteoporotic/osteopenic bone loss: from the basic science laboratory to the clinic. *Pharmacological research*. 2011;63(2):121-9.

166. Blum D, Chtarto A, Tenenbaum L, Brotchi J, Levivier M. Clinical potential of minocycline for neurodegenerative disorders. *Neurobiology of disease*. 2004;17(3):359-66.

167. Klein NC, Cunha BA. Tetracyclines. *The Medical clinics of North America*. 1995;79(4):789-801.

168. Barza M, Brown RB, Shanks C, Gamble C, Weinstein L. Relation between lipophilicity and pharmacological behavior of minocycline, doxycycline, tetracycline, and oxytetracycline in dogs. *Antimicrobial agents and chemotherapy*. 1975;8(6):713-20.

169. Yrjänheikki J, Keinänen R, Pellikka M, Hökfelt T, Koistinaho J. Tetracyclines inhibit microglial activation and are neuroprotective in global brain ischemia. *Proceedings of the National Academy of Sciences*. 1998;95(26):15769-74.
170. Yrjänheikki J, Tikka T, Keinänen R, Goldsteins G, Chan PH, Koistinaho J. A tetracycline derivative, minocycline, reduces inflammation and protects against focal cerebral ischemia with a wide therapeutic window. *Proceedings of the National Academy of Sciences*. 1999;96(23):13496-500.
171. Mejia RS, Ona VO, Li M, Friedlander RM. Minocycline reduces traumatic brain injury-mediated caspase-1 activation, tissue damage, and neurological dysfunction. *NEUROSURGERY-BALTIMORE*. 2001;48(6):1393-9.
172. Mei X-P, Xu H, Xie C, Ren J, Zhou Y, Zhang H, et al. Post-injury administration of minocycline: an effective treatment for nerve-injury induced neuropathic pain. *Neuroscience research*. 2011;70(3):305-12.
173. Thomas M, Le W. Minocycline: neuroprotective mechanisms in Parkinson's disease. *Current pharmaceutical design*. 2004;10(6):679-86.
174. Choi Y, Kim H-S, Shin KY, Kim E-M, Kim M, Kim H-S, et al. Minocycline attenuates neuronal cell death and improves cognitive impairment in Alzheimer's disease models. *Neuropsychopharmacology*. 2007;32(11):2393-404.
175. Thomas M, Ashizawa T, Jankovic J. Minocycline in Huntington's disease: a pilot study. *Movement disorders*. 2004;19(6):692-5.
176. Lee SM, Yune TY, Kim SJ, Kim YC, Oh YJ, Markelonis GJ, et al. Minocycline inhibits apoptotic cell death via attenuation of TNF- α expression following iNOS/NO induction by lipopolysaccharide in neuron/glia co-cultures. *Journal of neurochemistry*. 2004;91(3):568-78.
177. Basegmez C, Berber L, Yalcin F. Clinical and biochemical efficacy of minocycline in nonsurgical periodontal therapy: a randomized controlled pilot study. *The Journal of Clinical Pharmacology*. 2011;51(6):915-22.
178. Williams S, Wakisaka A, Zeng Q, Barnes J, Seyedin S, Martin G, et al. Effect of minocycline on osteoporosis. *Advances in dental research*. 1998;12(1):71-5.
179. Williams S, Wakisaka A, Zeng Q, Barnes J, Martin G, Wechter W, et al. Minocycline prevents the decrease in bone mineral density and trabecular bone in ovariectomized aged rats. *Bone*. 1996;19(6):637-44.
180. Klapisz-Wolikow M, Saffar J. Minocycline impairment of both osteoid tissue removal and osteoclastic resorption in a synchronized model of remodeling in the rat. *Journal of cellular physiology*. 1996;167:359-68.
181. Retzepi M, Donos N. The effect of diabetes mellitus on osseous healing. *Clinical oral implants research*. 2010;21(7):673-81.
182. Vestergaard P. Discrepancies in bone mineral density and fracture risk in patients with type 1 and type 2 diabetes—a meta-analysis. *Osteoporosis International*. 2007;18(4):427-44.
183. Wang W, Zhang X, Zheng J, Yang J. High glucose stimulates adipogenic and inhibits osteogenic differentiation in MG-63 cells through cAMP/protein kinase A/extracellular signal-regulated kinase pathway. *Molecular and cellular biochemistry*. 2010;338(1-2):115-22.
184. Balint E, Szabo P, Marshall C, Sprague S. Glucose-induced inhibition of in vitro bone mineralization. *Bone*. 2001;28(1):21-8.
185. Botolin S, McCabe LR. Chronic hyperglycemia modulates osteoblast gene expression through osmotic and non-osmotic pathways. *Journal of cellular biochemistry*. 2006;99(2):411-24.
186. Gopalakrishnan V, Vignesh R, Arunakaran J, Aruldas M, Srinivasan N. Effects of glucose and its modulation by insulin and estradiol on BMSC differentiation into osteoblastic lineages. *Biochemistry and cell biology*. 2006;84(1):93-101.
187. Brenner RE, Riemenschneider B, Blum W, Mörike M, Teller WM, Pirsig W, et al. Defective stimulation of proliferation and collagen biosynthesis of human bone cells by serum from diabetic patients. *Acta endocrinologica*. 1992;127(6):509-14.

188. Fulzele K, Riddle RC, DiGirolamo DJ, Cao X, Wan C, Chen D, et al. Insulin receptor signaling in osteoblasts regulates postnatal bone acquisition and body composition. *Cell*. 2010;142(2):309-19.
189. Li L, Xia Y, Wang Z, Cao X, Da Z, Guo G, et al. Suppression of the PI3K—Akt pathway is involved in the decreased adhesion and migration of bone marrow-derived mesenchymal stem cells from non-obese diabetic mice. *Cell biology international*. 2011;35(9):961-6.
190. Tolosa MJ, Chuguransky SR, Sedlinsky C, Schurman L, McCarthy AD, Molinuevo MS, et al. Insulin-deficient diabetes-induced bone microarchitecture alterations are associated with a decrease in the osteogenic potential of bone marrow progenitor cells: preventive effects of metformin. *Diabetes research and clinical practice*. 2013;101(2):177-86.
191. Stolzing A, Sellers D, Llewelyn O, Scutt A. Diabetes induced changes in rat mesenchymal stem cells. *Cells Tissues Organs*. 2010;191(6):453-65.
192. Thomsen JS, Laib A, Koller B, Prohaska S, Mosekilde L, Gowin W. Stereological measures of trabecular bone structure: comparison of 3D micro computed tomography with 2D histological sections in human proximal tibial bone biopsies. *Journal of Microscopy*. 2005;218(2):171-9.
193. Dobson K, Reading L, Haberey M, Marine X, Scutt A. Centrifugal isolation of bone marrow from bone: an improved method for the recovery and quantitation of bone marrow osteoprogenitor cells from rat tibiae and femuræ. *Calcified tissue international*. 1999;65(5):411-3.
194. Sekiya I, Larson BL, Smith JR, Pochampally R, Cui JG, Prockop DJ. Expansion of human adult stem cells from bone marrow stroma: conditions that maximize the yields of early progenitors and evaluate their quality. *Stem cells*. 2002;20(6):530-41.
195. Terada M, Inaba M, Yano Y, Hasuma T, Nishizawa Y, Morii H, et al. Growth-inhibitory effect of a high glucose concentration on osteoblast-like cells. *Bone*. 1998;22(1):17-23.
196. Bosetti M, Sabbatini M, Nicolì E, Fusaro L, Cannas M. Effects and differentiation activity of IGF-I, IGF-II, insulin and preptin on human primary bone cells. *Growth Factors*. 2013;31(2):57-65.
197. Wang N, Butler JP, Ingber DE. Mechanotransduction across the cell surface and through the cytoskeleton. *Science*. 1993;260(5111):1124-7.
198. Kilian KA, Bugarija B, Lahn BT, Mrksich M. Geometric cues for directing the differentiation of mesenchymal stem cells. *Proceedings of the National Academy of Sciences*. 2010;107(11):4872-7.
199. Goldberg DM, Martin JV, Knight AH. Elevation of serum alkaline phosphatase activity and related enzymes in diabetes mellitus. *Clinical biochemistry*. 1977;10:8-11.
200. Rezende A, Petenusci S, Urbinati EC, Leone F. Kinetic properties of osseous plate alkaline phosphatase from diabetic rats. *Comparative Biochemistry and Physiology Part A: Physiology*. 1993;104(3):469-74.
201. Fernandes SS, Furriel RP, Petenusci SO, Leone FA. Streptozotocin-induced diabetes: significant changes in the kinetic properties of the soluble form of rat bone alkaline phosphatase. *Biochemical pharmacology*. 1999;58(5):841-9.
202. Spanheimer RG, Umpierrez GE, Stumpf V. Decreased collagen production in diabetic rats. *Diabetes*. 1988;37(4):371-6.
203. Goldberg RB. Cytokine and cytokine-like inflammation markers, endothelial dysfunction, and imbalanced coagulation in development of diabetes and its complications. *The Journal of Clinical Endocrinology & Metabolism*. 2009;94(9):3171-82.
204. Ding J, Ghali O, Lencel P, Broux O, Chauveau C, Devedjian J, et al. TNF- α and IL-1 β inhibit RUNX2 and collagen expression but increase alkaline phosphatase activity and mineralization in human mesenchymal stem cells. *Life sciences*. 2009;84(15):499-504.
205. Seshi B, Kumar S, Sellers D. Human bone marrow stromal cell: coexpression of markers specific for multiple mesenchymal cell lineages. *Blood Cells, Molecules, and Diseases*. 2000;26(3):234-46.

206. Kotobuki N, Matsushima A, Kato Y, Kubo Y, Hirose M, Ohgushi H. Small interfering RNA of alkaline phosphatase inhibits matrix mineralization. *Cell and tissue research*. 2008;332(2):279-88.
207. Zhao Y-F, Zeng D-L, Xia L-G, Zhang S-M, Xu L-Y, Jiang X-Q, et al. Osteogenic potential of bone marrow stromal cells derived from streptozotocin-induced diabetic rats. *International journal of molecular medicine*. 2013;31(3):614-20.
208. Wan Y. PPAR γ in bone homeostasis. *Trends in Endocrinology & Metabolism*. 2010;21(12):722-8.
209. Muruganandan S, Roman A, Sinal C. Adipocyte differentiation of bone marrow-derived mesenchymal stem cells: cross talk with the osteoblastogenic program. *Cellular and molecular life sciences*. 2009;66(2):236-53.
210. Augello A, De Bari C. The regulation of differentiation in mesenchymal stem cells. *Human gene therapy*. 2010;21(10):1226-38.
211. Jaiswal RK, Jaiswal N, Bruder SP, Mbalaviele G, Marshak DR, Pittenger MF. Adult human mesenchymal stem cell differentiation to the osteogenic or adipogenic lineage is regulated by mitogen-activated protein kinase. *Journal of Biological Chemistry*. 2000;275(13):9645-52.
212. Ge C, Xiao G, Jiang D, Yang Q, Hatch NE, Roca H, et al. Identification and functional characterization of ERK/MAPK phosphorylation sites in the Runx2 transcription factor. *Journal of Biological Chemistry*. 2009;284(47):32533-43.
213. Zhang W, Shen X, Wan C, Zhao Q, Zhang L, Zhou Q, et al. Effects of insulin and insulin-like growth factor 1 on osteoblast proliferation and differentiation: differential signalling via Akt and ERK. *Cell biochemistry and function*. 2012;30(4):297-302.
214. Takada I, Kouzmenko AP, Kato S. Wnt and PPAR γ signaling in osteoblastogenesis and adipogenesis. *Nature Reviews Rheumatology*. 2009;5(8):442-7.
215. Hie M, Iitsuka N, Otsuka T, Tsukamoto I. Insulin-dependent diabetes mellitus decreases osteoblastogenesis associated with the inhibition of Wnt signaling through increased expression of Sost and Dkk1 and inhibition of Akt activation. *International journal of molecular medicine*. 2011;28(3):455-62.
216. López-Herradón A, Portal-Núñez S, García-Martín A, Lozano D, Pérez-Martínez FC, Ceña V, et al. Inhibition of the canonical Wnt pathway by high glucose can be reversed by parathyroid hormone-related protein in osteoblastic cells. *Journal of cellular biochemistry*. 2013;114(8):1908-16.
217. Suzuki A, Guicheux J, Palmer G, Miura Y, Oiso Y, Bonjour J-P, et al. Evidence for a role of p38 MAP kinase in expression of alkaline phosphatase during osteoblastic cell differentiation. *Bone*. 2002;30(1):91-8.
218. Hager S, Lampert FM, Orimo H, Stark GB, Finkenzeller G. Up-regulation of alkaline phosphatase expression in human primary osteoblasts by cocultivation with primary endothelial cells is mediated by p38 mitogen-activated protein kinase-dependent mRNA stabilization. *Tissue Engineering Part A*. 2009;15(11):3437-47.
219. Igarashi M, Wakasaki H, Takahara N, Ishii H, Jiang Z-Y, Yamauchi T, et al. Glucose or diabetes activates p38 mitogen-activated protein kinase via different pathways. *The Journal of clinical investigation*. 1999;103(2):185-95.
220. Stein GS, Lian JB, Owen TA. Relationship of cell growth to the regulation of tissue-specific gene expression during osteoblast differentiation. *The FASEB journal*. 1990;4(13):3111-23.
221. Miao J, Brismar K, Nyrén O, Ugarph-Morawski A, Ye W. Elevated Hip Fracture Risk in Type 1 Diabetic Patients A Population-Based Cohort Study in Sweden. *Diabetes care*. 2005;28(12):2850-5.
222. Vestergaard P, Rejnmark L, Mosekilde L. Diabetes and its complications and their relationship with risk of fractures in type 1 and 2 diabetes. *Calcified tissue international*. 2009;84(1):45-55.

223. Thrailkill KM, Lumpkin CK, Bunn RC, Kemp SF, Fowlkes JL. Is insulin an anabolic agent in bone? Dissecting the diabetic bone for clues. *American Journal of Physiology-Endocrinology And Metabolism*. 2005;289(5):E735-E45.
224. Silva J, Sampaio P, Fernandes M, Gomes P. The osteogenic priming of mesenchymal stem cells is impaired in experimental diabetes. *Journal of cellular biochemistry*. 2015;116(8):1658-67.
225. Brinckerhoff CE, Matrisian LM. Matrix metalloproteinases: a tail of a frog that became a prince. *Nature reviews Molecular cell biology*. 2002;3(3):207-14.
226. Krane SM, Inada M. Matrix metalloproteinases and bone. *Bone*. 2008;43(1):7-18.
227. Ortega N, Behonick D, Stickens D, Werb Z. How proteases regulate bone morphogenesis. *Annals of the New York Academy of Sciences*. 2003;995(1):109-16.
228. Golub L, Lee H-M, Ryan M, Giannobile W, Payne J, Sorsa T. Tetracyclines inhibit connective tissue breakdown by multiple non-antimicrobial mechanisms. *Advances in dental research*. 1998;12(1):12-26.
229. Wu X, Downes S, Watts DC. Evaluation of critical size defects of mouse calvarial bone: an organ culture study. *Microscopy research and technique*. 2010;73(5):540-7.
230. Hamann C, Kirschner S, Gunther K-P, Hofbauer LC. Bone, sweet bone - osteoporotic fractures in diabetes mellitus. *Nat Rev Endocrinol*. 2012;8(5):297-305.
231. Ryan M, Ashley R. How do tetracyclines work? *Advances in dental research*. 1998;12(1):149-51.
232. Payne J, Stoner J, Nummikoski P, Reinhardt R, Goren A, Wolff M, et al. Subantimicrobial dose doxycycline effects on alveolar bone loss in post-menopausal women. *J Clin Periodontol*. 2007;34:776-87.
233. Payne J, Golub L, Stoner J, Lee H, Reinhardt R, Sorsa T, et al. The effect of subantimicrobial-dose-doxycycline periodontal therapy on serum biomarkers of systemic inflammation: a randomized, double-masked, placebo-controlled clinical trial. *J Am Dent Assoc*. 2011;142:262-73.
234. Golub L, Lee H, Stoner J, Reinhardt R, Sorsa T, Goren A, et al. Doxycycline effects on serum bone biomarkers in postmenopausal women. *J Dent Res*. 2010;89:644-49.
235. Park J-B. Low dose of doxycycline promotes early differentiation of preosteoblasts by partially regulating the expression of estrogen receptors. *J Surg Res*. 2012;178:737-42.
236. Gomes P, Fernandes M. Effect of therapeutic levels of doxycycline and minocycline in the proliferation and differentiation of human bone marrow osteoblastic cells. *Arch Oral Biol*. 1997;52:251-9.
237. Eglence A, Colterjohn N, Duivenvoorden W, Ghert M, Singh G. Effect of bone morphogenetic protein-2 and doxycycline on the differentiation of osteoprogenitors from human femoral bone. *Open Bone J*. 2009;1:1-7.
238. Walter M, Frank M, Satué M, Monjo M, Rønold H, Lyngstadaas S, et al. Bioactive implant surface with electrochemically bound doxycycline promotes bone formation markers in vitro and in vivo. *Dent Mater*. 2014;30:200-14.
239. Zhang Z, Qu Y, Li X, Zhang S, Wei Q, Shi Y, et al. Electrophoretic deposition of tetracycline modified silk fibroin coatings for functionalization of titanium surfaces. *Appl Surf Sci*. 2014;303:255-62.
240. Park J-B. Effects of doxycycline, minocycline, and tetracycline on cell proliferation, differentiation, and protein expression in osteoprecursor cells. *J Craniofac Surg*. 2011;22:1839-42.
241. Almazin S, Dziak R, Andreana S, Ciancio S. The effect of doxycycline hyclate, chlorhexidine gluconate, and minocycline hydrochloride on osteoblastic proliferation and differentiation in vitro. *J Periodontol*. 2009;80:999-1005.
242. Duewelhenke N, Krut O, Eysel P. Influence on mitochondria and cytotoxicity of different antibiotics administered in high concentrations on primary human osteoblasts and cell lines. *Antimicrob Agents Chemother*. 2007;51:54-63.

243. Golub L, Lee H, Stoner J, Sorsa T, Reinhardt R, Wolff M, et al. Subantimicrobial-dose doxycycline modulates gingival crevicular fluid biomarkers of periodontitis in postmenopausal osteopenic women. *J Periodontol.* 2008;79.
244. Brinckerhoff C, Matrisian L. Matrix metalloproteinases: a tail of a frog that became a prince. *Nat Rev Mol Cell Biol.* 2002;3:207–14.
245. Schneir M, Ramamurthy N, Golub L. Minocycline-treatment of diabetic rats normalizes skin collagen production and mass: possible causative mechanisms. *Matrix.* 1990;10:112–23.
246. Sasaki T, Ramamurthy N, Yu Z, Golub L. Tetracycline administration increases protein (presumably procollagen) synthesis and secretion in periodontal ligament fibroblasts of streptozotocin-induced diabetic rats. *J Periodontal Res.* 1992;27: 631–9.
247. Craig R, Yu Z, Xu L, Barr R, Ramamurthy N, Boland J, et al. A chemically modified tetracycline inhibits streptozotocin-induced diabetic depression of skin collagen synthesis and steady-state type I procollagen mRNA. *Biochim Biophys Acta.* 1998;1402:250-6.
248. Yu Z, Ramamurthy N, Leung M, Chang K, McNamara T, Golub L. Chemically-modified tetracycline normalizes collagen metabolism in diabetic rats: a dose-response study. *J Periodontal Res.* 1993;28:420-8.
249. Sasaki T, Ramamurthy N, Golub L. Tetracycline administration increases collagen synthesis in osteoblasts of streptozotocin-induced diabetic rats: a quantitative autoradiographic study. *Calcif Tissue Int.* 1992;50:411-9.
250. Kol R, Palattella A. The use of doxycycline in periodontology. Histologic in vivo study on mice affected by diabetes mellitus. *Minerva Stomatol.* 2006;55:77-86.
251. Llambés F, Silvestre F, Hernández-Mijares A, Guiha R, Caffesse R. Effect of non-surgical periodontal treatment with or without doxycycline on the periodontium of type 1 diabetic patients. *J Clin Periodontol.* 2005;32:915-20.
252. Eickholz P. Systemic doxycycline and nonsurgical periodontal treatment in diabetic patients. *Evid Based Dent.* 2007;8:14.
253. Amid R, Sovaid M, Saadati H. Comparison of the effect of non-surgical periodontal therapy with and without systemic doxycycline on the health of periodontium and HbA1c in type 2 diabetic patients without good glycemic control. *J Periodontol Implant Dent.* 2009;1:20-7.
254. Tal H, Weinreb M, Shely A, Nemcovsky CE, Moses O. Tetracycline impregnation affects degradation of porcine collagen matrix in healthy and diabetic rats. *Clinical oral investigations.* 2016:1-6.
255. Bain S, Ramamurthy N, Impeduglia T, Scolman S, Golub L, Rubin C. Tetracycline prevents cancellous bone loss and maintains near-normal rates of bone formation in streptozotocin diabetic rats. *Bone.* 1997;21:147-53.
256. Sasaki T, Kaneko H, Ramamurthy N, Golub L. Tetracycline administration restores osteoblast structure and function during experimental diabetes. *Anat Rec.* 1991;231:25-34.
257. Lemann J, Lennon E, Piering W, Prien E, Ricanati E. Evidence that glucose ingestion inhibits net renal tubular reabsorption of calcium and magnesium in man. *The Journal of laboratory and clinical medicine.* 1970;75(4):578-85.
258. Schneider LE, Schedl HP. Diabetes and intestinal calcium absorption in the rat. *American Journal of Physiology--Legacy Content.* 1972;223(6):1319-23.
259. Goodman SB, Yao Z, Keeney M, Yang F. The future of biologic coatings for orthopaedic implants. *Biomaterials.* 2013;34(13):3174-83.
260. Matos AC. Investigation of New Formulations of Acrylic Bone Cement Containing Antibiotics. Lisbon: Faculty of Pharmacy; 2015.
261. Kretlow JD, Shi M, Young S, Spicer PP, Demian N, Jansen JA, et al. Evaluation of soft tissue coverage over porous polymethylmethacrylate space maintainers within nonhealing alveolar bone defects. *Tissue Engineering Part C: Methods.* 2010;16(6):1427-38.
262. Samuel S. Antibiotic Loaded Acrylic Bone Cement in Orthopaedic Trauma. In: Mauricio S, editor. *Osteomyelitis: InTech;* 2012. p. 131-52.

263. Kelly K, Sutton T, Weathered N, Ray N, Caldwell E, Plotkin Z, et al. Minocycline inhibits apoptosis and inflammation in a rat model of ischemic renal injury. *American Journal of Physiology-Renal Physiology*. 2004;287(4):F760-F6.
264. Ishikawa C, Tsuda T, Konishi H, Nakagawa N, Yamanishi K. Tetracyclines modulate protease-activated receptor 2-mediated proinflammatory reactions in epidermal keratinocytes. *Antimicrobial agents and chemotherapy*. 2009;53(5):1760-5.
265. Matos A, Gonçalves L, Rijo P, Vaz M, Almeida A, Bettencourt A. A novel modified acrylic bone cement matrix. A step forward on antibiotic delivery against multiresistant bacteria responsible for prosthetic joint infections. *Mater Sci Eng C*. 2014;38:218-26.
266. Matos A, Marques C, Pinto R, Ribeiro I, Gonçalves L, Vaz M, et al. Novel doped calcium phosphate-PMMA bone cement composites as levofloxacin delivery systems. *Int J Pharm*. 2015;490(1-2):200-8.
267. World Health Organization (WHO). Fact sheet Nº 310; Top 10 causes of death, updated May 2014. Geneva: World Health Organization. 2015.
268. Thonse R, Conway J. Antibiotic cement-coated interlocking nail for the treatment of infected nonunions and segmental bone defects. *Journal of orthopaedic trauma*. 2007;21(4):258-68.
269. Diegelmann RF, Lindblad WJ, Cohen IK. A subcutaneous implant for wound healing studies in humans. *Journal of Surgical Research*. 1986;40(3):229-37.
270. Socarrás TO, Vasconcelos AC, Campos PP, Pereira NB, Souza JP, Andrade SP. Foreign body response to subcutaneous implants in diabetic rats. *PloS one*. 2014;9(11):e110945.
271. Thomson S, McLennan S, Hennessy A, Boughton P, Bonner J, Zoellner H, et al. A novel primate model of delayed wound healing in diabetes: dysregulation of connective tissue growth factor. *Diabetologia*. 2010;53(3):572-83.
272. Ochoa O, Torres FM, Shireman PK. Chemokines and diabetic wound healing. *Vascular*. 2007;15(6):350-5.
273. Gerritsen M. Problems associated with subcutaneously implanted glucose sensors. *Diabetes Care*. 2000;23(2):143-.
274. Khanna S, Biswas S, Shang Y, Collard E, Azad A, Kauh C, et al. Macrophage dysfunction impairs resolution of inflammation in the wounds of diabetic mice. *PloS one*. 2010;5(3):e9539.
275. Kumar V, Abbas AK, Fausto N, Mitchell R. *Acute and Chronic Inflammation*. Robbins Basic Pathology. 8th ed. Philadelphia: Elsevier Health Sciences; 2007. p. 31-58.
276. Pereira MAA, Sannomiya P, Leme JG. Inhibition of leukocyte chemotaxis by factor in alloxan-induced diabetic rat plasma. *Diabetes*. 1987;36(11):1307-14.
277. Nolan CM, Beaty HN, Bagdade JD. Further characterization of the impaired bactericidal function of granulocytes in patients with poorly controlled diabetes. *Diabetes*. 1978;27(9):889-94.
278. Tan JS, Anderson JL, Watanakunakorn C, Phair JP. Neutrophil dysfunction in diabetes mellitus. *The Journal of laboratory and clinical medicine*. 1975;85(1):26-33.
279. Marhoffer W, Stein M, Maeser E, Federlin K. Impairment of polymorphonuclear leukocyte function and metabolic control of diabetes. *Diabetes care*. 1992;15(2):256-60.
280. Mowat AG, Baum J. Chemotaxis of polymorphonuclear leukocytes from patients with diabetes mellitus. *New England Journal of Medicine*. 1971;284(12):621-7.
281. Alba-Loureiro T, Munhoz C, Martins J, Cerchiaro G, Scavone C, Curi R, et al. Neutrophil function and metabolism in individuals with diabetes mellitus. *Brazilian Journal of Medical and Biological Research*. 2007;40(8):1037-44.
282. Smythies LE, Maheshwari A, Clements R, Eckhoff D, Novak L, Vu HL, et al. Mucosal IL-8 and TGF- β recruit blood monocytes: evidence for cross-talk between the lamina propria stroma and myeloid cells. *Journal of leukocyte biology*. 2006;80(3):492-9.
283. Cassatella MA. Neutrophil-derived proteins: selling cytokines by the pound. *Advances in immunology*. 1999;73:369-509.

284. Baggiolini M, Clark-Lewis I. Interleukin-8, a chemotactic and inflammatory cytokine. *FEBS letters*. 1992;307(1):97-101.
285. Hatanaka E, Monteagudo P, Marrocos M, Campa A. Neutrophils and monocytes as potentially important sources of proinflammatory cytokines in diabetes. *Clinical & Experimental Immunology*. 2006;146(3):443-7.
286. Salamone G, Trevani A, Martínez D, Vermeulen M, Gamberale R, Fernández-Calotti P, et al. Analysis of the mechanisms involved in the stimulation of neutrophil apoptosis by tumour necrosis factor- α . *Immunology*. 2004;113(3):355-62.
287. Shine W, McCulley J, Pandya A. Minocycline effect on meibomian gland lipids in meibomianitis patients. *Experimental eye research*. 2003;76(4):417-20.
288. Weisberg SP, McCann D, Desai M, Rosenbaum M, Leibel RL, Ferrante AW. Obesity is associated with macrophage accumulation in adipose tissue. *The Journal of clinical investigation*. 2003;112(12):1796-808.
289. Goren I, Müller E, Schiefelbein D, Christen U, Pfeilschifter J, Mühl H, et al. Systemic anti-TNF α treatment restores diabetes-impaired skin repair in ob/ob mice by inactivation of macrophages. *Journal of Investigative Dermatology*. 2007;127(9):2259-67.
290. Singer AJ, Clark RA. Cutaneous wound healing. *New England journal of medicine*. 1999;341(10):738-46.
291. Rosen A, Casciola-Rosen L. Autoantigens as substrates for apoptotic proteases: implications for the pathogenesis of systemic autoimmune disease. *Cell Death & Differentiation*. 1999;6(1).
292. Fadok VA. Clearance: The Last and Often Forgotten Stage of Apoptosis. *Journal of Mammary Gland Biology and Neoplasia*. 1999;4(2):203-11.
293. Koch AE, Polverini PJ, Kunkel SL, Harlow LA, DiPietro LA, Elnor VM, et al. Interleukin-8 as a macrophage-derived mediator of angiogenesis. *SCIENCE-NEW YORK THEN WASHINGTON*-. 1992;258:1798-.
294. Olerud JE. Models for diabetic wound healing and healing into percutaneous devices. *Journal of Biomaterials Science, Polymer Edition*. 2008;19(8):1007-20.
295. Ward WK. A review of the foreign-body response to subcutaneously-implanted devices: the role of macrophages and cytokines in biofouling and fibrosis. *Journal of diabetes science and technology*. 2008;2(5):768-77.
296. Morais JM, Papadimitrakopoulos F, Burgess DJ. Biomaterials/tissue interactions: possible solutions to overcome foreign body response. *The AAPS journal*. 2010;12(2):188-96.
297. Luttkhuizen DT, Harmsen MC, Luyn MJV. Cellular and molecular dynamics in the foreign body reaction. *Tissue engineering*. 2006;12(7):1955-70.
298. Siqueira MF, Li J, Chehab L, Desta T, Chino T, Krothpali N, et al. Impaired wound healing in mouse models of diabetes is mediated by TNF- α dysregulation and associated with enhanced activation of forkhead box O1 (FOXO1). *Diabetologia*. 2010;53(2):378-88.
299. Loots MA, Lamme EN, Zeegelaar J, Mekkes JR, Bos JD, Middelkoop E. Differences in cellular infiltrate and extracellular matrix of chronic diabetic and venous ulcers versus acute wounds. *Journal of Investigative Dermatology*. 1998;111(5):850-7.
300. Breslin RJ, Wasserkrug HL, Efron G, Barbul A. Suppressor cell generation during normal wound healing. *Journal of Surgical Research*. 1988;44(4):321-5.
301. Barbul A, Regan M. The regulatory role of T lymphocytes in wound healing. *Journal of Trauma and Acute Care Surgery*. 1990;30:97-9.
302. Kilzer P, Chang K, Marvel J, Rowold E, Jaudes P, Ullensvang S, et al. Albumin permeation of new vessels is increased in diabetic rats. *Diabetes*. 1985;34(4):333-6.
303. Witte M, Kiyama T, Barbul A. Nitric oxide enhances experimental wound healing in diabetes. *British journal of surgery*. 2002;89(12):1594-601.
304. Dulak J, Józkwicz A. Regulation of vascular endothelial growth factor synthesis by nitric oxide: facts and controversies. *Antioxidants and redox signaling*. 2003;5(1):123-32.

305. Chbinou N, Frenette J. Insulin-dependent diabetes impairs the inflammatory response and delays angiogenesis following Achilles tendon injury. *American Journal of Physiology-Regulatory, Integrative and Comparative Physiology*. 2004;286(5):R952-R7.